



Skolkovo Institute of Science and Technology

STUDY OF DEFORMATIONAL BEHAVIOR OF ELECTRICAL CONDUCTIVITY  
OF POLYMER COMPOSITES WITH DIFFERENT NANOFILLER DISTRIBUTION  
TYPES

*Doctoral Thesis*

by

OLEG V. LEBEDEV

DOCTORAL PROGRAM IN MATERIALS SCIENCE AND ENGINEERING

Supervisor  
Assistant Professor Sergey Abaimov

Moscow - 2020

© Oleg V. Lebedev 2020

I hereby declare that the work presented in this thesis was carried out by myself at Skolkovo Institute of Science and Technology, Moscow, except where due acknowledgement is made, and has not been submitted for any other degree.

Candidate (Oleg V. Lebedev)  \_\_\_\_\_

Supervisor (Sergey Abaimov)  \_\_\_\_\_

## Abstract

In this work, the correlation between electrical conductivity and uniaxial deformation of polymer composites with different nanofiller distribution types was studied.

First, a material with highly segregated distribution of conductive filler was investigated. Multi-walled carbon nanotubes (MWCNTs) were used as a model filler. A numerical model was proposed that can be used to predict changes in conductive structure made of MWCNTs in response to uniaxial deformation of material. At the first stage, numerical simulations were conducted for uniformly distributed MWCNTs providing confinement of the filler in a two-dimensional film structure with high volume fraction of the filler. At next stage, conductivity response to uniaxial deformation of reconstructed real 3D highly segregated distribution of the filler was investigated numerically. Embedded element method was implemented to conduct realistic and computationally efficient simulation of MWCNTs behavior during deformation of the composite material. The results of numerical simulations of changes in electrical conductivity of composite during deformation were compared with the experimental data to prove the correctness of assumptions used in the models.

Next, electrically conductive composites based on polypropylene (PP) and filled with MWCNTs and carbon black (CB) were studied. The composites were manufactured using melt mixing of the filler powder and PP pellets. The composites electrical conductance was measured while they were subjected to uniaxial deformation. A numerical modeling approach based on finite element method was proposed to predict the conductive system transformation as a response to composite material deformation. This approach considered experimentally observed composite structure and deformational behavior of the MWCNTs or clusters of CB particles, while also taking into account highly agglomerated state of the nanoparticles that was obtained in the tested samples. The numerical predictions of correlation between applied deformation and electrical conductance of the composites were compared against the experimental data and it was concluded, that the proposed numerical methods provide satisfactory estimations.

Finally, a multi-scale and multi-physics model taking into account structure-property relationships that are interconnected across the length scales was developed to predict electrical conductance deformational behavior for glass fiber reinforced electroconductive nanocomposites (GFRNCs). To verify numerical model predictions, composites with PP matrix filled with nanoparticles and reinforced with woven glass fibers were manufactured. As nanosized electroconductive fillers MWCNTs and CB were used. Uniaxial deformation of the obtained GFRNCs with simultaneous continuous electrical conductance measurements was performed experimentally and numerically. Results of the numerical modeling were compared with experimental data obtained for modified PP and for GFRNCs. It was concluded that introduction of woven glass fiber in the electrically conductive matrix noticeably affects electrical conductivity changes with deformation for the material, which can be adequately predicted numerically using proposed multi-scale modeling approach for correct composite structure representation.

## Publications

1. Lebedev, O. V., Abaimov, S. G., & Ozerin, A. N. (2020). Modeling the effect of uniaxial deformation on electrical conductivity for composite materials with extreme filler segregation. *Journal of Composite Materials*, 54(3), 299–309. <https://doi.org/10.1177/0021998319862045> (Q2 Scopus, WoS)
2. Lebedev, O. V., Trofimov, A., Abaimov, S. G., & Ozerin, A. N. (2019). Modeling of an effect of uniaxial deformation on electrical conductance of polypropylene-based composites filled with agglomerated nanoparticles. *International Journal of Engineering Science*, 144, 103132. <https://doi.org/10.1016/j.ijengsci.2019.103132> (Q1 Scopus, WoS)
3. Lebedev, O. V., Abaimov, S. G., Ozerin, A. N., Kurkin T.S. & Trofimov, A. (2020). Multi-Scale Modeling of Uniaxial Deformation of Electroconductive Polypropylene/Nanoparticles Composites Reinforced with Woven Glass Fiber, *Proceedings of the 36th International Conference of the Polymer Processing Society (PPS)*, AIP Publishing (accepted) (WoS, Scopus)

## **Personal Contribution**

The following results presented in this work were obtained by the author personally:

- Manufacturing of the laboratory samples.
- Mechanical testing of the samples, as well as measurements of conductance of the samples in the course of deformation.
- Electron microscopy images processing.
- Development of numerical models and performance of the numerical simulations.
- Experimental and numerical simulations data processing and analysis.

The following results were obtained with personal participation of the author:

- Electron microscopy studies of the filler powders and the samples.

## **Acknowledgements**

I want to thank Prof. Sergey Abaimov for valuable advices and help given to me in the course of my whole work on my PhD thesis.

I would like to express my sincere gratitude to Dr. Alexander Ozerin, who inspired me to start working on the topic of my dissertation, being world-known expert in this field. I also want to thank him for all the advice he provided me concerning experimental part of my work.

I am very grateful to Prof. Iskander Akhatov for providing me with necessary resources to conduct my research at Skoltech.

Special thanks to my friend Dr. Anton Trofimov, who supported me in many different ways, such as providing advice on numerical simulation, and helping me with writing articles and conference proceedings.

I also like to thank my friends Dr. Tikhon Kurkin and Evgeny Golubev for assisting me with many miscellaneous tasks, thus saving me a lot of time needed for my research.

This work was supported by the RFBR, namely the reported in chapter 3 study was funded by RFBR under the research project № 19-03-00369. The reported in chapter 4 and 5 study was funded by RFBR under the research project № 18-33-00688.

## Table of Contents

Abstract.....	3
Publications.....	5
Personal Contribution .....	6
Acknowledgements.....	7
Table of Contents .....	8
List of Abbreviations .....	10
Chapter 1. Introduction .....	11
Chapter 2. Literature review .....	19
2.1. Polymer Composites with Segregated Structure.....	19
2.2. Non-destructive Testing of Electroconductive Polymer Composites.....	26
Chapter 3. Materials and Methods.....	29
3.1. Experimental Part.....	29
3.1.1. Materials .....	29
3.1.2. Methods.....	33
3.2. Numerical part .....	44
3.2.1. Modeling of thin MWCNTs layer.....	44
3.2.2. Modeling of PP-based Nanocomposites .....	54
3.2.2.1. Distribution Creation .....	54
3.2.2.2. Finite Element Analysis.....	61
3.2.2.3. Relative Electrical Conductance Calculations.....	64
Chapter 4. Modeling the Effect of Uniaxial Deformation on Electrical Conductivity for a Compacted Thin Layer of MWCNTs .....	67
4.1. Comparison Between Numerical and Experimental Results.....	67
4.2. Influence of the Model Parameters .....	70
4.3. Conclusions to Chapter 4 .....	75
Chapter 5. Modeling the Effect of Uniaxial Deformation on Electrical Conductivity for Composite Materials with Extreme 3D Filler Segregation.....	77
5.1. Results and Discussion. ....	77

5.2. Conclusions to Chapter 5 .....	86
Chapter 6. Modeling of an effect of uniaxial deformation on electrical conductance of polypropylene-based composites filled with agglomerated nanoparticles .....	88
6.1. Results and Discussion .....	88
6.1. Conclusions to Chapter 6 .....	98
Chapter 7. Multi-Scale Modeling of Uniaxial Deformation of Electroconductive Polypropylene/Nanoparticles Composites Reinforced with Woven Glass Fibers.....	100
7.1. Multi-scale Modeling.....	100
7.1.1. Modified PP Properties .....	102
7.1.2. Modeling at the Micro-scale Level .....	104
7.1.3. Modeling at the Meso-scale Level .....	109
7.2. Comparison of the Experimental and Numerical Results.....	112
7.3. Conclusions to the Chapter 7 .....	115
Chapter 8. General Conclusions .....	117
Bibliography .....	121

## **List of Abbreviations**

BET - Brunauer–Emmett–Teller

CB – carbon black

CNT - carbon nanotube

FE - finite element

FEA - finite element analysis

FEM - finite element method

GFRNC - glass fiber reinforced electroconductive nanocomposite

MWCNT – multi-walled carbon nanotube

NN - no new contacts assumption

NNHC - no new contacts and highly conductive particle/electrode contacts assumptions

PE - polyethylene

PP – polypropylene

PTFE – polytetrafluoroethylene

RVE - representative volume element

UHMWPE - ultra-high-molecular-weight polyethylene

## Chapter 1. Introduction

Electrically conductive polymer composites filled with different types of carbon nanoparticles, such as carbon nanotubes, graphene, fullerenes, finely dispersed graphite, or carbon black, attract a lot of attention as potentially cheap, lightweight, and chemically resistant conductive materials [1]. As of this time, trend to develop deformation control methods providing correlation between non-destructively measured characteristics of the material and its state becomes more popular. One of the characteristics that allow to do that efficiently is electrical conductivity [2]. Since not all the materials, such as polymers, intrinsically possess high levels of conductivity, the modification by the addition of an electroconductive filler can be considered [1]. The modified polymers' electrical conductivity is dependent on the type and volume fraction of the nanosized filler. This allows a wide range of their applications, from insulating materials, electrostatic protection and electromagnetic interference shielding materials, to composite materials acting as metal replacement. The sensitivity of percolation network to deformations allows to apply such nanocomposites in sensors [3].

There are several types of fillers that are used for modification of the polymer materials, including carbon black (CB), due to their fairly cheap price and simple form, and multi-walled carbon nanotubes (MWCNTs) that are widely used due to their high electrical conductivity and high aspect ratio. [4–6]. High values of filler's aspect ratio provide low values of percolation threshold, which is important because of the requirement to minimize impact of the filling on the initial polymer material properties [7,8].

In the last two decades carbon nanotubes (CNTs), particularly MWCNTs, have become the most investigated type of filler for composites, with multiple research papers dedicated to the subject [7,9,10]. MWCNTs are often used due to their high electrical conductivity and high aspect ratio that provides low percolation threshold values.

Properties of a composite, especially its electrical conductivity are, to a great extent, determined by the distribution and dispersion of filler in a matrix [11,12]. Uniform distribution and dispersion can potentially lead to predictable mechanical and electroconductive properties, which is well described experimentally and analytically [13–15]. However, it is very difficult to achieve for nanosized particle fillers because of their tendency to agglomerate, as was demonstrated in previous works on the methods of MWCNTs dispersion in polymer matrices [9,10,16,17]. Besides, MWCNTs agglomeration is difficult to account for in a model, which results in a high uncertainty in the model parameters that are usually varied to fit experimental data. Another problem associated with the uniform dispersion and distribution of filler is a relatively high filler volume fraction required to reach percolation threshold and high level of electrical conductivity [7,9]. Thus, instead of attempts to achieve the uniform dispersion of filler, a simpler solution to these problems would be to create within a composite a certain structure made of filler particles, where the volume fraction of filler would be much higher compared to the rest of a composite. Such materials are usually called composites with segregated structure, and are often characterized by very low percolation threshold the value of which is strongly affected by the method of composite preparation (segregation method) [12,18].

Formation of segregated structures and investigation of their properties is of special importance for nanocomposites based on ultra-high-molecular-weight polyethylene (UHMWPE) as a matrix [19,20]. This is due to a limited number of processing methods available for that type of polymer, which results from the high viscosity of the UHMWPE's melt. One of the most popular methods of obtaining UHMWPE-based composites is a mechanical mixing of matrix polymer powder with nanofiller, followed by sintering at temperatures above melt temperature of polyethylene (PE) [20]. Inability of filler to enter the matrix deep enough because of the high viscosity of polymer melt leads to formation of strongly pronounced segregated structures. Melting of UHMWPE particles and pressing them together results in formation of elastic rubber-like structure of the material. This is not desirable if the UHMWPE powder in use can be further processed into ultra-strong fibers, because the entanglement prevents any shear deformations required for transition to a highly oriented state of polyethylene (PE) molecules [21]. This type of reactor powder can be processed in a solid state (below melting temperature of PE), which is a prerequisite for obtaining polymers with a high degree of orientation. The fiber-forming UHMWPE reactor powder can be used to obtain most extreme types of segregated structures, because while it is still possible for a filler particle to enter the volume of UHMWPE's melt during sintering, it cannot do so during solid-state processing. Additionally, the presence of filler does not significantly affect the process of strengthening through orientation, making it possible to obtain flexible electroconductive materials with high tensile strength [19,21].

Currently, one of the popular trends in the industry is the development of effective methods for non-destructive control of a polymer material (its deformation or extent of

damage) [22]. Electroconductivity of materials makes it possible to establish a relation between electrophysical properties of material and the state of material. The easiest way to establish this relation can be through the knowledge of initial distribution of filler particles, followed by the analysis of changes in mutual position and contacts of particles during deformation or damage of material. For MWCNTs-filled composites it is also important to account for orientation and overall alignment of MWCNTs, which can significantly affect electrical conductivity of material [23–25]. Several works have been published to this moment, making attempts at prediction of electrophysical properties of MWCNTs-filled composites [24,26,27], but there is still a need for a working model capable of describing the filler behavior during deformation for relatively high deformation degrees (with strains of 5 % and higher), especially taking into account possible complex (not rod-like) shape of MWCNTs.

Various numerical models currently exist, in particular, finite element method (FEM) based [22,28–33]. These methods allow more or less successful estimation of mechanical characteristics and electroconductivity of nanocomposites filled with particles of different types. However, considering the volume fraction of filler required for percolation, conductivity calculations for systems with filler content above this value can be a very heavy computational task, especially in 3D setting [28,31,32]. Thus, they are rarely used for large systems of nanoparticles, and finite element analysis (FEA) typically would require serious simplifications to reach reasonable computational times.

One way to increase computational efficiency of FEA simulations is to use the so-called embedded element method for mesh creation. This method implies creation of two

separate independent meshes — for the matrix and for the filler (embedded). Nodes of filler elements lying within matrix elements have constraints on translational degrees of freedom. The method was used earlier to characterize mechanical and conductive properties in two-dimensional setting for a composite filled with MWCNTs [33]. The embedded element method can also provide results for calculation of 3D stress fields in MWCNTs filled composites, close to the results obtained using continuous meshing technique [31,32]. Due to the peculiarities of MWCNTs behavior during deformation, the representation of MWCNTs as hollow tubes meshed with shell elements with isotropic mechanical properties, used in this work, might not be suitable for high deformations. The reason is that while MWCNTs theoretically possess high bending and tensile strength [34], they can assume very complex shapes, such as statistical coils, for example, when left suspended in a solution [35], partially because of a number of defects accumulated within a certain segment of MWCNT.

To understand the correlation between the level of deformation and electrical conductivity of a composite material with conductive network made of the filler inside the material, it is important to know the initial distribution of the particles inside the composite volume as well as deformational behavior of the nanoparticles of different types. Various numerical and theoretical studies were performed up until this moment, however, the fundamental understanding of the working mechanisms that can relate the complex filler behavior during the deformation to the material electrical conductance changes are still under investigation [4–6].

Thermoplastic polypropylene (PP) is one of the most promising polymers that can be used as a matrix in composite materials providing correlation between electrical conductance and deformation response due its ability to withstand high level of deformations without cracks formation. For this type of polymer high electrical conductivity can be obtained by different processing methods, such as solution blending or in situ polymerization [36]. But the simplest method to mix thermoplastic matrix and nanofiller that can be integrated in large manufacturing process is melt mixing. It is important to mention, that this method of processing when applied to the mixtures containing nanoparticles will lead to formation of nanoparticle agglomerates, which is inevitable due to their high specific surface area [17], and can seriously affect the results of modeling since typically in these models the distribution of the filler particles is considered to be uniform.

Composites based on polymer materials, for example PP, filled with carbon nanoparticles, such CB and MWCNTs, were investigated previously by [2,28,29,37]. However, correspondence between experimental data and numerical model predictions for the composite electrical conductance response to the uniaxial deformation up to relatively high strain values (0.1 and higher) is rather poor, especially considering the agglomerated state of the nanoparticles.

Smart composites capable of structural health monitoring present attractive solution to improve the safety and performance of parts. One way to control strain state of a material is by correlating the deformation degree with the material's electrical conductance [6,38].

For composites having non-conductive polymer matrix reinforced with dielectric fibers (e.g. glass fibers), high levels of electrical conductivity can be achieved by filling polymer with electrically conductive nanosized particles, i.e. MWCNTs or CB [6]. In this work, conductance-deformation behavior of a woven glass fibers reinforced polymer nanocomposites (GFRNCs) based on PP filled with MWCNTs and CB was studied.

The structure of GFRNC is hierarchical. At the meso-scale, it is made of the modified polymer matrix and glass fiber tows that are classified as warp (longitudinal) and weft (transverse). At the micro-scale, tows are represented by bundles of glass fibers and the modified polymer matrix. Therefore, the prediction of conductance-deformation relation requires an efficient multi-scale procedure [39,40].

This work was aimed to solve the fundamental problem in the field of multifunctional composites, providing models for the correlation of electrical properties and applied deformation, taking into account the structure of materials, and verified by experimental methods.

To achieve this goal, it was necessary to solve the following problems:

- 1) Analysis and selection of the most suitable types of fillers and methods for their introduction into the polymer matrix, followed by the production of representative laboratory batches of materials optimized in structure and properties for studying their physical properties. This approach includes the identification of structural and functional relationships between the type, quantity, size and degree of dispersion of conductive nanoparticles introduced

into the system and the corresponding changes in the physico-mechanical characteristics of multicomponent polymer systems;

- 2) Study of the structure and properties of composite materials by experimental methods, as well as changes in these properties during the deformation of composites;
- 3) Numerical modeling of representative composite structures based on experimental data and analytical methods of homogenization to calculate the effective mechanical and electrical properties of composite structures;

## **Chapter 2. Literature review**

### **2.1. Polymer Composites with Segregated Structure.**

Polymer composites become an increasingly attractive object for research recently, which can be observed by assessing the number of publications on this subject over the last ten years (according to Web of Science database). At the same time, a lot of articles are also related to the study of the electrophysical characteristics of materials, which indicates a great interest in conductive polymer composites.

Electrically conductive polymer composites possess useful and interesting combinations of properties, including low weight, non-linear current-voltage characteristics, conductivity that is sensitive to external influences and many more. Because of this, they are in high demand in the development of antistatic, electrostatic, shielding coatings and elements, sensors, devices, etc. [41–44].

In order to obtain an electrically conductive polymer composite, in addition to choosing a polymer matrix and a filler for the future material, it is also necessary to make a choice of the method that will be further used to obtain composites. Possible methods for mixing conductive nanoparticles (CB, CNTs, graphite and graphene) in a polymer matrix include melt mixing, polymerization filling, solution mixing, latex technology, etc. [16,45,46]. In a review [47], using the example of composites modified with carbon nanofibers, the role of the method and conditions for obtaining a composite material on its electrical conductivity was demonstrated. Also, the influence of the distribution of filler particle sizes and its dispersion on the possibility of obtaining high electrical conductivity values with a minimum degree of composite filling was studied.

To obtain electrically conductive polymer composite material, the concentration of the modifying electrically conductive filler should be higher than the so-called percolation threshold, at which the material begins to exhibit a high level of electrical conductivity [7,8,48]. Recently, epoxy resin modified with graphene flakes and carbon fibers was studied by [49,50], it was shown that addition of nanofillers decreases electrical resistivity by several orders of magnitude. Since the percolation threshold is reached, as a rule, at high degrees of filling, this creates serious problems with regard to the processability of electrically conductive polymer composites, the surface quality of products made from these materials and their final cost.

To solve this problem, it is possible to create a so-called segregated, or separated, structure made from the filler in a composite. It is characterized by the fact that the filler is not distributed evenly throughout the volume, but in some areas with a higher concentration of filler particles, which is mostly determined by the method of processing of the composite [12]. Moreover, if areas with increased filler concentration also form a percolation cluster, then for a material to reach a high level of electrical conductivity an average amount of filler is required significantly less than in the case of uniform distribution in volume [51,52]. Percolation threshold decrease is determined by the type of segregated structure [12,53,54]. Over the past years, more than one thousand of articles have been devoted to the problem of producing polymer composites with a segregated structure made of nanosized fillers (data from the Web of Science portal).

Segregated structure can be achieved, for example, by organizing special microfibrillar morphology of composites [55,56]. This approach is an example of

multiphase mixing, where as a result the filler remains in the volume of only one phase or is located at the interface of the polymer phases in the composite, being immiscible with one or both phases at certain values of thermodynamic parameters. This kind of separation into the conductive and non-conductive phases can also be achieved, for example, for the PP/polystyrene/CB system. Such system was described in [57], in which nanosized filler (CB) was introduced by the authors in the polystyrene phase solely. The authors of the work were also able to increase the local concentration of the filler by removing the polystyrene phase by dissolution and creating a heterophasic PP/CB composite by additional hot pressing.

The simplest approach to create a composite with a segregated structure made of nanosized filler is the hot-pressing method. The polymer granules are pre-coated with particles of the filler, after which the granules are pressed together at a temperature above the melting temperature of the polymer. Due to the high viscosity of the polymer, nanosized particles continue to remain in the vicinity of granule boundaries that no longer exist at that time, forming a percolation network (Figure 1). This approach was tried, in particular, on polyethylene granules [52,58], where graphene and carbon nanotubes were used as a nanosized filler. Such method allows one to obtain materials with high electrical conductivity and electromagnetic radiation shielding ability at very small volumetric filling. Unfortunately, often this approach is not the best due to the fact that the nanoscale filler still has the ability to leave the exact boundary of the granule due to the presence of some mobility in the melt.

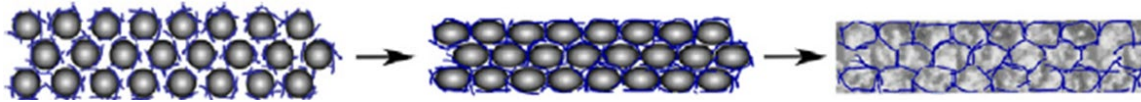


Figure 1. Schematic illustration of formation of the segregated conductive structure in a composite material during the molding of pre-coated with nanofiller particles polymer granules [52].

In order to minimize the movement of nanoparticles in the melt, it is necessary to select a material that would possess very high melt viscosity, thereby preventing any significant movement of the nanoparticles into the polymer volume during hot pressing. Lately, UHMWPE, which is not capable of flowing at temperatures above the melting point of polyethylene, has been increasingly used as such material for the production of composites. In the view of that, a lot of research was conducted demonstrating that, in the case of a combination of UHMWPE/nanosized filler, a very small amount of nanoparticles is required to achieve the percolation threshold in samples obtained by coating UHMWPE granules with nanoparticles, which is followed by hot pressing [53,59–62]

However, for a model type of study of segregated structures, the most effective way to implement a combination of high deformability of the polymer matrix and a minimum filler content is the method of dry mixing of finely dispersed components (matrix polymer - functional filler) followed by solid-phase molding of the composite [63].

UHMWPE can be used as a matrix polymer in the form of a highly dispersed UHMWPE reactor powder with a special morphology that is capable of solid-phase processing into high-strength high-modulus film filaments and fibers [63]. Such approach allows reaching a minimum value close to the limiting value for the filler concentration

required for percolation and the highest possible local concentration thereof, due to the fact that during solid-state (at room temperature) molding, the filler does not have the ability to go into the polymer volume during the composite molding process, providing thus, the conductivity is  $\sim 2$  orders of magnitude higher than for the same filler concentrations in the case of composites with UHMWPE obtained by hot pressing [19].

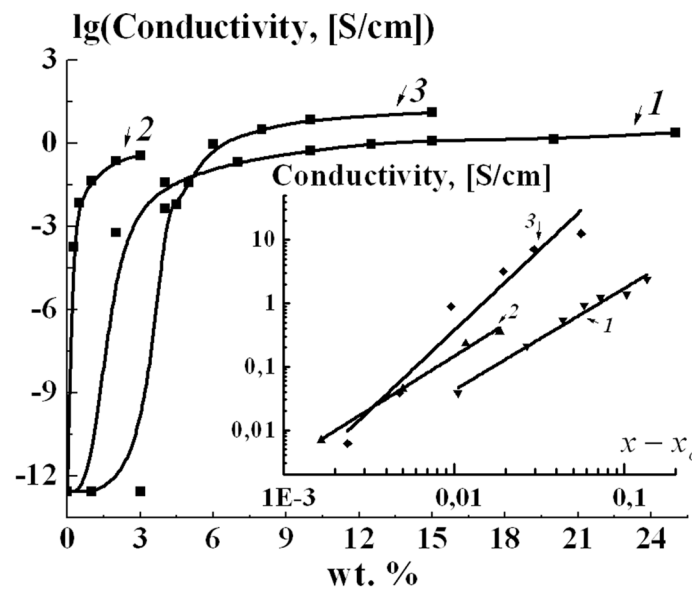


Figure 2. Conductivity of solid-state processed composites based on UHMWPE filled with CB (1), MWCNTs (2), and GNP (3) as a function of the filler mass fraction [19].

The inset illustrates fitting of the data with the percolation equation.

The above examples show that composites with a segregated structure are of undoubted practical and scientific interest, as a result of which the development of scientific research in the field of new methods and techniques for their design, optimization of functional properties and a complex of their characteristics seems to be very relevant.

The literature review on this subject demonstrates that no multiscale models have been developed to date for the discussion of functional polymer composite materials with a segregated structure of the filler, which allow one to evaluate the characteristics of the material considering the structure of the composite, filler realistic representation and its concentration. Systematic studies in the area on composites with segregated structure on a wide range of subjects will be important for the development of this field of knowledge and related scientific disciplines. These subjects may be: identification of structural and functional dependencies between the quantity, size, degree of dispersion, surface functionalization and surface structure of conductive nanoparticles introduced into the system; corresponding changes in the physicochemical characteristics of multicomponent polymer systems; correlation dependencies electrical conductivity-deformation for the model range of polymer/conductive nanofiller systems.

Among the works in the field of modeling composites with a segregated filler structure, one can note, for example, an attempt by the team of authors to construct a mathematical model of segregation of nanofibers in a solvent between densely packed emulsion particles using the Monte Carlo method [64]. The authors of this work calculated the conductivity of the calculated volume for several values of the diameter of nanofibers depending on the concentration of nanofibers, for which was used the classical power law of the change in conductivity with a change in concentration during percolation.

In a number of other works, attempts were made to interpret the experimental dependences obtained for changing the electrical conductivity of a composite material with a change in the nanofiller concentration using semiempirical models. For example, in the

paper [65], an analytical model was proposed that relates the conductivity of a material having a double percolation structure formed by a filler pre-mixed with PE during its subsequent dispersion in PP at a temperature below the melting point of PP, with a filler concentration, and with the distribution of the filler between the two phases of PP and PE. The developed model took into account the mutual solubility of each of the components. The classical percolation theory was used to interpret the results.

A large number of works conducted was simply limited by observation of percolation network formation in segregated structures obtained for different systems from polymer matrices and fillers, as was done, for example, in [53,66,67]

The problem of multiscale modeling of the dependence of the electrical conductivity of a material on its deformation has not been seriously investigated for composites with a segregated structure. For systems with a uniform distribution of nanoparticles in the matrix, several works can be noted that describe attempts to numerically simulate relatively small uniaxial strains of nanotube-filled composites [22,24,68]. There are also several examples of studies that offer semi-empirical models of the deformation of composites filled with nanoparticles with a uniform distribution in the volume of the composite [69,70]. In view of the that, it is safe to say that the important task has not yet been resolved on the following subject: conducting multiscale modeling, comparing the results with experimental data, and ultimately obtaining a workable model that allows us to describe the characteristics of a material with a segregated structure of nanoparticles depending on the degree and type of segregation, concentration and type of

filler, as well as to assess the change in the electrical conductivity of such a material during its deformation.

## **2.2. Non-destructive Testing of Electroconductive Polymer Composites**

Over the years, a large number of various systems have been developed aimed at monitoring the state of structural parts used, for example, in the aerospace industry [71], energy industry [72], or various elements of civilian infrastructure [73]. So, for example, the optical fibers built into the system allow you to measure the change in the intensity or frequency of the reflected light from the loaded material depending on the applied load. Unfortunately, such fibers easily break during operation, violating the integrity of the detection system, and also act as stress concentrators, increasing the likelihood of defects [74]. Therefore, non-invasive methods of control, such as thermography, ultrasound and acoustic emission, are particularly popular today [75]. On the other hand, the use of thermography and ultrasound to control the deformation or integrity of the composite material suggests the presence of a complex exciter-receiver system, as well as a sufficiently strong constant effect on the structure, which otherwise could easily be noisy by environmental factors. In the case of thermography, the causative agent is a heat flux source that should give a fairly uniform heating of the material, which is not always possible due to changes in the ambient temperature conditions, as well as the complexity of the design form. At the same time, the receiver is a thermographic camera (thermal imager) - rather expensive equipment if high sensitivity to temperature changes is necessary (which is necessary if the heat flux is created as small as possible). When using

ultrasound, a vibrator (emitter) and a detector are required. In order not to affect the operational characteristics of the structure, the power of ultrasonic emission should be minimal, but at the same time stand out against the background noise created by the interaction of the material with the environment. Therefore, detectors are usually used quite nontrivial and expensive.

In order to overcome the above-mentioned limitations, systems have been more and more actively developed lately that could provide an ability to control one's state due to the features inherent in the material itself and its structure. Such a system can be obtained by creating an electrically conductive grid in a dielectric polymer matrix. To date, some similar systems have been studied, for example, using CNTs as a filler for a polymer material, which may be, for example, epoxy [76,77]. CNTs are of particular interest due to their exceptional physicochemical and electrical properties [78]. [79] shows the effect of nanotubes on the electrical properties of the composite, when only 0.1 vol.% was used to modify the dielectric polymer matrix to obtain noticeable electrophysical characteristics. Later on, a more detailed analysis of composite systems was also carried out, in which CNTs successfully acted as sensors allowing correlation of mechanical and electrical properties [80]. An experimental analysis of the effect of cyclic loads on multifunctional systems was carried out by [81], where it was shown that carbon nanotubes are able to form a highly sensitive structure in the polymer volume that can respond to various types of damage during operation of the composite material as a whole. Graphene nanoplates have also been successfully used as a filler to impart conductive properties to a dielectric matrix in [82], providing better mechanical properties compared with those for systems where

CNTs were used as filler, but at high cost for filler to form a conductive network. In work [83] the authors proposed an experimental approach for measuring deformations by compiling a conductivity map in the sample, obtaining more detailed information about the location and type of defect compared to the usual measurement of voltage changes. However, this approach implies connecting a complex system of sensors to the material, the number of which determines the resolution of the maps, and this is not always appropriate during operation. At present, Russia has a team of scientists involved in the modeling of polymer composites [84]. However, often their approach is based on the molecular dynamics method, thereby not allowing to describe all possible levels of the material structure and limiting the possibility of studying its macroscopic properties and their mutual correlation.

All of the above studies focus mainly on experimental analysis or numerical analysis at only one scale, without developing models that can take into account the multiscale nature of such a complex object as a multifunctional composite. In this regard, the goal of this project is to solve the fundamental problem in the field of development and creation of multifunctional composite materials, which consists in constructing a numerical model that will be based on experimental studies and will describe the properties of the composite material, taking into account its structure and the correlation of its electrical properties with the value and the type of strain applied.

## Chapter 3. Materials and Methods

### 3.1. Experimental Part

#### 3.1.1. Materials

As one of the model fillers, the Nanocyl™ NC 7000 type MWCNTs were used in this work [85]. The specification of the MWCNTs is presented in Table 1. The morphology of the filler is shown in Figure 3. The choice of NC 7000 MWCNTs as a model filler was due to the narrow distribution of their diameter and size, as well as their high purity and affordable price. The MWCNTs of choice are also characterized by low degree of entanglement, which is a significant issue for commercially available SWCNTs, some of which are known to be grown in bundles [86].

Table 1. Specification of the MWCNTs Nanocyl™ NC 7000 [85].

Parameter	Method of testing	Value
Specific area, m <sup>2</sup> /g	BET	250-300
Purity, %	TGA	90
Average diameter, nm	SEM	9.5
Average length, nm	SEM	1500
Metal content, %	Inductively coupled plasma mass spectrometry	<1
Resistivity, Ohm·cm	Powder conductivity measurements	10 <sup>-4</sup>

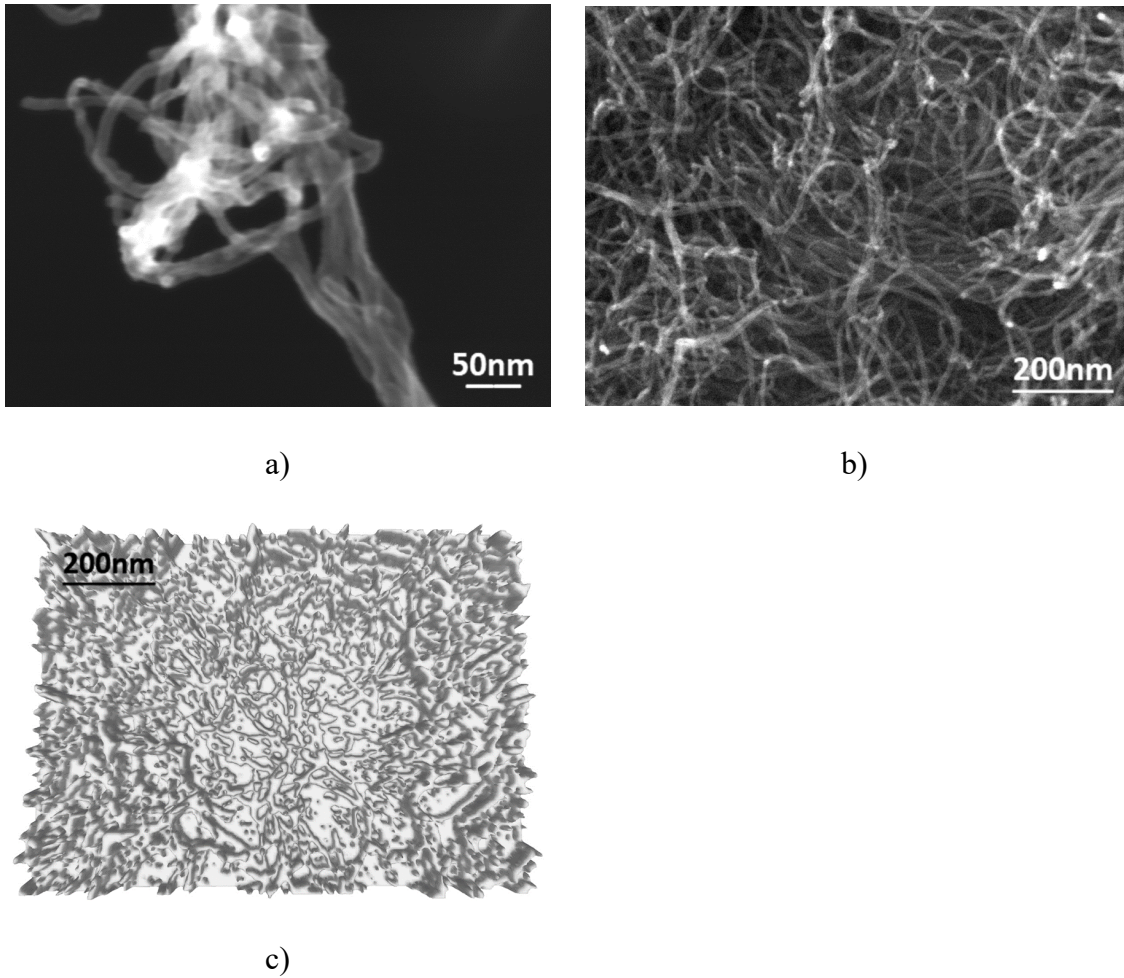


Figure 3. Scanning electron microscopy images of the MWCNTs used in this work: (a) in a free state, (b) on a plane surface, and (c) 3D representation of the (b), required for estimation of MWCNT volume fraction in the conductive layer.

In contrast to MWCNTs, characterized by high aspect ratio, CB particles were used as another model filler, as they can be considered as isometric and spherical. Particularly, commercially available P267E type CB was used [87], specification of which is presented

in Table 2. The morphologies of the MWCNTs and CB particles, obtained using transmission electron microscopy are shown in Figure 4.

Table 2. Specification of the CB P267E [87].

Parameter	Method of testing	Value
Specific area, $\text{m}^2/\text{g}$	ASTM D3765	144
Iodine number, $\text{g}/\text{kg}$	ASTM D 1510	226
DBP absorption, $\text{cm}^3/100\text{g}$	ASTM D 2414	165
Humidity, %	ASTM D1509	0,5
Ash content, %	ASTM D1506	0.27
Mass fraction of sulfur, %	ASTM D1619	0.38
Sieve 0.045 residue, wt. %	ASTM D1514	0.0005
Bulk density, $\text{kg}/\text{m}^3$	ASTM D1513	230
Dust content, %	ASTM D1508	5.0
Resistivity (bulk density $0.5 \text{ g}/\text{cm}^3$ ), $\text{Ohm}\cdot\text{m}$	-	$2\cdot 10^{-3}$

Construction class woven glass fabric (T26, Comfiber) with areal weight of 285  $\text{g}/\text{m}^2$  was used as the additional composite reinforcement.

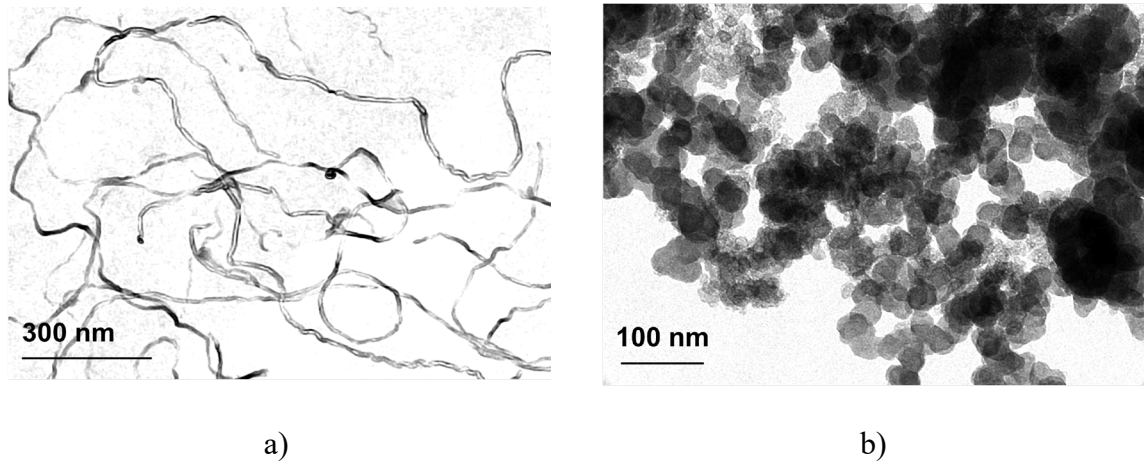


Figure 4. Electron microscopy images of the nanofillers used in this work: MWCNTs (a) and CB (b).

UHMWPE nascent reactor powder with a special nodular morphological structure [63] was used as a matrix for the composites (MM weight  $5 \cdot 10^6$ , bulk density of the reactor powder  $0.058 \text{ g/cm}^3$ ).

Commercial grade of PP (H030 GP, manufactured by Tobolsk-Polymer LLC) distributed in a pellet form [88] was used as the matrix material for nanocomposites. The specification of the H030 GP PP is presented in Table 3.

Table 3. Specification of the PP H030 GP [88].

Parameter	Method of testing	Value
Melt flow rate, g/10 min	ASTM D1238	3.0
Tensile yield strength, MPa	ASTM D638	30
Yield elongation, %	ASTMD638	8
Flexural modulus, MPa	ASTM D790	1300
Izod impact strength, kJ/m <sup>2</sup>	ASTM D 256	2.5
Vicat softening point, °C	ASTM D1525	155
Bending under load temperature, °C	ASTMD 648	70÷120

### 3.1.2. Methods

The electron microscopy studies of the filler powders morphology were performed using HITACHI SU8000 electron microscope.

To test the electrical conductance response of MWCNTs layer to uniaxial deformation, several specimens were prepared using the following technique: two commercially available rectangular polytetrafluoroethylene (PTFE) plates of 50\*12\*3 mm were polished with fine sandpaper, followed by deposition of MWCNTs on the surface of one of the plates from a suspension in hexane (Figure 3b), forming a ~10 µm thick layer. The MWCNTs particles were deposited on the PTFE plate surface in the amount calculated from the layer dimensions and volume fraction of MWCNTs within the layer, using the following formula:

$$w = V \cdot \frac{\rho_f}{v_f} \quad (1)$$

where  $w$  is the weight of filler,  $V$  is the volume of the layer,  $v_f$  is the volume fraction of filler within the layer, and  $\rho_f$  is the density of filler [22]. The volume fraction of filler within the conductive layer (55 %), used in calculations, was evaluated using image processing results of electron microscopy (Figure 3c).

The pieces of 10  $\mu\text{m}$  thick aluminum foil were put at the ends of the second plate at the distance between them of 10 mm, with thin copper wires glued down to each foil piece. Two plates were then pressed together and fixed in the grips of a testing machine (Figure 5). Resistance of such specimens in undeformed state constituted  $\sim 5$  kOhm.

Deformation of the specimens was performed at room temperature, using Instron 5969 dual column testing system in a strain mode with a nominal strain rate of  $0.1 \text{ min}^{-1}$ . The base of specimens constituted 10 mm.

Electrical conductance of specimens during deformation was determined with 34401A multimeter (Agilent) using four-probe resistance measurement methods. Current was applied in a cross-wise manner from two sides of a sample, while electrical voltage was measured in a opposite manner.

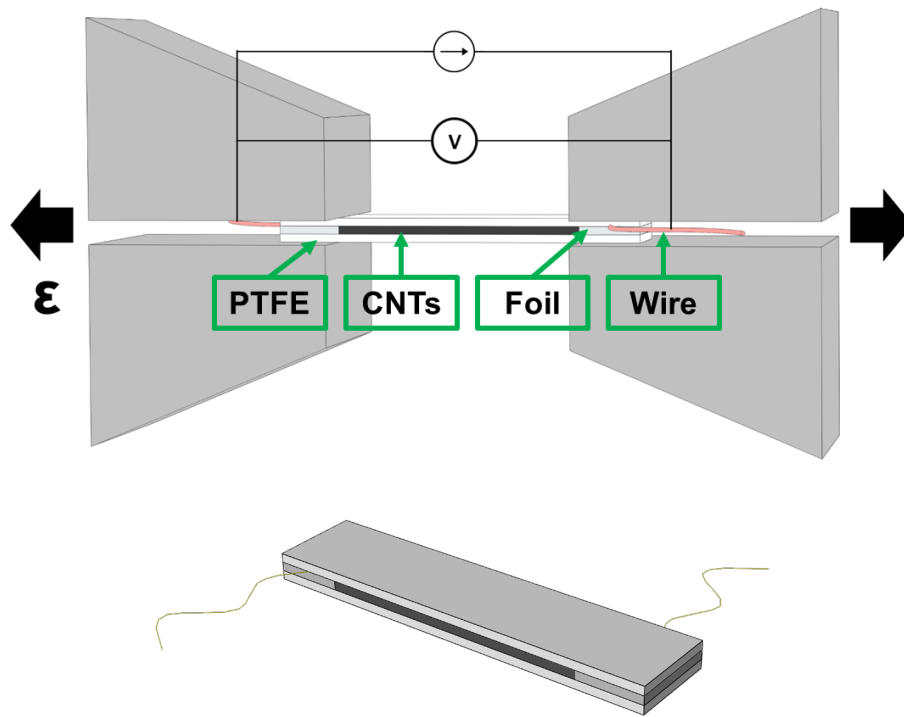


Figure 5. Conductance measurement scheme used in the experiments. PTFE: polytetrafluoroethylene; CNT: carbon nanotubes.

At the next stage, samples of composite materials with a segregated structure of nanoscale filler were manufactured. UHMWPE nascent reactor powder with a special nodular morphological structure [63] was used as a matrix for the composites (MM weight  $5 \cdot 10^6$ , bulk density of the reactor powder  $0.058 \text{ g/cm}^3$ ). Nanocyl NC7000 MWCNTs were used as the filler. The components were mixed in a non-solvent volatile liquid (hexane) using a CUD-500 ultrasonic disperser from Criamid, Russia (5–10 min, 250 W, 30 kHz). Such melt-free mechanical method allows to obtain materials with a lower percolation threshold compared to other mixing methods, because the filler is not distributed evenly in the polymer's volume, but covers the polymer particles with a thin layer, thereby forming

a segregated conductive network. The uniformity of the distribution of nanoparticles on the surface of the granules of the UHMWPE reactor powder was evaluated using a HITACHI SU8000 electron microscope. The results of microscopy showed the presence of areas uncovered by nanoparticles on the surface of the UHMWPE reactor powder. Subsequent compactification of this mixture at room temperature (20°C) in a closed mold under pressure of 200 MPa produced the initial plates of composite materials with dimensions 50×12×0.5 mm. The distribution of nanoparticles in the compacted composite samples was also studied by electron microscopy. The microscopy demonstrated a denser coating of surface of UHMWPE granules with MWCNTs, which was attributed to reduction of UHMWPE particles volume after compaction (~ 20 times). Electrical conductivity of composite samples with various concentrations of MWCNTs measured and percolation thresholds were estimated. The electrical conductivity of the formed composite plates was measured using the four-probe resistance measurement method and an Agilent 34401A multimeter. The results obtained — the percolation threshold is several times lower than that predicted by the classical percolation theory (~0.1 vol% against >0.4 vol.%) — indicated the formation of a segregated structure from the filler in the composite, regardless of its type. For subsequent tests, samples were used with a concentration of fillers known to be higher than the percolation threshold determined for them.

A series of samples of composites containing MWCNTs in various quantities was also subjected to repeated pressing in a heated mold under a pressure of 200 MPa and a mold temperature of 160°C for 5 minutes. The samples thus obtained had 2 orders of magnitude lower conductivity compared to composites based on UHMWPE, obtained

without a stage of processing through the melt. This effect is due to the fact that although UHMWPE does not have the ability to flow in a melted state due to its extremely high viscosity, there is possibility of penetration to a certain depth for MWCNT particles. It is also possible for polymer melt to get into the contact zone between the nanoparticles. This leads to a decrease in the density of the layer of nanoparticles and the number of contacts between them, which, in turn, leads to a decrease in the electrical conductivity of the composite sample as a whole.

To study the deformation behavior of the electrical conductivity of composites, the Instron 5969 test complex was used in tension mode with a nominal strain rate of  $0.1 \text{ min}^{-1}$ . The base of the samples was 10 mm. Samples at the ends were wrapped in thin copper foil, which, in turn, was insulated from the clamps of the testing machine with fine-grained sandpaper. During the deformation, a voltage of 2 V was supplied to the foil by the AKIP 1147/1 power source, while using an ADC with a frequency of 100 Hz, the value of the electric current passing through the sample and measured by a Keithley 6485E picoammeter was recorded. The obtained values of the electric current were converted into the value of the relative electrical conductivity — the ratio of the value of the electrical conductivity in the deformed state to the value corresponding to the electrical conductivity of the undeformed sample.

Mixture of the components in a melted state was obtained using DACA twin-screw microcompounder. Deformation of the samples was performed using the 5969 Dual Column Testing System (Instron) in a stretching mode at room temperature, with a nominal

strain rate of  $0.1 \text{ min}^{-1}$ . Strain was controlled using the in-built sensors of the Instron 5969 and stress values were calculated using initial cross section of a sample.

Distance between grips of the testing machine was set as 20 mm, which was also the distance between electrodes. As electrode a layer of thin ( $\sim 100 \text{ }\mu\text{m}$ ) copper wires was used due to high roughness of such electrode type. The electrodes were dipped in a silver paste and isolated from the grips by pieces of sandpaper, which additionally helped to prevent slippage of a sample. Electrical conductance of the samples in the course of deformation was determined with 34401A multimeter (Agilent) using four-probe resistance measurement methods.

The electron microscopy studies were performed using Supra 50 VP LEO electron microscope with INCA Energy+ Oxford microanalysis system and Hitachi SU8000 scanning electron microscope. The specimens were prepared via freeze fracturing of the test samples at the liquid nitrogen temperature.

To obtain the composite material, dry mixture of the filler powder and PP pellets in desired proportion was initially prepared. At the next step, it was melted and compounded using twin-screw compounder for 10 minutes at  $200 \text{ }^\circ\text{C}$  and the rotation speed of screws of 500 rpm. After the mixing procedure was completed, the composite material in a strand form was cut into small pieces and molded for 1 min in a closed mold at  $200 \text{ }^\circ\text{C}$  and 20 atm following by instant cooling in cold water to obtain strips of 1.2 mm thickness, width of 12 mm and length of 100 mm. The resulting distributions of the filler for each filler type and concentration are presented in Figure 6.

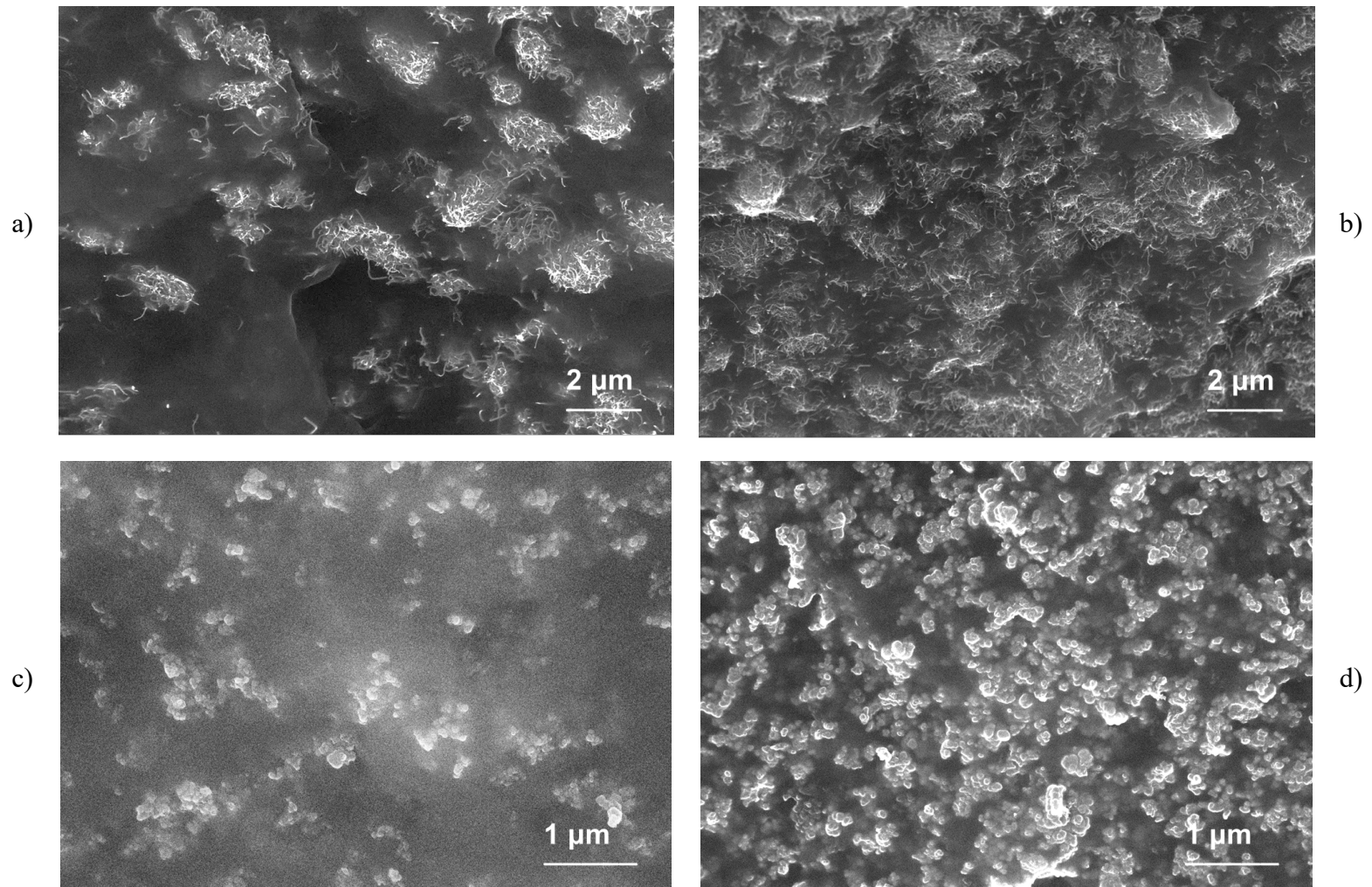
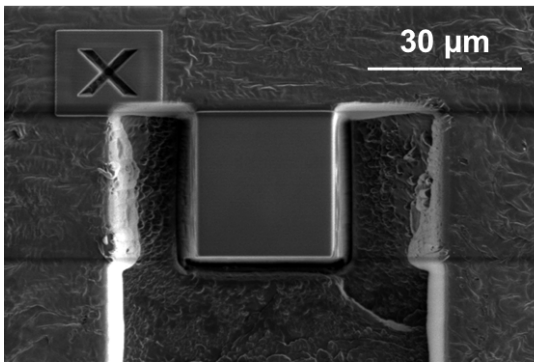


Figure 6. Distribution of MWCNTs in the PP matrix for concentration of the filler 7.5 wt.% (a) and 15 wt.% (b), and CB in PP for its concentration of 15 wt.% (c) and 30 wt.% (d) obtained with electron microscopy of the composite fracture surface.

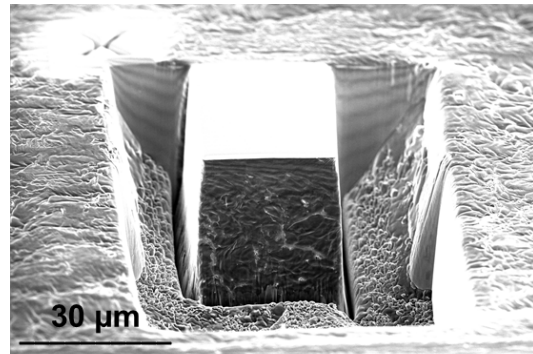
As it can be seen from the microscopy images, both MWCNTs (Figure 6a,b) and CB (Figure 6c,d) are present in the PP in a highly agglomerated state. It was noted that a size of the agglomerates is not highly dependent on the filler concentration, so for the future analysis it was assumed that increase in concentration can lead only to an increase of number of agglomerates in the composite volume. Of course, this assumption may be valid for concentrations of filler above percolation threshold that were investigated in this work.

To assure that contacts between particles in PP-based composites are Ohmic, current-voltage dependencies was measured for samples PP + 7.5 wt.% MWCNTs and PP + 25 wt.% CB in a range of voltages 1 – 10 V. It was observed that the dependencies have character very close to linear, proving that the contacts can be considered as Ohmic.

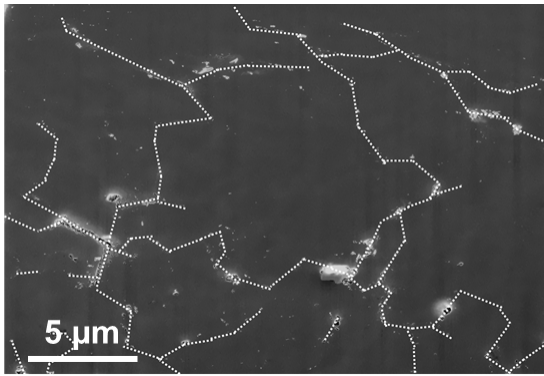
The compacted UHMWPE + 2 wt.% MWCNTs composite samples were studied using Helios NanoLab 660 electron microscope layer by layer using focused ion beam etching with a layer spacing of 100 nm and a photographic region of 20×25 microns (Figure 7a,b). The final number of images (layers) was 290.



a)



b)



c)

Figure 7. (a, b) - Electron microscopy images of the investigated with focused ion beam scanning electron microscopy volume of composite UHMWPE + 2 wt.% MWCNTs and (c) - one of the resulting slice images with artificially reconstructed distribution of highly-filled MWCNTs areas (dotted white line).

PP was filled with carbon nanoparticles using a commonly applied melt mixing procedure at 200°C. The volume fractions of MWCNTs and CB were chosen to be 4.75% and 10% respectively. Next, the obtained composite strands were cut into small pellets and

pressed at 3MPa into rectangular plates (10×50×2mm) for the measurements of electrical conductance response of modified polymer to its uniaxial deformation.

Modified PP matrix was reinforced with glass fibers using a multi-step procedure. At the first step the pellets were repressed into small circular plates of ~ 600 μm thickness and diameter of 2 cm. After that, each individual layer of textile was placed between two circular composite plates obtained earlier and hot pressed at 200°C and pressure of 5 MPa. To avoid fabric deformation the pressure was applied gradually. Such resulting impregnated with modified PP material layers were characterized by thickness of ~250 μm and diameter of ~7 cm. Then, not impregnated fabric was cut off from the sides of the specimens. Four of such newly obtained layers were stacked together and hot pressed again at the same conditions as used before, resulting in a sandwiched structure with thickness of ~900 μm. The layers stacking was done in a 0-90 manner to ensure isotropy of electrical conductivity of the composite material in the fabric plane. To study the influence of the number of layers on the investigated effect, GFRNC samples were made including 2, 4, and 6 layers of fiberglass for each type of filler. From the measurements of weight of the obtained samples and considering the glass fiber fabric areal weight, it was concluded that the volume fraction of glass fibers could be estimated as ~50%. Results of the electron microscopy for the obtained GFRNC sample cross-section are presented in Figure 8. It can be seen that polymer has successfully impregnated space between glass fiber tows (Figure 8a), as well as space between separate glass fibers (Figure 8b) in the course of the manufacturing process.

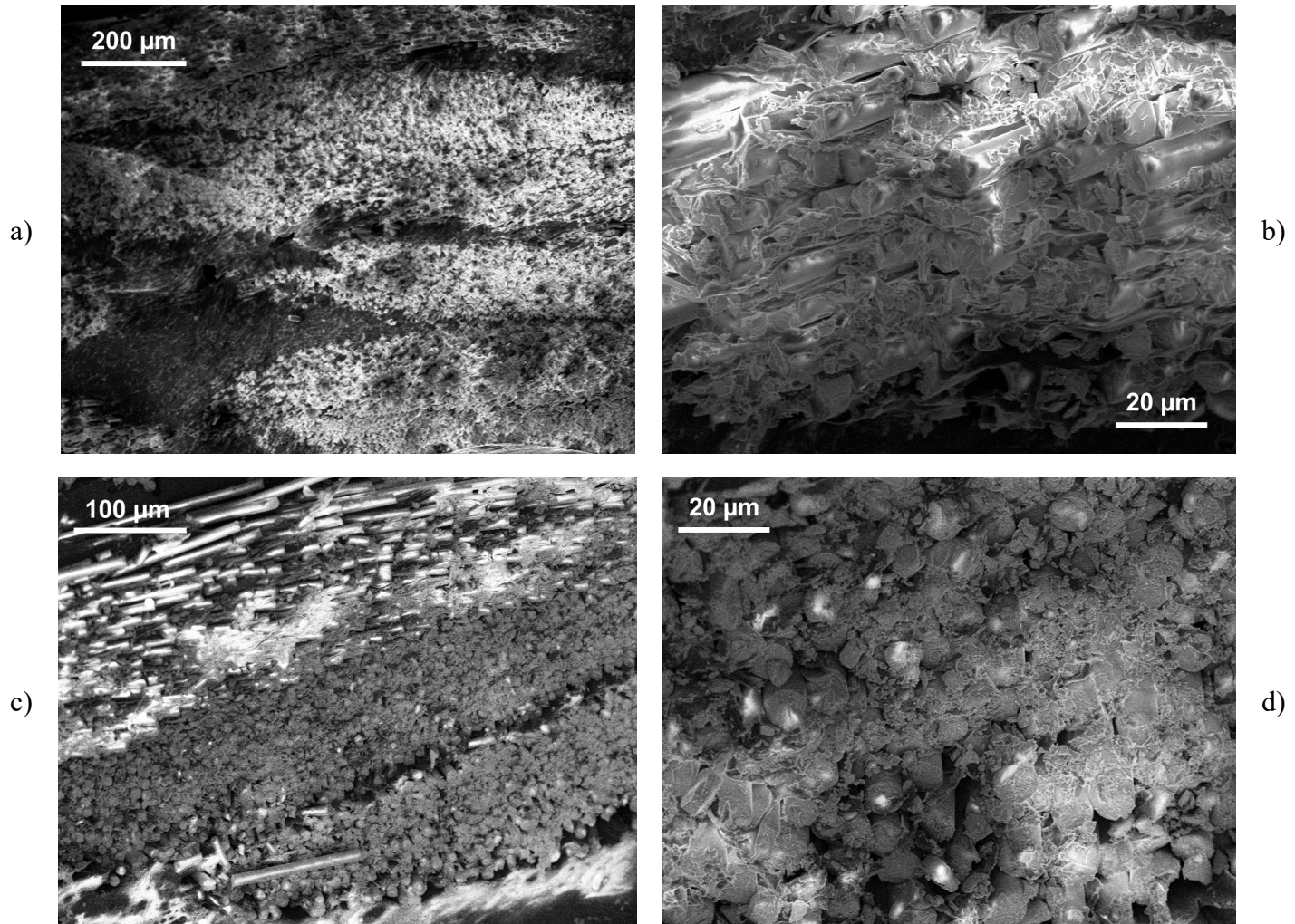


Figure 8. Electron microscopy of the obtained PP-based composite filled with 50% of glass fibers and 2.375 vol.% of MWCNTs (a) and 50% of glass fibers and 5 vol.% of CB (b) at different scales.

Uniaxial tensile deformation of the specimens was performed using the 5969 Dual Column Testing System (Instron) at room temperature, with a strain rate of 0.01 mm/min. The distance between grips of the testing machine was set to 10 mm as well as the distance between electrodes. As an electrode a layer of thin ( $\sim 50 \mu\text{m}$ ) copper wires was used. The electrodes were dipped in a silver paste and isolated from the grips by pieces of sandpaper.

## **3.2. Numerical part**

### *3.2.1. Modeling of thin MWCNTs layer*

The simplest representation of the conductive layer located between two plates, as it was used in the experimental study, is as filler particles uniformly dispersed in a rectangular parallelepiped with one dimension limited by the supposed thickness of the segregated conductive layer.

In this work, nanotubes were represented as chains of two-node 3D truss segments, characterized by the ability to freely rotate around the joints between the elements. A similar approach was successfully implemented earlier for percolation threshold calculation for wavy nanotubes [27,89]. Number of elements (segments) in a single MWCNT was determined by dividing the MWCNT length ( $1.5 \mu\text{m}$  in this work) by the equivalent of the statistical (Kuhn) length for a nanotube, the value of which ( $\sim 250\text{--}500 \text{ nm}$ ) was estimated using literature data [35] and results of electron microscopy. In this work the value of statistical length of  $375 \text{ nm}$  was used. Assumption was made that joints with free rotation at the ends of Kuhn segments should be used in numerical simulations of CNT-based nanocomposites. Indeed, this hypothesis is based on studies [35]

demonstrating that at the lengths exceeding the statistical length CNTs can deform without application of external loading.

To imitate periodical boundary conditions for MWCNTs network conductance calculations, a special type of volume element was constructed (Figure 9). First, the initial (one of the ends) points of the future MWCNTs were distributed uniformly in  $0.1 \times 5 \times 5 \mu\text{m}$  volume. Number of MWCNTs was chosen according to the volume fraction of the filler in the conductive layer (55 %), obtained experimentally (see section 3.2.1). The layer thickness of 100 nm was taken from the thickness of conductive layer formed around UHMWPE grains in solid-state processed UHMWPE/MWCNTs composites with ~1% volume fraction of the filler.

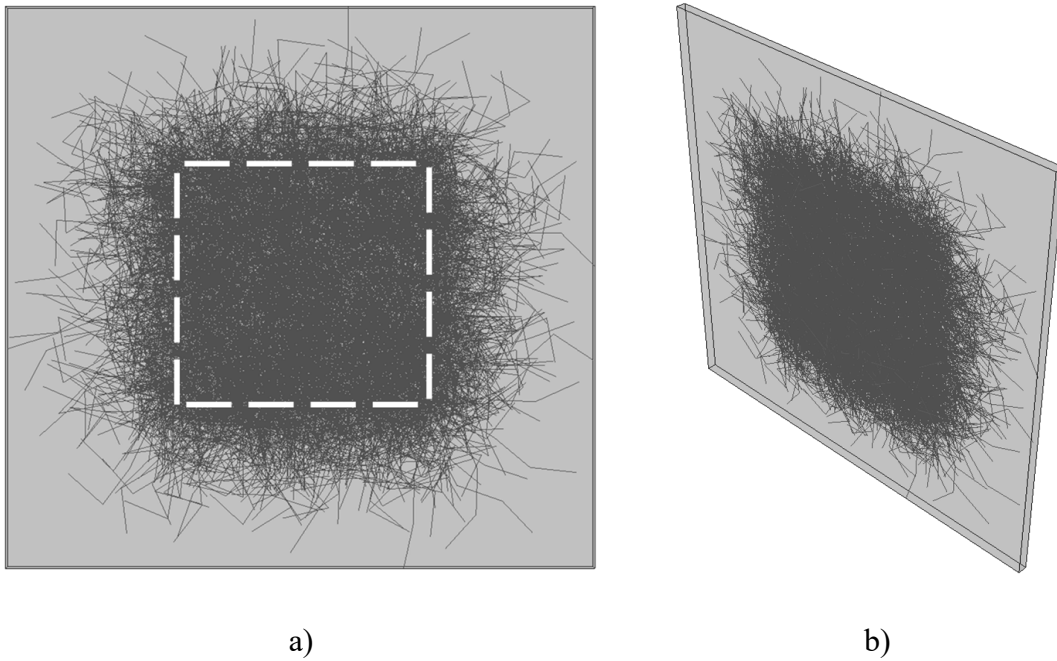


Figure 9. (a) Volume element constructed for deformation tests and conductance calculations with imitated periodic boundary conditions, where the white dashed square contours the investigated sub-volume (“inner” volume), to which the deformation was applied and conductance of which was calculated later; and (b) side view of the volume element. MWCNT: multi-walled carbon nanotube.

From each initial point, MWCNTs were “grown” following a simple procedure: at the distance from the initial point corresponding to the statistical length, and at a random angle, a next point was created, forming a segment of the MWCNT. A finite element (FE) was created spanning this distance with the free rotation joint at its end. Then the process was repeated with the previously created joint serving as a new reference point, generating the next MWCNT segment, and so on. Similar idea was illustrated earlier [89], however,

used in this work approach is different in that no limit on the angle between the MWCNTs segments and allow mutual penetration of MWCNTs was set. The coordinates of new points are limited by the dimensions of selected volume so that MWCNTs are deflected inwards by the edges of the created MWCNT layer.

For correct representation of the experimentally investigated layer the confinement of MWCNTs is allowed only in the thickness direction. To eliminate deflection of MWCNTs from the edges of the created MWCNT layer in the plane perpendicular to the thickness direction, only the “inner” part of the layer was studied. All MWCNTs not crossing the “inner”  $0.1 \times 2 \times 2 \mu\text{m}$  volume (shown with the white dashed line in Fig. 3a) located in the center of the layer were removed. All MWCNTs crossing the “inner” volume were kept, even those with their segments lying outside of the “inner” volume. This allowed us to imitate periodic boundary conditions for conductance for the ‘inner’ volume as is shown in Figure 9a,b. Electrical conductance of the “inner” volume was calculated later. The reason for not using the representative volume element obtained by truncation of the initial to the boundaries of the ‘inner’ volume is because in that case some MWCNTs segments cut by the new boundaries would have lengths shorter than the statistical length. Presence of the segments of different lengths can result in unpredictable outcomes (see section 3.3) and, therefore, is undesirable. At the same time, periodic boundary conditions cannot be created for the truncated volume due to the specifics of the meshing method selected in this work — the embedded element method — that eliminates all the MWCNTs elements’ degrees of freedom.

Principle scheme of the embedded element technique is depicted in Figure 10. The main idea behind this technique is creation of two separate independent meshes – for matrix (“host”) and for the filler (“embedded”). Nodes of embedded elements that lie within host elements have their translational degrees of freedom being eliminated (constrained to the interpolated values of the corresponding degrees of freedom of the host elements). Thus, these nodes become the “embedded” nodes. Rotational degrees of freedom of the embedded elements are not constrained by the embedding, if the elements have them initially (for example, beam elements). Since truss elements that were used for MWCNTs meshing do not initially have rotational degrees of freedom it is impossible to add any additional constraints on their nodes after the embedding.

The embedding element technique can be considered very computationally effective for volume elements with high level of filling with small particles due to independency of the host and embedded meshes. That allows to control number of FEs freely, providing that the final meshing can ensure reliable results. Compared to the continuous meshing technique that assumes fine meshing near the filler elements - the total amount of elements (matrix plus filler) becomes very high (tens of millions) - the embedded element method can decrease number of required elements by several orders of magnitude [31,32], which can accelerate calculation time drastically.

It is worth noticing that the embedded element method accounts for the volume of matrix that should be occupied by the embedded elements, thus making the effect of that volume error to be uncertain. But in opinion of the authors of this work, for conductance calculation these artefacts can be neglected, since all that is important for the set goal

achievement is to find a way to provide homogeneous strain field during the conductance investigation with deformation, which can be done successfully using this method. Also, one of the main drawbacks of this method is that the embedded elements can interact only through matrix, so mutual penetration and passing through of the filler elements is possible.

The method was implemented earlier successfully for two-dimensional case of MWCNTs filled polymer volume for mechanical and conductive properties characterization of the composite [90]. It was also demonstrated [31,32] that embedded element method can provide interesting results for 3D stresses field calculations in composite materials filled with MWCNTs, which can be very close to the results obtained using continuous meshing technique. Although, the way of MWCNT representation used – hollow tubes meshed with shell elements with isotropic mechanical properties - might not be suitable for high degrees of deformations. This is so due to the specific type of MWCNTs behavior with deformation. Although they do theoretically possess very high tensile and bending strength, which was also demonstrated experimentally [34], the number of defects accumulated on certain length allow them to easily assume very complex shapes, such as statistical coils, for example, if to leave them suspended in a solution [35]. But if to try to deform them in isotropic matrix with mechanical characteristics, such as elastic modulus, values of which are much lower than such for the MWCNTs, the isotropic behavior of MWCNT properties will lead to inability to deform a particle at all and it will stay in the same coiled form. If to implement boundary conditions that will force high stresses on MWCNTs through the matrix, then their deformation will be linear and instead of changing conformation it will be simple stretching of the MWCNTs elements in the

direction of the deformation applied. This was tested on few distributes randomly MWCNTs in a small volume with Poisson effect-forcing boundary conditions used for the second test. The results of these tests demonstrated unreliability of this approach if to consider implementation of relatively large deformation degrees to the composite volume for such method of CNT representation and meshing.

The resulting distribution of MWCNTs segments was imported to SIMULIA Abaqus<sup>TM</sup> FEA software suite. Two-node 3D truss element (T3D2) mesh was created for the MWCNTs distribution, with cross section area calculated from the Nanocyl NC7000 MWCNTs parameters. The following properties were assumed for matrix and MWCNT materials respectively: elastic modulus of 100 MPa and 1000 GPa (data taken from the MWCNTs NC7000 specifications), and Poisson coefficient of 0.46 and 0.3 [91]. Elastic modulus of matrix is assumed to be equal to that of PTFE (~500 MPa) used in the experiment as the substrate, containing certain number of pores. Since contrast between the matrix and the MWCNTs mechanical properties is very high, the precise value of matrix elastic modulus was considered to be irrelevant.

Matrix mesh was generated using equally sized eight-node cubic elements (C3D8, edge size 20 nm) for the volume surrounding MWCNTs in Figure 9. After that the MWCNTs mesh was embedded in the matrix mesh.

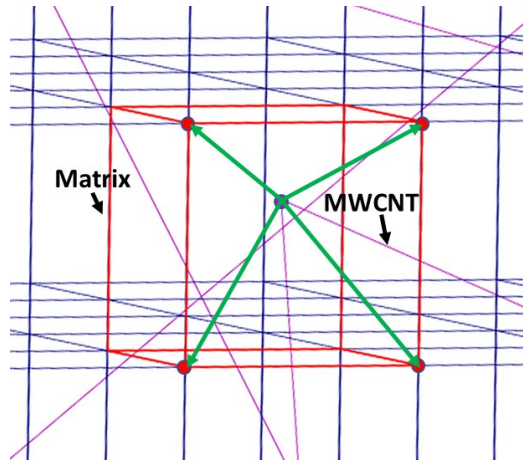


Figure 10. Close-up view of finite element mesh used in simulations, where blue and red color indicate edges of the matrix cubic elements, and purple indicates truss elements representing the MWCNT segments (dashed arrows symbolize constrains of the MWCNT node by the matrix nodes that are created during the embedding). MWCNT: multi-walled carbon nanotube.

Tensile displacement (Figure 11) was applied to the planes coplanar with the upper and lower faces of the inner volume (white dotted lines in Figure 11). In the course of deformation, the coordinates of all MWCNTs nodes were recorded.

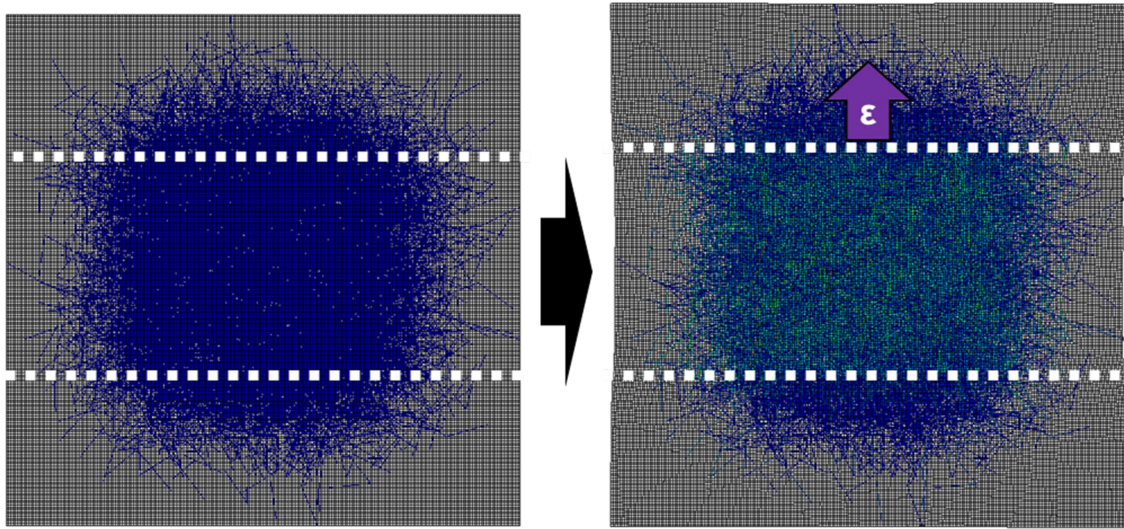


Figure 11. Scheme of deformation application used in the model for the investigated volume (additional colors on the right image illustrate tensile stress distribution in MWCNT elements).

The obtained dataset of MWCNTs nodes coordinates at different moments of deformation was exported for further conductance calculations.

CNTs can display very strong relation between their mechanical deformation and conductivity[92], which can affect the properties of a composite material filled with such particles and subjected to deformation. Molecular mechanics calculations quantifying the CNT band gap change due to mechanical deformation of CNT may be needed to get precise value of conductance of the deformed composite material volume. The processing temperatures can also influence the resulting conductance values. Conductance calculations for CNT-filled composites with regard to the band gap changes for each segment of CNT can be very complex. For simplification, in order to calculate the

conductance of the investigated volume element at a given deformation, the inner resistance of MWCNTs was assumed to be negligible compared to the contact resistance between MWCNTs or between the MWCNT and the electrode [93,94]. The relative conductance (the ratio of conductance for a selected degree of deformation to conductance of non-deformed volume) was obtained using Kirchhoff's circuit laws for the grid of unit contact resistances and unit input and output electrical currents flowing through upper and lower faces of the "inner" volume. The principle of contact grid formation is illustrated in Figure 12. Efficiency of a similar approach for conductance calculations in CNTs networks was demonstrated earlier in several papers [24,26,33,89]. All distances between the MWCNT elements equal or less than two MWCNT radii were considered as contacts. To take into account the tunneling effect, the law of the exponential decrease of contact conductance was implemented with characteristic distance of 0.5 nm [93,94]. The contact between electrodes and MWCNTs is formed if an MWCNT is crossing one of the faces of the "inner" volume to which the deformation is applied (upper or lower). One of MWCNTs (chosen at random) is characterized by zero value of electrical potential. After that all other MWCNTs potentials are calculated using a relation:

$$I_i = Q_{ij}U_j \quad (2)$$

where  $I_i$  is a vector of differences between input and output electrical currents for all MWCNTs and electrodes,  $U_j$  is a vector of electrical potentials (voltages) for all MWCNTs and electrodes, and  $Q_{ij}$  is a matrix of conductance values for all possible MWCNT/MWCNT junctions and for MWCNT/electrode junctions with respect to the

direction of the current flow. The effective conductance of the “inner” volume was calculated as reciprocal voltage difference between the first electrode and the second.

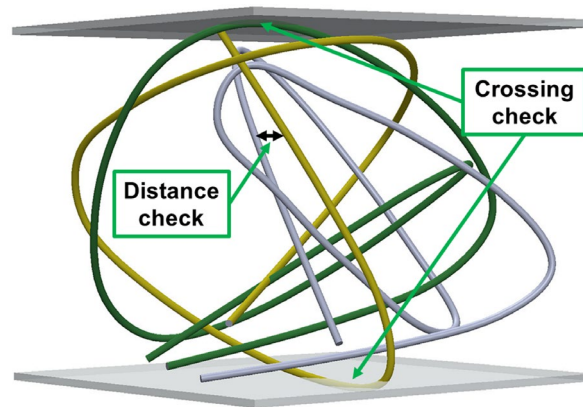


Figure 12. Electrical conductance calculation scheme for MWCNT composite, where yellow MWCNT crosses the plane of the first electrode and the green one crosses the plane of the second electrode.

### 3.2.2. Modeling of PP-based Nanocomposites

#### 3.2.2.1. Distribution Creation

Distributions of the filler were generated in a unique way for each type of the investigated filler based on experimental data. For MWCNTs a special type of volume element was generated (Figure 13), development of which consisted of several stages.

First, using the electron microscopy data (i.e. Figure 6a,b) an average MWCNTs agglomerate was evaluated to be around  $1\mu\text{m}$  in diameter. Next, for numerical simulations it was assumed that the agglomerates are distributed uniformly and periodically such that conductivity of composite material is isotropic. Therefore, overall properties were

calculated from investigation of the volume element consisting of matrix and one agglomerate embedded into it.

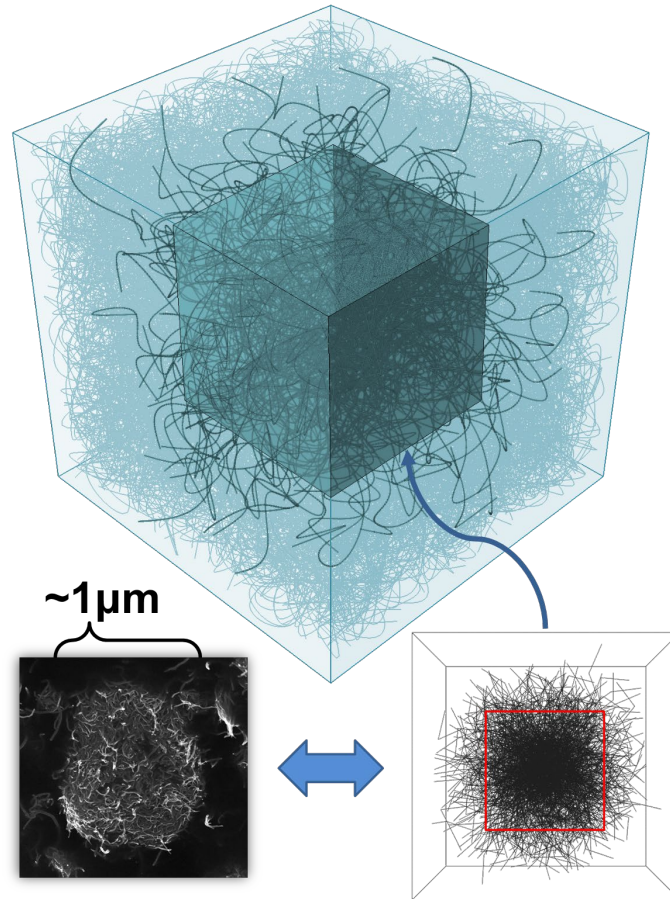


Figure 13. Volume element created using electron microscopy data for numerical simulation of PP-based composites containing 7.5 wt.% of MWCNTs.

To evaluate the volume fraction of agglomerated MWCNTs an 8-bit image depicting a single MWCNTs agglomerate was duplicated several times, so each copy would contain only intensities that correspond to MWCNTs laying in a layer of thickness roughly equal to nanotube diameter (10nm). These images were later converted into the

binary images, with non-zero values of pixels corresponding to the volume occupied by the MWCNTs. From the top layer image, a relation between number of non-zero pixels to the total number of pixels was calculated, which can be used as estimation of volume fraction of the filler in the layer. From each non-top layer images, the similar procedure was performed while accounting partial obscurity of these layers by the higher ones. Averaged value of the MWCNTs volume fractions calculated for different layers was used as an estimation of the volume fraction of MWCNTs in an agglomerate. Consequently, the volume fraction was estimated considering MWCNTs as solid cylindrical objects.

Weight fraction of MWCNTs values ( $\phi_w$ ) used during compounding were used for evaluation of the total volume fraction of MWCNTs ( $\phi_v$ ), assuming that the density of MWCNT wall is 2.1g/cm, number of walls – 10, and thickness of the wall – 0.45nm. The ‘free’ MWCNTs volume fraction ( $\phi_{vf}$ ), as well as volume fraction of MWCNTs in an agglomerate ( $\phi_{va}$ ), were estimated using an assumption that the average agglomerate size is the same for all of the volume fraction of MWCNTs in the composites for the selected range of the MWCNTs weight fraction, so with an increase of the total volume fraction only the average distance between the agglomerates and the volume fractions of “free” and agglomerated MWCNTs are changed. Period dimension values were estimated using the electron microscopy data. This information allowed to evaluate  $\phi_{vf}$  values. Resulting values of total MWCNTs volume fraction, period dimension, volume fraction of “free” and agglomerated MWCNTs corresponding to weight fraction values used in the experimental study are presented in Table 4.

Table 4. Parameters of the simulated MWCNTs distributions in the investigated composite volumes.

$\phi_w, \%$	$\phi_v, \%$	Period, $\mu\text{m}$	$\phi_{vf}, \%$	$\phi_{va}, \%$
7.5	3.5	1.51	0.36	3.14
10	4.74	1.36	0.48	4.26
12.5	6.01	1.25	0.6	5.41
15	7.31	1.17	0.69	6.62

Each nanotube was represented as a chain of one-dimensional segments that can freely rotate around the joint, since nanotubes can assume very complex conformations. Such representation of nanotubes was implemented earlier for evaluation of percolation threshold for nanotube-filled composites by [27,89], and can be related to the concept of statistical (Kuhn) length used widely in polymer physics [95]. The length of the segment of the MWCNTs used in this work was evaluated to be  $\sim 250\text{-}500$  nm using literature data [35] and results of electron microscopy. Particularly, a value of statistical length of 375 nm was used. The maximum angle between the segments was chosen to be of  $180^\circ$ , which satisfies the statistical length definition. Investigation of the influence of the statistical length (CNT waviness) and angle between the segments on the numerically evaluated electrical conductive properties of CNT-filled composites is discussed elsewhere [26,96].

At the next stage of the volume element formation, a MWCNTs agglomerate was created in the center of a cubic volume with dimensions of  $5 \times 5 \times 5 \mu\text{m}$  (the “initial” volume). To accomplish that, the initial points of the nanotubes were randomly distributed

in a sphere with diameter of MWCNTs agglomerate located in the center of the “initial” volume. From these points the nanotubes were “grown” by generation of consequent points positioned at the distance from previous nanotube point corresponding to the statistical length value. Number of segments in one MWCNT was calculated by dividing the nanotube length (1.5 $\mu$ m) by the statistical length value. The growth was always done in one direction, starting from one of the MWCNT end points. For MWCNTs in agglomerated state all their points were constrained by the sphere mentioned before. Next, the non-agglomerated MWCNTs were distributed according to their volume fraction determined previously for selected concentration of MWCNTs in the composite. For that, initial points of the MWCNTs were distributed in the “initial” volume uniformly, while the segment “growth” procedure was constrained by the dimensions of the “initial” volume.

After that, a cubic sub-volume (the “inner” volume) was selected in the “initial” volume. The “inner” volume edge length was chosen to be equal to the period of the agglomerate distribution (red square in the bottom part of Figure 13). All MWCNTs that didn’t have any points inside this “inner” volume (obscure nanotubes in the top part of Figure 13) were removed from the ‘initial’ volume. This allowed to avoid consideration of the nanotubes located close to the boundaries of the “initial” volume. In this work electrical conductance of the “inner” volume was studied. This approach was implemented since the alternative method - simple truncation of the ‘initial’ volume to the “inner” volume - can result in creation of MWCNT short segments distribution along the “inner” volume boundaries. It is undesirable, since it can lead to unpredictable results for the volume element conductance behavior with deformation. At the same time, it is not possible to

enforce any additional constraints on the segments of MWCNTs split by the new formed boundaries due to specifics of the embedded element method used in this work (see appendix).

Finally, the “initial” volume was cut so its size would be minimal while it still contained inside all the MWCNTs points.

In the case of composites filled with CB particles the following procedure was used to generate an investigated volume element (Figure 14).

At first, the average diameter of the CB agglomerate was evaluated to be  $\sim 0.4\mu\text{m}$  after post processing of the images obtained with electron microscopy (Figure 6c,d) according to the standardized image processing procedure [97]. The images were also used for estimation of the number of agglomerates in the investigated volume element for different concentrations of CB in the composite. The number of particles in agglomerate was determined using the assumption of fractal geometry of the agglomerate, which can be calculated using the expression:

$$n = C \cdot (R/r)^D \quad (3)$$

where  $n$  is the number of particles in the agglomerate of radius  $R$  and  $r$  is the radius of the CB particle, while  $C$  and  $D$  are the pre-factor and the mass fractal dimension [4]. For a typical level of structural branching of CB agglomerates these values can be chosen as  $C = 1$  and  $D = 2.34$  [98]. Radius of a CB particle ( $\sim 20\text{nm}$ ) value was evaluated using the electron microscopy images obtained for nanofiller powders (Figure 4a).

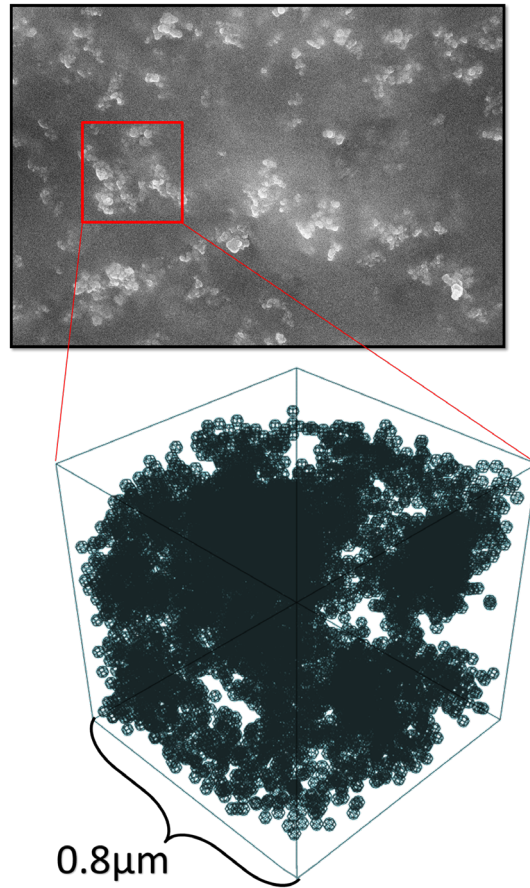


Figure 14. Volume element constructed with the help of electron microscopy data for numerical simulation of PP-based composites containing 15 wt.% CB

Using the obtained CB agglomerates parameters, the agglomerates center points were uniformly distributed in the  $1.5 \times 1.5 \times 1.5 \mu m$  cubic volume. The agglomerates center points coordinates were limited by the selected cubic volume boundaries accounting that they cannot be located closer to them than one agglomerate radius. Then the CB particles center coordinates were distributed in the agglomerate while preventing interpenetration between different CB particles by enforcing minimal distance between the

centers of CB particles equal to the two CB particle radii. After the agglomerates were created for chosen concentration, all particles outside the agglomerated state were distributed uniformly in the volume without interpenetration. The relative number of not agglomerated CB particles was <0.2% for all investigated filler volume fractions.

Finally, the initial volume was trunked from all sides to form a new cubic volume of  $0.8 \times 0.8 \times 0.8 \mu\text{m}$ . It was done to ensure that there is no influence of the volume boundaries on the uniformity of CB particle distribution. Example of the trunked volume element with CB concentration of 15wt.% can be seen in Figure 14.

#### *3.2.2.2. Finite Element Analysis*

Obtained distribution of the MWCNTs and CB points were imported in SIMULIA Abaqus<sup>TM</sup> CAE FEM package. Using the information on the affiliation of points to the specific MWCNT and their order inside this MWCNT, two-node 3D truss element (T3D2) mesh was created for the distribution of MWCNTs in a cubic domain. Cross section area of the truss elements was calculated from the Nanocyl NC3100 MWCNTs parameters. Each CB particle was represented as a sphere meshed with shell elements with characteristic thickness of 5 nm and mesh size of ~25nm. According to specifications provided by the manufacturer for the MWCNTs used in the experimental study, for simulations the MWCNT Young's modulus value should be ~1000GPa. Since the truss elements are characterized by the cross-section area of a solid cylinder, properties of which are set during the FE simulations, a correction was made to the assumed by manufacturer value taking into the account the hollowness of the MWCNTs and the interlayer gaps,

resulting in Young's modulus of  $\sim 500$  GPa. Young's modulus value of 500 GPa was also assumed for CB particles represented as shell-meshed sphere with wall thickness of 5 nm. Overall, since the systems studied have high contrast in values of mechanical characteristics between matrix and inclusions properties, the exact values of Young moduli are not important. The sensitivity study shows that starting from a contrast of 1000 there is no significant difference in the simulation results. For the matrix, value of 600 MPa for elastic modulus (see section 4.4) was chosen. Such low Young's modulus value for matrix was set taking into account manufacturing method used in the experimental study, specifically the fast cooling of the melted composite samples. This approach results in very low crystallinity degree of PP that, in its turn, strongly affects its mechanical properties [99]. Poisson coefficient values equal to 0.3 and 0.46 were chosen for MWCNT/CB particles and PP respectively.

An embedded element method was used for meshing of volume element so it can be suitable for representation of deformational behavior of conductive particle network. For more details on this method see appendix. Matrix mesh was created using equally sized eight-node brick elements (C3D8). Size of the elements was chosen to be noticeably lower compared to the characteristic sizes of the filler elements to reduce computational costs. For the MWCNT-filled composite the edge of the brick element was  $\sim 40$  nm, while for CB-filled composites it was set as  $\sim 15$  nm.

The obtained volume elements were subjected to the deformation that was applied to the plane coincided with the top face of the "inner" volume for the composites filled with MWCNTs, while the bottom face was fixed (Figure 15a). In the case of CB filled

composites, the displacement was applied to the top face of the constructed volume element, while the bottom was fixed (Figure 15b). The strain of the investigated volume element was set at 10% value for each type of filler and filler concentration.

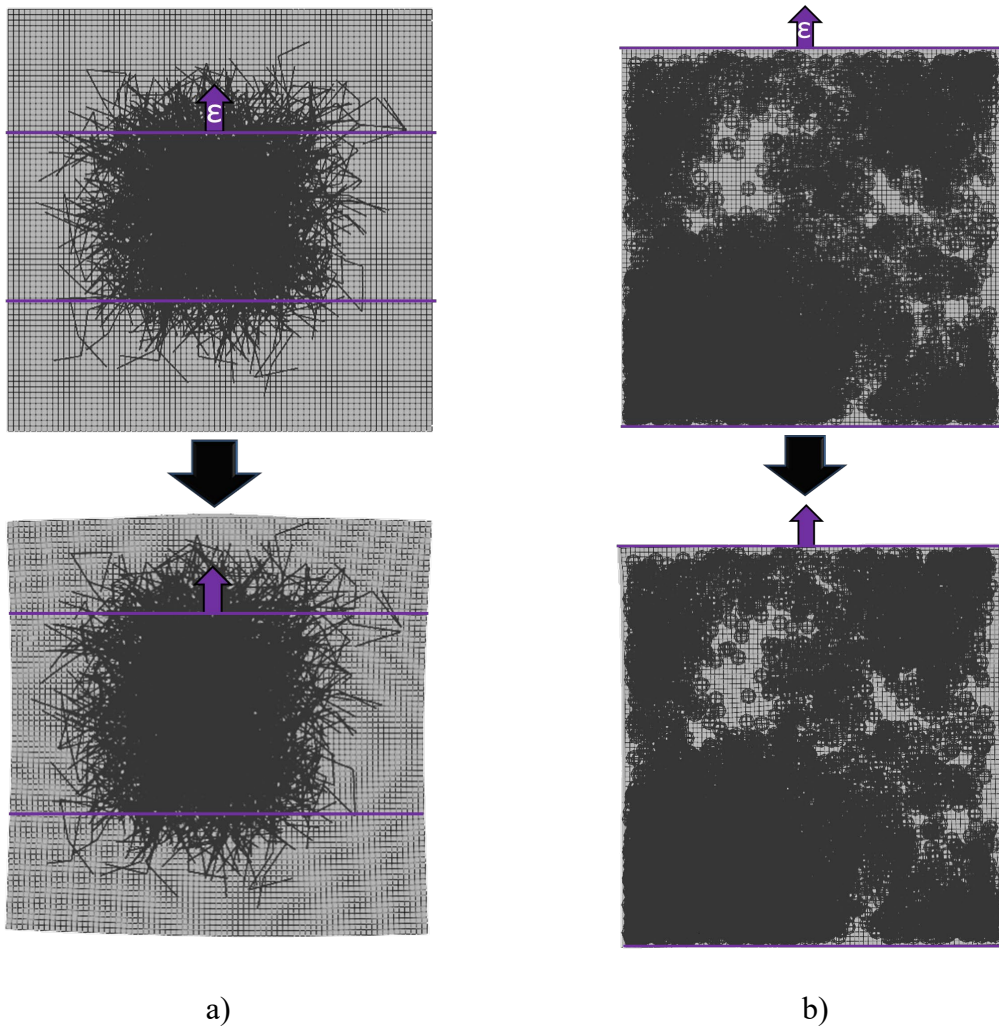


Figure 15. Illustration of the deformation application to the constructed volume elements and the results of deformation in case of MWCNTs filled composite (a) and CB filled composite (b).

At each step of deformation, the coordinates of filler points were recorded. These coordinates were used to calculate conductance of the investigated composites volumes (“inner” volume in case of MWCNTs-filled composites and whole volume element in case of CB-filled composites).

### *3.2.2.3. Relative Electrical Conductance Calculations*

Relative electrical conductance of the investigated volume at selected value of deformation was calculated using the assumption of negligible resistance of filler particle volume compared to the contact (junction) resistance between filler particle or between particle and electrode [93,100]. Since the contact resistance values for selected filler particles in the selected matrix are unknown, it was considered that they all have value of 1 (unit), for the sake of simplicity. The relative value of conductance (conductance for selected degree of deformation divided by conductance value of non-deformed composite volume) was obtained according to the Kirchhoff’s circuit laws for a 3D grid of unit contact resistances and unit input and output electrical currents flowing through two opposite faces (top and bottom) of the investigated volumes, to which the deformation was applied. Principle scheme of the contact grid definition is presented in Figure 16 for both types of the filler studied. Effectiveness of that approach for evaluation of the of composite volume with CNTs network was demonstrated earlier in [24,26,89,90].

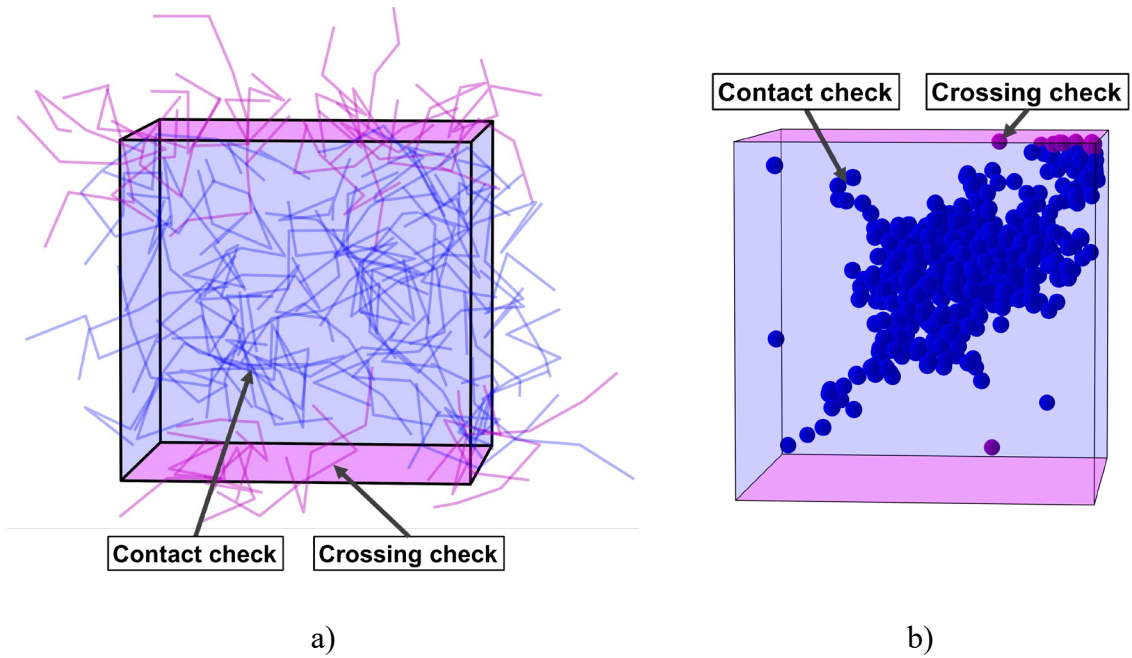


Figure 16. Electrical conductance calculation scheme for MWCNTs- (a) and CB-filled (b) composites. Blue color indicates the particles that are far from the assumed electrodes, while the purple particles are crossing the electrodes planes.

The distances between MWCNTs elements equal or less than two MWCNT radii and distances between CB particles centers equal or less than CB particle diameter were considered as contacts. To account for tunneling effect an exponential decrease of the contact conductance was used with characteristic distance of 0.5nm from the MWCNT or the CB particle supposed surfaces according to the studies conducted for polymer mediated contacts between nanoparticles [93,94]. The contact between electrodes and MWCNTs/CB was considered to be formed if a particle crosses top or lower faces of the investigated volume. A randomly chosen filler particle was characterized by the zero value of electrical

potential. After that all unknown MWCNTs potentials were calculated using a relation (2). The effective conductance of the “inner” volume was calculated as reciprocal voltage difference between the first electrode and the second.

## **Chapter 4. Modeling the Effect of Uniaxial Deformation on Electrical Conductivity for a Compacted Thin Layer of MWCNTs**

The goal of this part of the work was to create an experimentally verified, computationally effective multi-scale numerical model capable to predict electrical conductance of a thin layer of segregated MWCNTs and its response to uniaxial deformation for modeling of composites with highly segregated 3D structure, such as solid-state processed composites based on UHMWPE. The model should take into account the real deformational behavior of MWCNTs that comes from their ability to freely change their conformation.

### **4.1. Comparison Between Numerical and Experimental Results**

The averaged results of experimental determination of relative conductance response of a thin layer of MWCNTs to applied deformation were compared to the FEA results for three simulations (Figure 17). Simulations were conducted for different positions of randomly generated initial and subsequent points of MWCNTs. Several numerical simulations were required to compensate for possible unrepresentativeness of the investigated inner volume. Supposed unrepresentativeness was attributed to the comparability between dimensions of the investigated “inner” volume (2  $\mu\text{m}$ ) and the length of MWCNT used (1.5  $\mu\text{m}$ ). The absolute value of conductance for the simulated volume in undeformed state constituted  $\sim 90$  (units of contact conductance) for each simulation. Here and further the smoothing of the curves was performed using Savitzky-

Golay method, and was used only for better representation of the data, otherwise being presented as large number of scattered data points. All data processing operations, such as curve fitting, were performed on initial set of data points, obtained for three simulations. Difference of the conductance values numerically obtained during different simulation, conducted with the same sets of parameters (see raw numerical data in Figure 17), can be attributed to the assumed earlier unrepresentativeness of the investigated distributions of the filler particles.

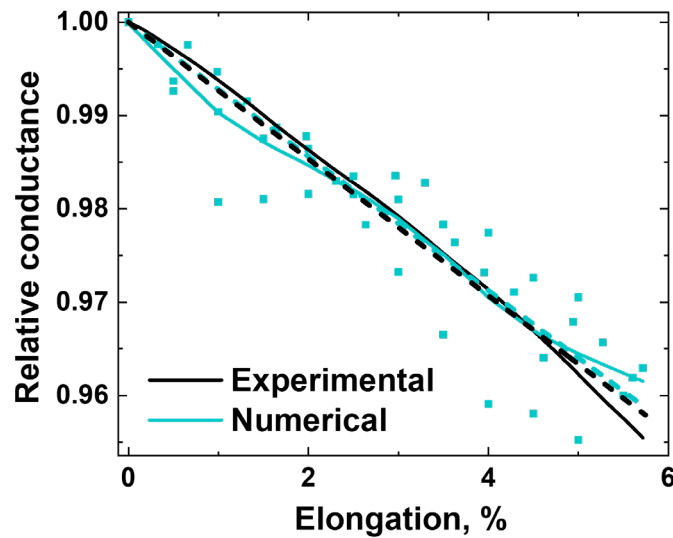


Figure 17. Numerical simulation and experimental results for MWCNT layer relative conductance response to deformation. For experimental results, the raw data and the linear fit of the data are presented. For numerical results, the raw data points obtained from three simulations, the smoothed raw data curve, and the linear fit are shown.

The obtained dependencies demonstrate monotonous decrease of the conductance with deformation. This result can be explained by decreasing number of contacts between the MWCNTs in the direction of deformation. Since the relative conductance values are compared, no correction to geometry of the investigated volumes is introduced.

For the purposes of future analysis, the experimental relationship between relative conductance and the elongation value can be considered linear within the investigated range, with relatively high accuracy (coefficient of dispersion  $\sim 0.993$ ). The linear fit was done with intercept parameter set a 1 to reflect physical meaning of the curve. For three numerical simulations and conductance calculations that were performed for three different distributions, the best averaged fit for the normalized conductance vs elongation relation was also linear, with the slope very close to that of the experimentally obtained (solid line in Figure 17) curve:  $(-7.2 \pm 0.2) \cdot 10^{-3}$  and  $(-7.330 \pm 0.004) \cdot 10^{-3}$ , respectively. Fitting and fitting error calculations were performed using OriginPro™ 2019b software.

Since during simulations only network of contacts between particles was considered, this allows to ignore orientation of the particles influence on the numerically obtained value of conductance. It can be concluded that the closeness of values of the slopes obtained experimentally and numerically conductance dependencies correspond well to the assumption made during numerical simulations that the resistances of MWCNTs segments located between contact points are negligibly small compared to the contact resistances.

## 4.2. Influence of the Model Parameters

In the previous section, the model was identified by the experimentally determined parameters of segregated structures and therefore represented the particular case of the material studied. In this section, model parameters to study results' sensitivity to parameter values were varied.

To correctly evaluate the limitations of the developed model in terms of parameters selection, the influence of different parameters of the model on changes in MWCNTs layer conductance with deformation was investigated. To quantify the model's response to variation of its parameters, the slope of the linear fit for the relative conductance dependency on elongation was chosen as a characteristic representative. While a certain parameter was varied other parameters were fixed at the experimentally verified values given in the previous section. For each varied parameter value more than three simulations were performed for randomly generated MWCNTs distributions.

First, the influence of the thickness of conductive layer was investigated. The results of simulations are shown in Figure 18. As can be seen in the graphs (Figure 18b), the dependency of the characteristic value on the conductive layer thickness demonstrates no obvious tendency and results differ mostly due to scatter (Figure 18a). That means that for the sake of computational efficiency one might use lower thickness values, while not losing much in the slope evaluation accuracy.

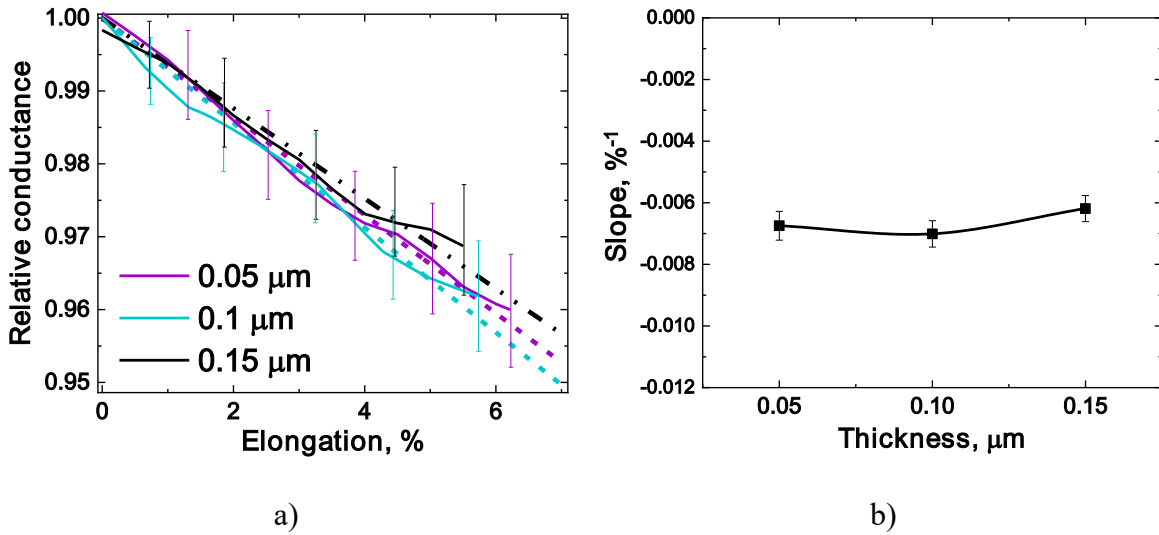


Figure 18. (a) Relative conductance as a function of elongation for simulations for different thicknesses of a conductive layer and (b) slope as a function of layer thickness for linear approximations of relative conductance vs elongation plots.

Next, the influence of filler volume fraction in the investigated inner volume was studied (Figure 19). The legend shows volume fractions of the filler. The results are similar to those obtained for the thickness value parameter (Figure 18b) in that there is no pronounced dependency on the volume fraction of MWCNTs as far as volume fraction changes remain within reasonable bounds. The seeming decrease in characteristic value with MWCNTs volume fraction (Figure 19b) can be attributed to errors in simulation and conductance calculations. Since the number of MWCNTs directly affects the computation time (mostly of conductance calculations performed externally from FEM), it would be reasonable to use lower volume fractions of MWCNTs for simulation. Although, as can be seen from the graphs (Figure 19b), relatively small volume fractions of MWCNTs produce

larger errors in characteristic value. This can also justify the suggested imitation of periodic boundary conditions that leads to formation of regions within the host volume that have lesser volume fractions of MWCNTs, compared to the inner volume (outside regions of the dashed square in Figure 9). It is also worth noting the very linear relation between the absolute conductance in the investigated volume in undeformed state and the volume fraction in the selected range of values.

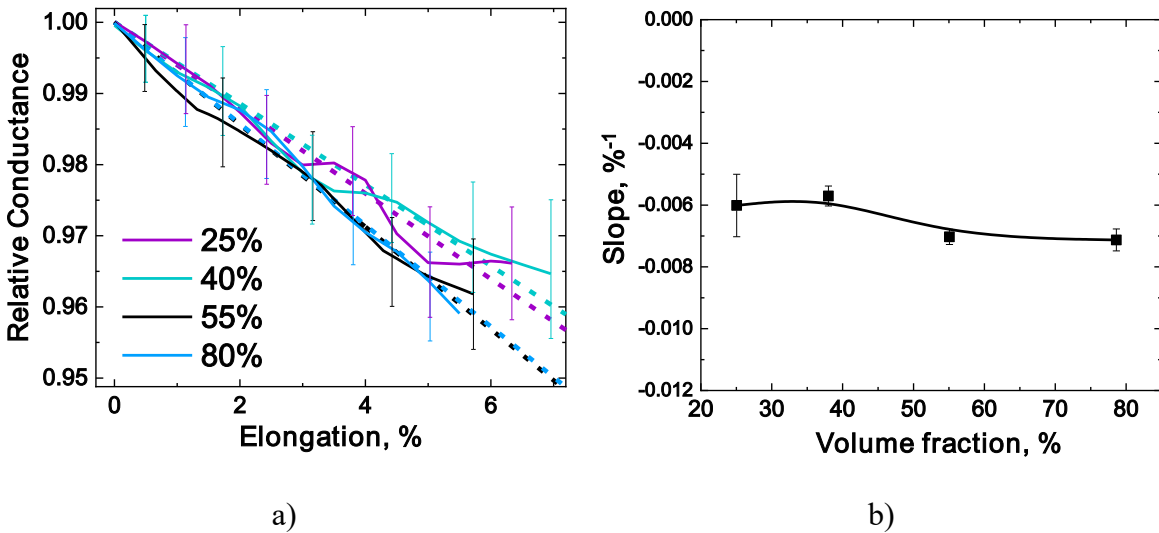
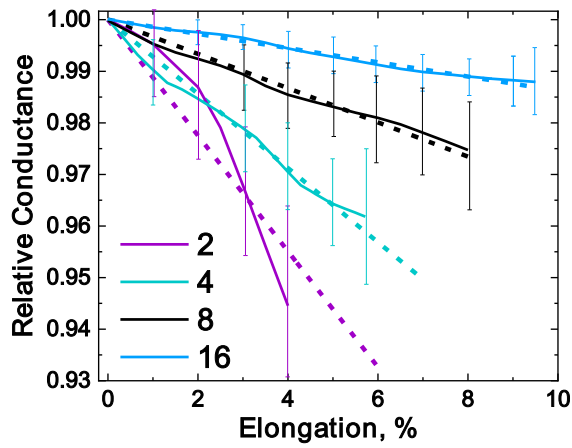


Figure 19. (a) Relative conductance as a function of elongation for simulations with different volume fractions of the filler in the investigated conductive layer and (b) slope as a function of volume fraction of MWCNTs for linear approximations of relative conductance vs elongation plots.

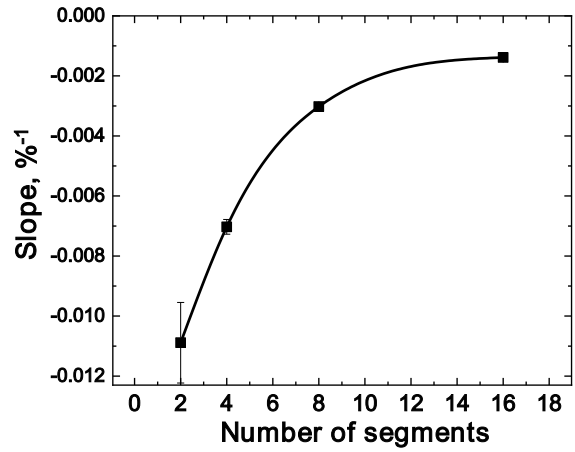
Lastly, the length of segments of MWCNTs, which is directly related to statistical length was varied, and its influence on the relation between relative conductance and the

degree of deformation was investigated (Figure 20). Statistical length is a very important parameter for simulations based on the method proposed in this work. It affects not only the correctness of MWCNTs representation in simulations, it also affects how the interactions between the host and embedded meshes are implemented. The smaller statistical length requires finer meshing of the matrix, because, as the density of the MWCNTs nodes increases, so does the probability of several nodes being embedded in the same host element. Since the application of the same constraints on degrees of freedom for different MWCNTs nodes can result in rigid bonding of those nodes, it is advisable to decrease the host element dimensions for more realistic simulation of the MWCNTs behavior during deformation. The rigid bonding between the neighboring MWCNTs can also result in unbreakable contact, which can explain the dependency of characteristic value on the MWCNT segment length (see Figure 20a).

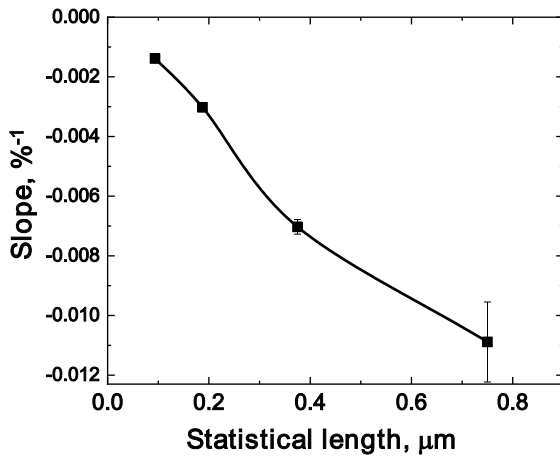
Because of limited computing resources it is difficult to simulate very thick layers containing high amount of MWCNTs. In order to demonstrate that conductance response to the deformation for thick layers is relatively close to that for the thin ones, the characteristic value was determined for simulations with 2  $\mu\text{m}$  thick layer but with 7.5 vol.% of MWCNTs. The resulting value is very close  $((-6.3 \pm 0.3) * 10^{-3})$  to the values obtained for the thicknesses investigated previously, thus supporting the conclusions made earlier.



a)



b)



c)

Figure 20. (a) Relative conductance as a function of elongation for simulations with different 1.5-mm long MWCNT segment number in the investigated conductive layer, (b) slope as a function of the number of segments in the 1.5-mm long MWCNT, and (c) slope as a function of statistical length, for linear approximations of relative conductance vs elongation plots.

From the obtained data it was concluded that the assumptions used in the model produce reasonable results. Strong dependency of the results on the statistical length clearly demonstrates that statistical length is a key parameter in numerical simulations and that ignoring the free rotation of CNTs for larger lengths may lead to wrong predictions.

It can also be said that the embedded element technique ensures that the strain field is close to uniform (Figure 9), which correctly reproduces what happens inside the layer of filler pressed between two plates of polymer material. Using relatively effective computational methods and conductive layer parameters derived from experimental data (thickness of 0.1  $\mu\text{m}$ , MWCNTs volume fraction of 0.55, and MWCNT statistical length of 0.375  $\mu\text{m}$ ) it was possible to obtain results that are very close ( $\pm 1.5\%$  for characteristic value) to the experimental data on the relative conductance dependency on deformation.

### **4.3. Conclusions to Chapter 4**

Several specimens consisting of thin MWCNTs layer pressed between PTFE plates were tested to determine the electrical conductance response of thin MWCNTs layer to the applied uniaxial deformation, and the numerical model describing the deformational behavior of MWCNTs layer electrical conductance was proposed. The model takes into account the ability of MWCNTs to assume various conformations, such as random coil, by using a concept of statistical length. The FE model of the volume imitating periodical boundary conditions was built for conductance calculations, ensuring that the deformational behavior of the investigated volume is as close as possible to the one determined experimentally.

The results of experimental and numerical study were compared using a chosen characteristic value — the slope of linear function fitted to the data. Parameters of numerical simulations were selected based on the experimental data to match the specific case of specimen tested. The difference between numerical and experimental results for characteristic value was found to be small enough ( $<2\%$ ) to suggest that numerical methods used can provide reliable estimation of the deformational response of electrical conductivity for materials with highly segregated MWCNTs. The sensitivity of the numerical model to its parameters was additionally studied and it was demonstrated that the assumptions used in construction of simulated volume can be considered as correct.

It was found that the sensitivity of conductance response to deformation is low for changes both in the thickness of filler layer and in the volume fraction of MWCNTs, as long as they remain within reasonable bounds. On the contrary, the sensitivity of results to the statistical length as a representation of the scale of free MWCNT rotation is very high. Therefore, the correct choice of statistical length plays the crucial role in numerical simulations.

## **Chapter 5. Modeling the Effect of Uniaxial Deformation on Electrical Conductivity for Composite Materials with Extreme 3D Filler Segregation**

The next stage of the study was obtaining a model of the three-dimensional MWCNTs distribution in a composite based on UHMWPE for further modeling the deformation behavior of the electrical conductivity of the composite material with segregated structure.

### **5.1. Results and Discussion.**

The obtained images were processed in the ImageJ software package to obtain a three-dimensional surface reflecting the estimated spatial distribution of interlayers from MWCNTs in the composite. Since the volume fraction of MWCNTs in the composite investigated was very low (~1 vol%), although the distribution of MWCNTs could be discerned from the images of the slices (Figure 7c), the segregated structure was not completely interconnected when thresholding of the images was performed using different threshold values. To fix that, series of 3D dilution and erosion operation were performed, allowing to obtain approximated 3D structure made of densely packed MWCNTs in the composite's volume. Using the MeshLab software package, the obtained three-dimensional surface (Figure 21a) were simplified and corrected (Figure 21b), which allowed to successfully imported it into the Abaqus software package for further modeling using FEM.

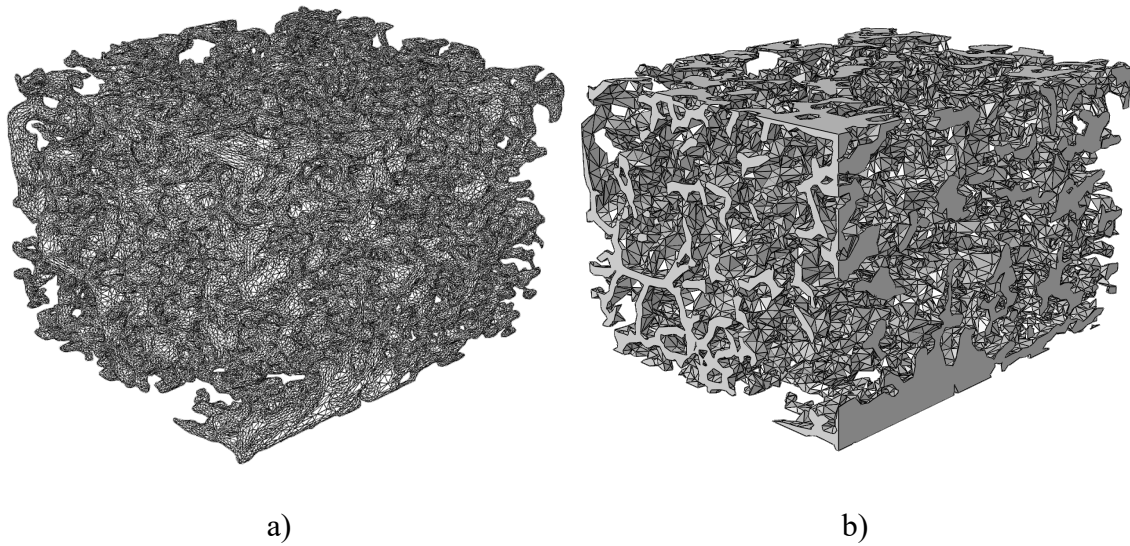


Figure 21. 3D triangular shell element meshes of the reconstructed structure made of densely packed MWCNTs in the composite UHMWPE + 2 wt.% MWCNTs before (a) and after (b) simplification and correction.

A parallelepiped with dimensions 20 \* 25 \* 29 was created in Abaqus, to which the mechanical properties of UHMWPE were imparted. This parallelepiped was meshed uniformly with cubic element edge length of  $\sim 0.5$  microns. Subsequently, this matrix parallelepiped served as the “host” for the embedded element method, where the “embedded” elements were the elements of the structure from the filler (Figure 22).

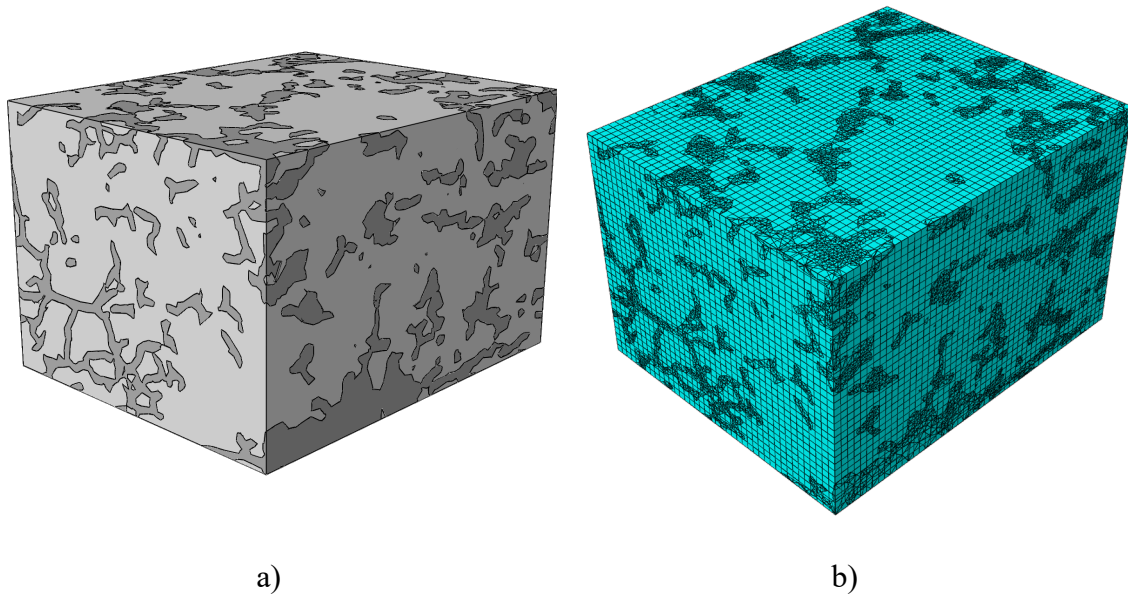


Figure 22. (a) - Geometry reflecting distribution of densely packed MWCNTs (dark gray) in UHMWPE matrix (light grey) reconstructed for composite UHMWPE + 2 wt.% MWCNTs sample; and (b) – result of separate meshing of the matrix parallelepiped volume and MWCNTs-formed surface followed with embedding of the filler elements into the matrix element mesh.

The mesh for the filler structure was created using two-dimensional triangular Shell elements. The embedded element method implementation made it possible to significantly reduce the total number of elements for FE modeling (to  $\sim 2.5 \cdot 10^5$  compared with the estimated  $> 2 \cdot 10^6$  for the case of continuous meshing).

Due to the use of the structure of the filler in the composite as a spatial distribution of two-dimensional small-sized elements with different orientations as a numerical representation, as a next step, a thin layer of MWCNTs was deformed at different angles

to its plane (Figure 23). This corresponds to the concept of a three-dimensional structure of filler interlayers observed in the UHMWPE/MWCNT composite, in which, with uniaxial deformation, elementary interlayer segments, which are also planes, will be located at different angles to the axis of deformation of the composite.

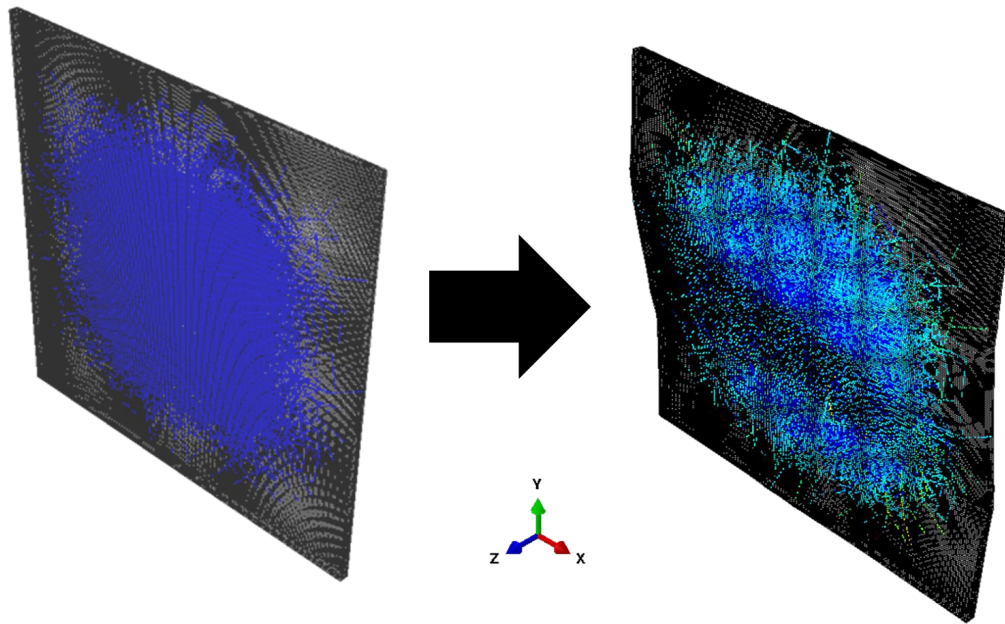


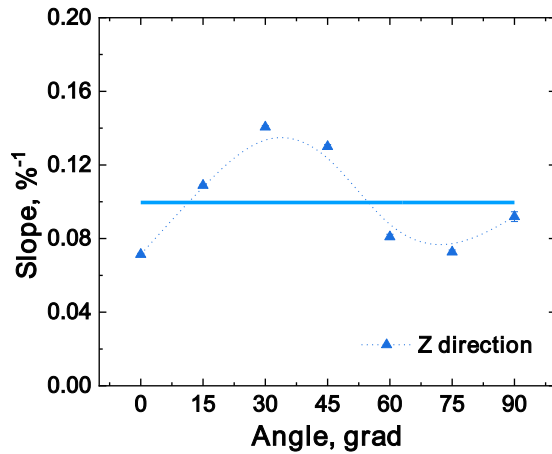
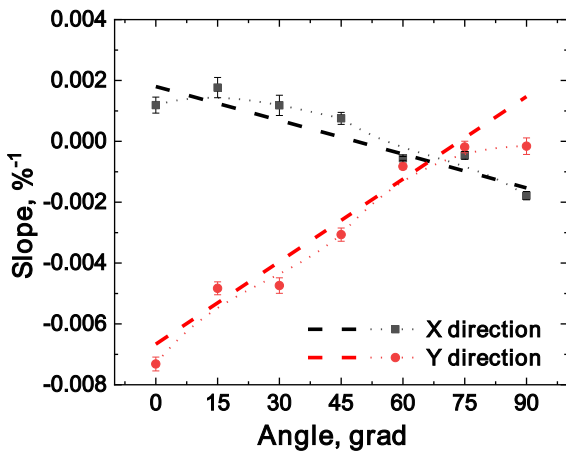
Figure 23. Scheme of deformation application under certain angle to the plane of the layer for the investigated thin volume containing MWCNTs (additional colors on the right image illustrate tensile stress distribution in MWCNT elements).

Deformation was applied in Y-Z plane of the layer. Angle between the global coordinate system Y axis and the applied deformation direction was varied. Y axis of the layer corresponded to the direction of composite deformation and global coordinate system Y axis when the angle equals 0. X axis was perpendicular to the layer's Y axis while also

being located in the plane of the layer, and Z axis was perpendicular to the plane of the layer.

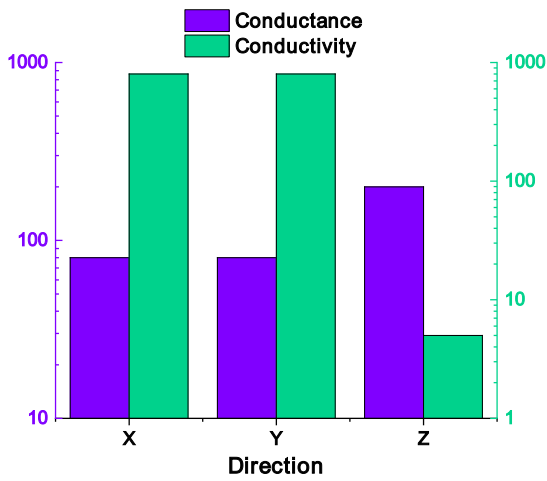
Since the deformational behavior of the electrical conductivity of an elementary segment of the segregated structure made from MWCNTs in all its directions can change significantly depending on the angle between the global coordinate system Y axis and the applied deformation direction, it was decided to calculate the electrical conductivity of the volumes under study for all dimensions of the MWCNTs layer.

Obtained dependencies of the slopes of relative conductance versus elongation curves for the layer's X and Y directions (Figure 24a) were approximated with linear functions, parameters of which were used in the future analysis. Difference in conductivity in X-Y and Z direction (Figure 24c), as well as no notable trend for the slope values in Z direction (Figure 24b) allowed to consider as negligible the dependence of Z component of conductivity tensor deformation response from the deformation direction and its magnitude.



a)

b)



c)

Figure 24. Values of slopes of the conductivity dependencies from elongation for all directions (X and Y (a), and Z (b)) of the thin layer of MWCNTs versus angle between the deformation direction and Y direction. (c) - Values of conductance in units of MWCNT contact conductance and conductivities in different directions of MWCNTs layer for the angle = 0.

At the next step, the obtained linear laws of the conductivity changes for densely-filled with MWCNTs elements for different deformation directions were used for the homogenized elements of segregated MWCNTs structure to determine segregated network response to deformation depending on the element's orientation to the deformation direction. Due to the ability of linking the individual orientation and properties of each 2D Shell element (Figure 25a), the meshing was carried out using 2D triangular Shell elements. It was possible to implicitly set the dependence of the conductivity of each element in each of its dimensions volume depending on the degree of uniaxial deformation of the investigated composite using subroutine UMAT in the FEA Abaqus software. Because in the course of creation of the formed with shell elements surface representing the MWCNTs distribution, the structure was effectively doubled due to the initial thickness increase of the layer during the dilution-erosion operations (Figure 21a), thickness of the shell elements was set as 50 nm. As conductivity of the matrix a value of  $10^{-15}$  S/m was used, while for the MWCNTs layer elements value of  $10^5$  S/m was chosen. The precise values of the conductivity were not of the concern, since the contrast between conductivity of matrix and densely packed MWCNTs was very high. As mechanical properties, values of 500 and 5 GPa were chosen as elastic moduli for matrix and MWCNTs layer respectively, and Poisson coefficient of 0.46 was used for both matrix and MWCNTs layer. These values were used because it was assumed that filler does not influence mechanical properties of the matrix significantly since it is not integrated into the matrix, and simply follows the matrix movements due to the friction forces. Unit potential difference was applied to the volume in the deformation direction (global Y axis), while the total current value passing

through the top surface was measured for values of elongation in range from 0 to 5% with 0.5% step (Figure 25b).

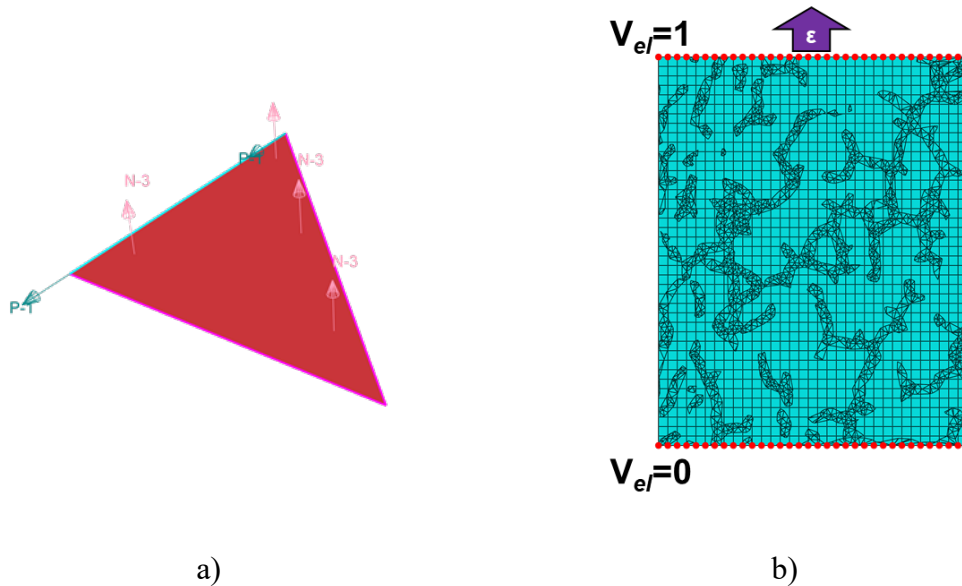


Figure 25. (a) – Illustration of a Shell element with set orientation; and (b) - scheme of deformation application with simultaneous conductance measurement for the investigated volume of composite with segregated structure used in the model.

Comparison of the experimentally obtained results for composite UHMWPE + 2 wt.% MWCNTs samples and results of numerical simulations are presented in the Figure 26. It can be seen that the relative conductance vs elongation dependency, obtained experimentally for composite UHMWPE + 2 wt.% MWCNTs, is close to the linear, with the slope insignificantly lower (in the range of the error) to that of the experimentally

obtained for MWCNTs layer curve (Figure 17):  $(-7.0 \pm 0.2) \cdot 10^{-3}$  versus  $(-7.2 \pm 0.2) \cdot 10^{-3}$ , respectively.

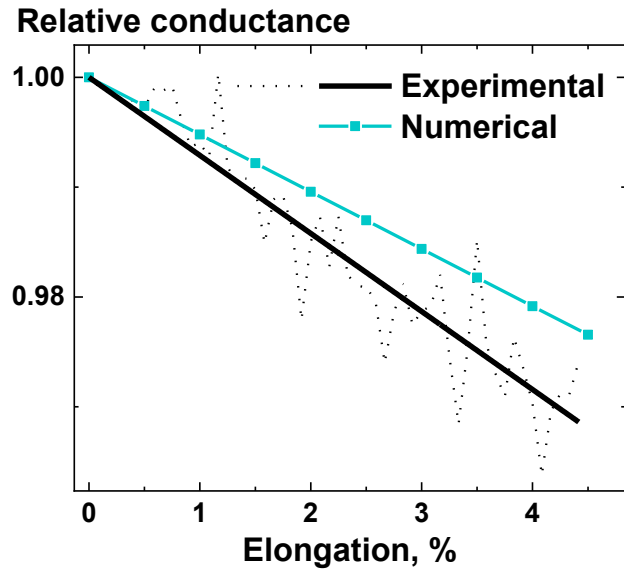


Figure 26. Experimental results for composites UHMWPE + 2wt.% MWCNT layer relative conductance response to deformation and numerical results, obtained for reconstructed using tomography data composite volume. For experimental results, the averaged for three experiments raw data (black dashed line) and the smoothed data (black solid line) are presented.

The slope of relative conductance dependency from elongation, obtained numerically, was lower in absolute value compared to that of the experimentally obtained for MWCNTs layer:  $-(5.21 \pm 0.01) \cdot 10^{-3}$  versus  $(-7.2 \pm 0.2) \cdot 10^{-3}$ , respectively. The reduced rate of conductance change for investigated composite's volume with deformation can be explained by presence in the conductive network regions, in which the direction of the

flowing electrical current is significantly diverted from the applied to the composite's volume deformation direction. It means that conductance of this regions in the direction of the flowing electrical current should decrease with slower rate (see Figure 24a), or may even increase with deformation of the composite's volume.

Difference between the results, obtained experimentally and numerically for composite with segregated structure may be explained by the presence of pores at the interface between polymer granules, observed for investigated experimentally samples. Because of that, the conductive pathways in the material are destroyed faster, and the whole composite sample has low mechanical properties, such as low elongation at break (~6%).

## **5.2. Conclusions to Chapter 5**

Using focused ion beam scanning electron microscopy, and implementing various image processing techniques, the 3D virtual structure of the filler in the solid-state processed composite material based on UHMWPE and filled with MWCNTs was created. The resulting structure was successfully imported into the software package for FEA.

To investigate response of the structure made of MWCNTs in the numerically recreated composite volume, electrical conductance of the MWNCTs layer response to deformation under different angles to the plane of the layer was obtained using numerical approach developed earlier. The obtained data allowed to impart electrical properties change law for each conducting element corresponding to the structure made of MWCNTs in the numerically investigated volume of composite with segregated structure, taking into account individual orientation of each element. Analysis of the deformational behavior of

conductance of the composite's volume using FEM allowed to estimate influence of the complexity of the filler segregation on deformational behavior of the composite's electrical conductance.

The numerical methods developed can find various applications where computationally effective simulation of systems with densely packed MWCNTs (with volume fraction well above percolation threshold) is required, and where MWCNTs are distributed within thin layers in generally non-conductive phase. An example of such systems is the composites based on solid-state processed UHMWPE reactor powder mechanically premixed with MWCNTs to obtain the extreme state of filler segregation in a composite structure. This type of materials can find many interesting applications in the future due to their ability to be further processed in a solid state in order to achieve highly oriented state and high mechanical characteristics while still maintaining high electrical conductivity.

## **Chapter 6. Modeling of an effect of uniaxial deformation on electrical conductance of polypropylene-based composites filled with agglomerated nanoparticles**

The aim of this part of thesis was to contribute to the process of development of numerical methods predicting correlation between deformation and conductance response of composite materials based on PP filled with different concentrations of CB and MWCNTs.

### **6.1. Results and Discussion**

After the specimens of composites filled with different concentrations of MWCNTs and CB particles were manufactured, their electrical conductivity was measured to determine the value of percolation threshold for each type of the filler (Figure 27). The resulting value was obtained from averaging the conductivity of three samples with same filler concentration. The estimated value of percolation threshold for MWCNTs-filled composite (~3wt.%) was much higher than it was expected for uniform distribution of the particles with the aspect ratio of ~150 (~0.7wt.%) according to the classical percolation theory [8], which means that aggregation of the nanoparticles highly negatively affected the electroconductive properties of the material obtained by the selected method of processing. On the other hand, for CB-filled composites the resulted percolation threshold (~12.5wt.%) was much lower than it should be for randomly distributed spherical particles (~35wt.%). It signifies that formed large agglomerates of predominantly non-unit aspect ratio are much more likely to form percolation cluster.

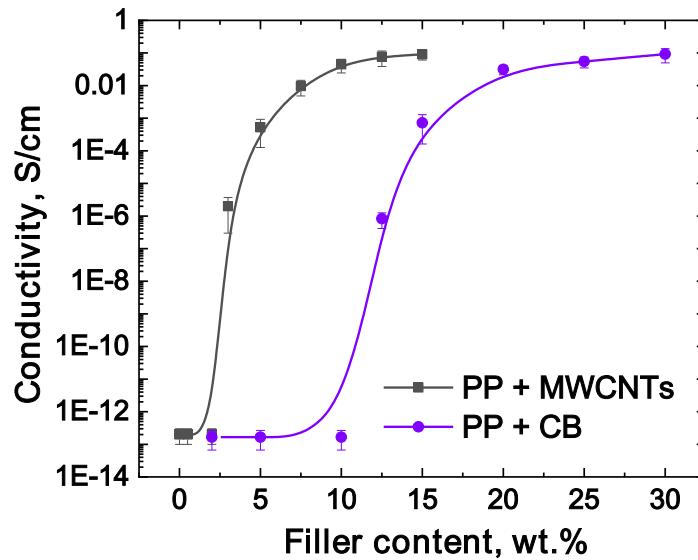


Figure 27. Conductivity of the composites filled with MWCNTs and CB particles versus concentration of the filler. Continuous curves are the results of spline interpolation for the data points.

Obtained samples with concentrations of filler above percolation threshold were subjected to uniaxial deformation in the course of which the conductance of the testing sample was constantly measured. The obtained results were averaged for three identical samples. The stress-elongation curves and dependencies of relative conductance from the deformation degree for the samples with different concentrations of the filler are presented in Figure 28.

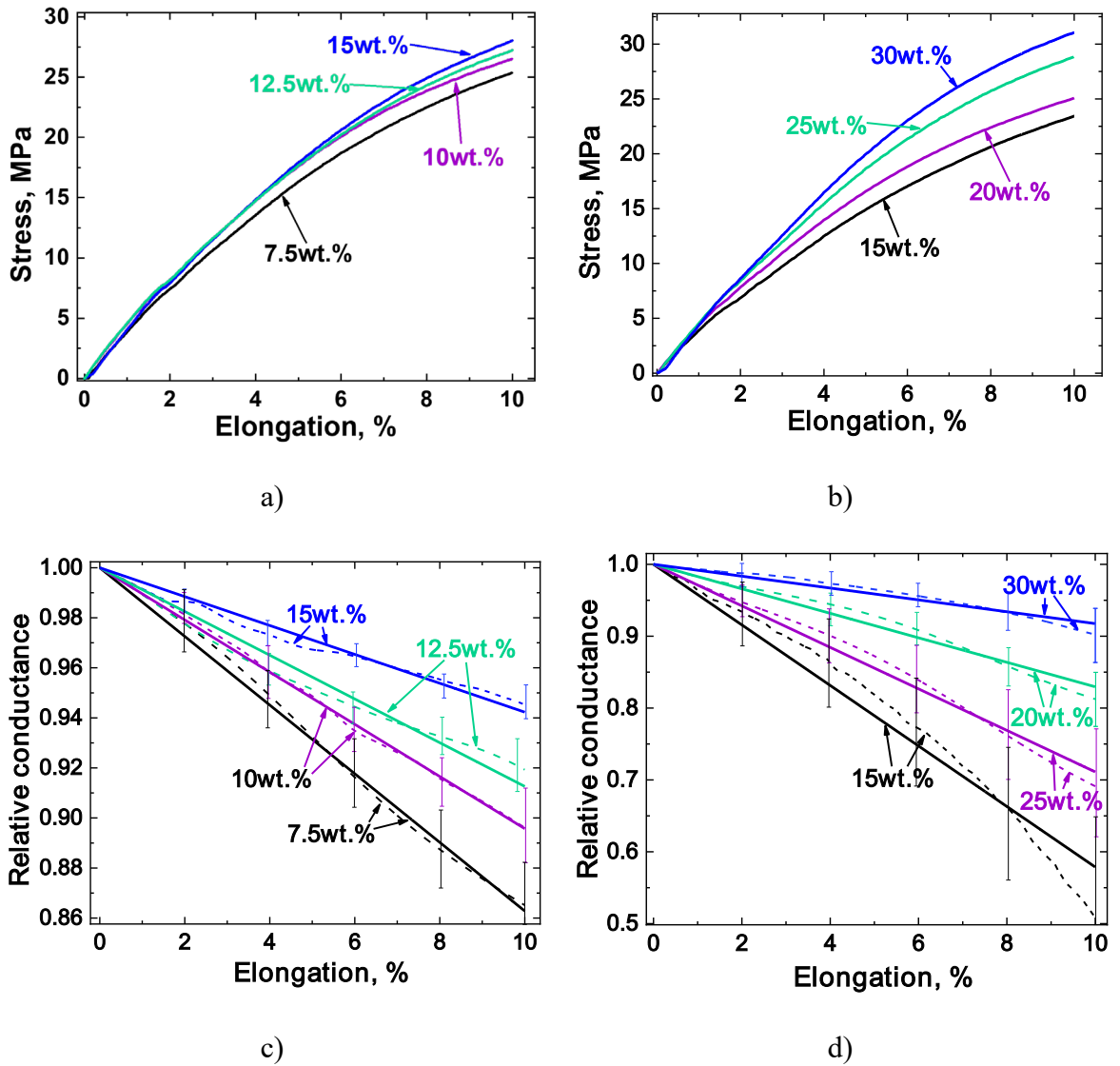


Figure 28. Stress-elongation curves for composites filled with MWCNTs (a) and CB particles (b) and relative conductance of composite samples filled with MWCNTs (c) and CB versus elongation.

The increase in modulus with increase of the filler concentration was expected and can be observed for both MWCNTs (Figure 28a) and CB filler particles (Figure 28b).

Monotonically increasing form of the deformational curves indicates that the deformation of the samples was dominantly elastic for both types of the filler. The relative conductance is changing linearly with increasing elongation for the MWCNTs-filled composites (Figure 28c), while the dependencies for high concentration of the CB particles start to demonstrate non-linear behavior at the elongation values of  $\sim >4\%$  (Figure 28d). But for the sake of simplicity when comparing the experimental data with results of numerical simulation a slope of the fitted line function with intercept of 1 was used as a characteristic value.

The results of numerical simulations of deformational behavior of conductance for the composites filled with MWCNTs are presented in Figure 29. The resulting curves (dashed lines) are the product of smoothing of averaged data for three simulations conducted with a same set of parameters. The multiple simulations were required to compensate for possible non-representativeness of the investigated volumes, size of which were comparable to the length of MWCNT used. In Figure 29a, the results of calculations of electrical conductance for unit contact resistances between MWCNTs and between MWCNTs and electrodes (the “Initial” assumption) demonstrate non-monotonic dependency of the fitted to the numerical simulation results linear function slope on the MWCNTs concentration in the composite. To understand the reasons behind the insensibility of the results to the filler concentration additional assumption that no new contacts can be formed in the course of the deformations were considered during the conductance calculations (no new contacts or “NN” assumption).

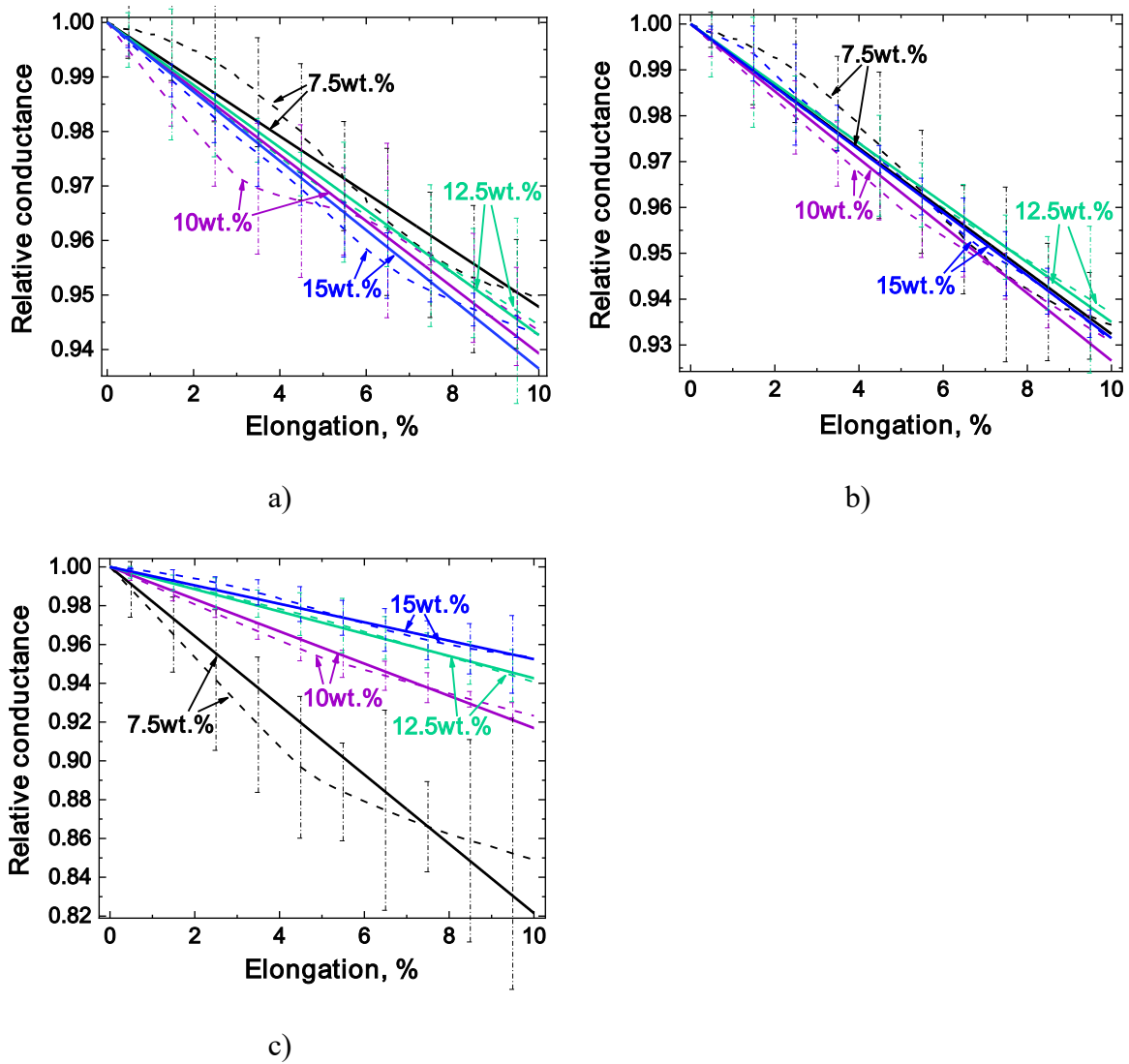


Figure 29. Relative conductance dependency from the elongation of the composite volume filled with MWCNTs obtained from the numerical simulations and calculated with “Initial” assumptions (a), with the “NN” assumption (b) and the “NNHC” assumptions (c). Error bars are given for selected number of points.

The idea behind the NN assumption is as follows: if no contact was formed between filler particles during the manufacturing (melt mixing) process, then the gap between them

is filled with polymer. That means that during the deformation it is possible to lose contact (pore creation) but not to form a new one, since the polymer will be in the way. As it can be seen from Fig. 9b, the results for the fitted function slope dependency from the concentration of the filler was still non-monotonic, but the absolute value of the slopes increased. The final assumption was that the MWCNT/electrode contact conductance value should be set at several magnitude higher than the MWCNT/MWCNT contact conductance (no new contacts and highly conductive particle/electrode contacts or “NNHC” assumptions). Particularly, a value of 1000 was set in the work for filler/electrode contact conductance. It was assumed that the increase of the MWCNT/electrode contact conductance could decrease the effect, since most interest presents what occurs in the bulk of the ‘inner’ volume (number of contact changes) rather than on the electrode faces, and above the top electrode and below the bottom (Figure 13), . In that case the conductance value for the ‘inner’ volume presumably will be determined mostly by the network of conducting contacts located in the depth of the ‘inner’ volume. The slope values for the fitted curves turned out to be generally lower than the ones obtained without this assumption and increased steadily with increasing concentration (Figure 29c), which corresponds to the experimentally obtained results for MWCNTs filled composites (Figure 28c).

The results of numerical simulations of a deformational behavior of the CB-filled composite electrical conductance are presented in Figure 30. In this case the resulting curves were also smoothed over averaged data from three and more simulations, since the investigated volume element size ( $1\mu\text{m}$ ) was comparable to the agglomerate size ( $0.4\mu\text{m}$ )

and distributions of the particles in the volumes could deviate strongly from one simulation to another, particularly for low concentrations of CB in the composite.

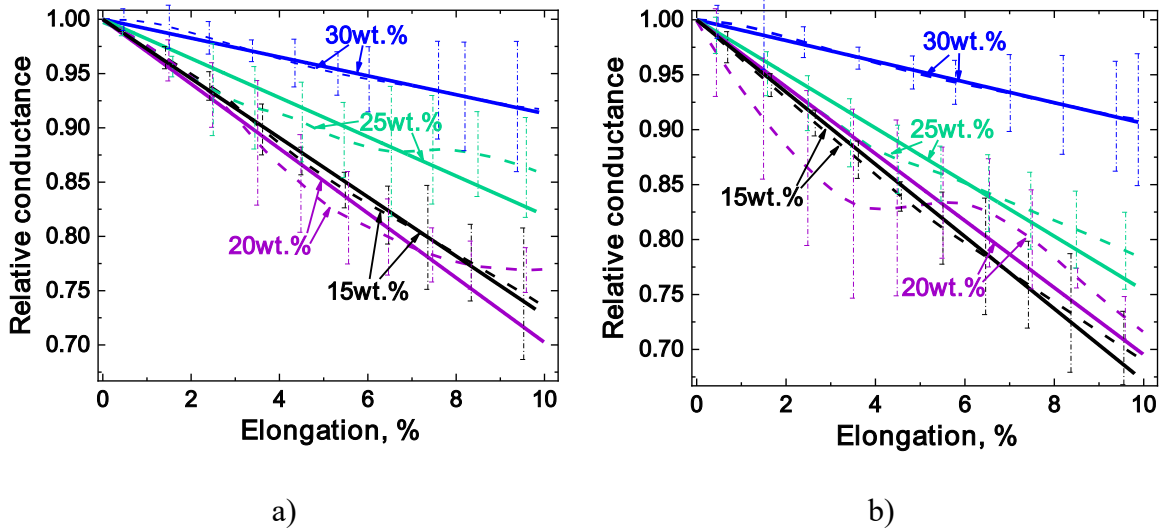


Figure 30. Relative conductance dependency from the elongation of the composite volume filled with CB particles obtained from the numerical simulations and calculated with “Initial” assumptions (a) and with “NNHC” assumptions (b). Error bars are given for selected number of points.

For dependencies of conductance calculated with assumptions of unit contact resistances between CB articles and between CB particles and electrodes a non-monotonic behavior at low filler concentrations can be noted (Figure 30a). The assumption that no new contacts between particles can be formed did not lead to significantly different results, so the assumption that the CB/electrode contact conductance is two order of magnitude higher than CB/CB particle contact conductance (also abbreviated as “NNHC”

assumptions) was made. As it can be seen in Figure 30b an increase of the concentration of CB in the investigated volume element leads to growth of the fitted line function slope value. It is worth noting that due to the error in the conductance value for averaged results of simulations, which is especially high for low filler concentrations, the positive trend for characteristic value with concentration of CB particles may be no longer observed if to analyze the elongation of a simulated volume up to its small values (<5%).

Comparison of the experimental results and the results obtained with numerical modeling for the composites filled with MWCNTs and CB particles is presented in Figure 31a. It can be noted, that for simulated composites filled MWCNTs the most reliable results provide the calculations of conductance made with “NNHC” assumptions, since they demonstrate consistent rise of the characteristic value (slope of the fitted linear curve) with the filler concentration increase, while also giving the values closest to the experimental in overall in terms of averaged relative error(Figure 31d). Relative errors were calculated as  $(S_{num} - S_{exp})/S_{exp}$ , where  $S_{num}$  and  $S_{exp}$  are the slope values obtained numerically and experimentally correspondingly.

Looking at the characteristic values corresponding to the low concentrations of MWCNTs for any set of assumptions it can be said that the calculations at low concentrations are the least reliable and have the highest error of value (Figure 31c).

Also, it is worth noting, that dependencies of the slope values on normalized concentration  $x_n = (x - x_c)/x_c$ , where  $x_c$  – percolation threshold, determined previously experimentally, are forming joined trend across the filler types investigated. This trend is characterized by saturation at high values of normalized concentration (Figure 31b).

It can also be said in the case of composites filled with CB particles, where for the lowest concentration of CB particles in the composite the characteristic value obtained numerically demonstrate high deviation from experimental data. The “NNHC” assumptions in the case of CB-contained composite simulation can ensure the monotonic increase of the characteristic value with concentration of CB particles, while “initial” set of assumptions produce characteristic values in average closer to the experimental results (Figure 31d).

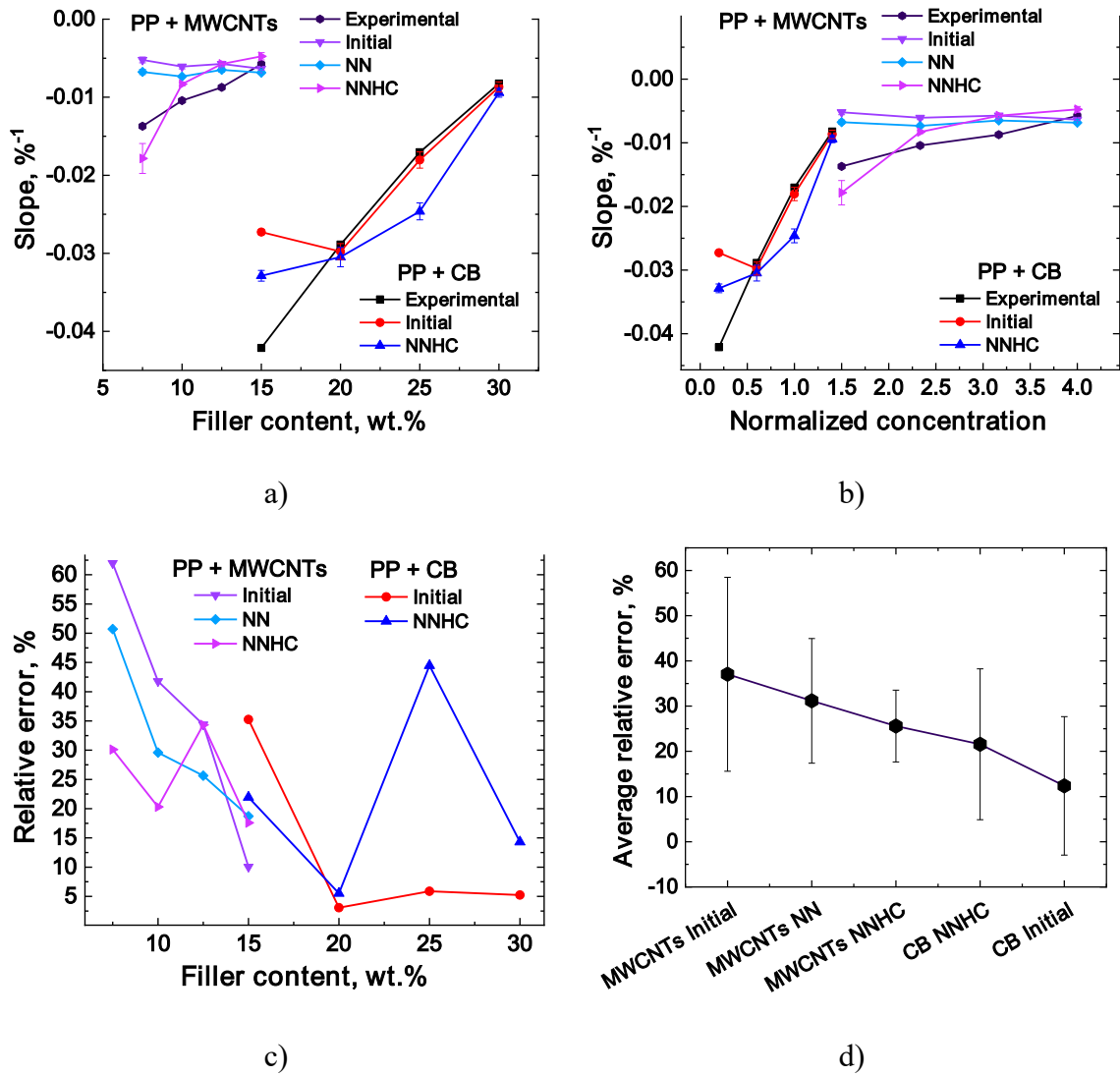


Figure 31. Slope of the relative conductance values dependency from elongation of the composite samples for different MWCNTs and CB particles concentrations (a) and normalized concentrations (b) obtained experimentally and numerically using different assumptions for conductance calculations; (c) relative error of the numerically obtained slope value for different conductance calculations assumptions and averaged over concentration range (d) error.

## 6.1. Conclusions to Chapter 6

Samples of composites containing different concentrations of the electroconductive filler of different types were obtained using melt mixing processing method. Electron microscopy data and conductivity dependencies on the filler concentrations demonstrated that both MWCNTs and CB particles used in the study as fillers presented in a highly agglomerated state in the investigated composites volume. The obtained composite samples were tested on the electrical conductance response to a uniaxial deformation.

The analysis of the experimental data was used to develop a numerical model that allowed to connect such characteristics of the composites as a type of the filler, its concentration in the composite volume and a distribution of the filler particles in the composite volume to a degree of uniaxial deformation to which the material is subjected.

For simulations of the composites filled with different types of inhomogeneities special volume elements were constructed for each type of the filler to account for experimentally obtained data while minimizing possible computational resource requirements. To ensure uniformity of the strain field applied and to maximize computational efficiency an embedded element technique for FEM was implemented. The constructed volume elements were deformed by applying displacement value (10% of elongation) between top and bottom planes of the investigated ‘inner’ volumes. The resulting particle spatial distributions for each step of deformation were used to calculate electrical conductance of the investigated composite volume.

Numerically obtained using different assumptions relative conductance dependencies from the elongation were compared to the experimental results. It was

concluded that embedded element method coupled with correct replication of the filler particles distribution and realistic representation of the filler deformational behavior can provide results close ( $\sim 10\%$  relative average deviation for both filler types) to the obtained during the experimental tests.

## **Chapter 7. Multi-Scale Modeling of Uniaxial Deformation of Electroconductive Polypropylene/Nanoparticles Composites Reinforced with Woven Glass Fibers**

In chapter 6, it was shown that uniaxial deformation of the PP filled with MWCNTs and CB decreases material's electrical conductance almost linearly. Slope of the obtained relative conductance changes was proven to be highly dependent on the filler type and its concentration in the matrix. It was also demonstrated that numerical methods using realistic representation of nanosized particles can be used to predict conductance-deformation relation for the nanocomposites. In this chapter, a multi-scale and multi-physics model is described that is capable of predicting changes in conductance deformational behavior coming from introduction of reinforcing glass textile into the nanocomposite materials investigated earlier.

### **7.1. Multi-scale Modeling**

The structure of a composite is hierarchical. At the meso-scale, it is made of tows that are classified as warp (longitudinal) and weft (transverse) and of polymer matrix. At the micro-scale, bundles of fibers and the polymer matrix represent tows. All of these features interact with each other and influence the overall part performance. Therefore, modeling of composite behavior requires a robust constitutive model for the polymer matrix and an efficient multi-scale procedure.

The process of multiscale modeling was divided into several stages (Figure 32). In the first step, the mechanical and electrical properties of the matrix filled with conductive

nanoparticles (S1) were determined. The mechanical properties of the modified matrix were obtained using the Mori-Tanaka analytical micromechanical scheme [101]. The dependencies of the change in the electrical conductivity of the matrix modified by nanoparticles on the applied strain were obtained experimentally. The data on the modified matrix was programmed into the subroutine UMAT for the Abaqus FE software and used for the simulation at the micro-scale. At the micro level, numerical homogenization was carried out to compute the mechanical and electrical properties of the fabric's tows (S2). The obtained data was again programmed into the UMAT subroutine and used as input for modeling at the meso-scale. At the meso-scale, an FE model of a representative volume element (RVE) was created, based on experimental data from the electron microscopy. The generated model was used to study the change in electrical conductivity depending on the applied load in composite.

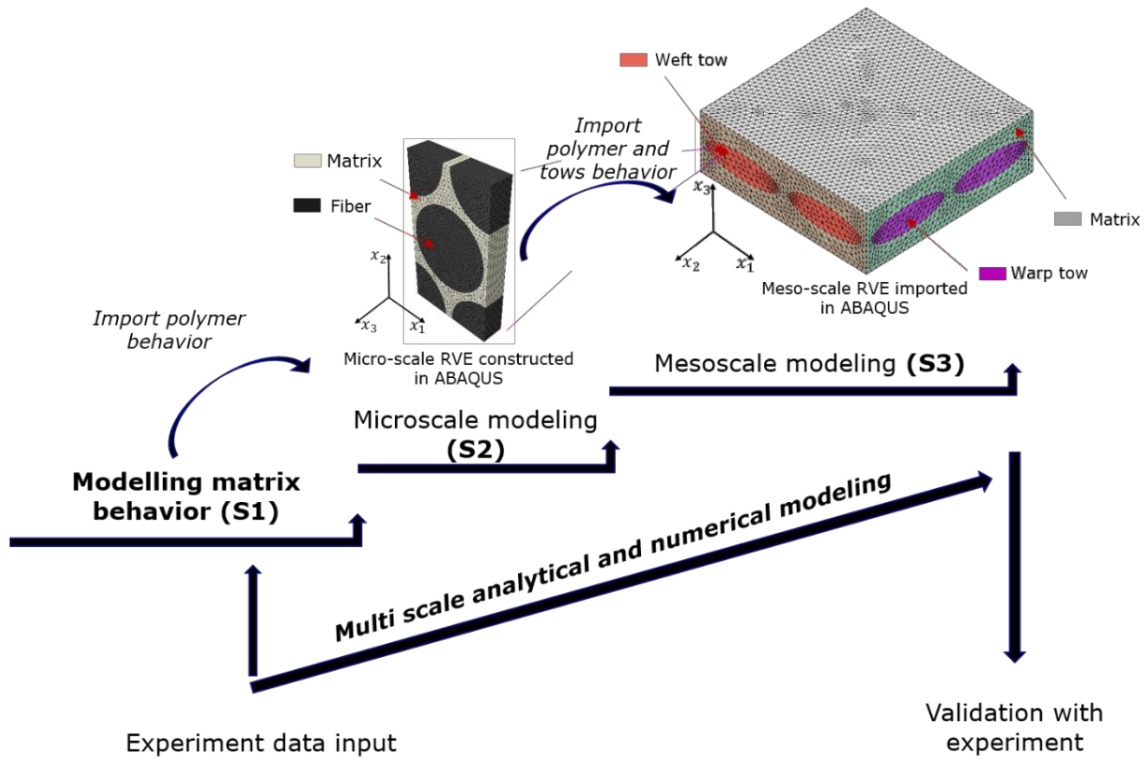


Figure 32. A multiscale approach to modeling the dependency of conductivity changes on the applied strain.

### 7.1.1. Modified PP Properties

In the present work, the contribution tensor formalism was used to estimate overall elastic properties of polymer matrix filled with nanoparticles (CB and MWCNTs). The contribution of an individual particle to the effective material response can be evaluated using the stiffness contribution tensor  $N$  [102–104]. The effective stiffness tensor of the material with particles was presented as:

$$C = C_0 + N_{RVE} \quad (4)$$

where  $C_0$  is the stiffness tensor of the matrix material and  $N_{RVE}$  is the contribution from all particles present in the RVE.

One of the most widely used micromechanical model is the Mori-Tanaka scheme, proposed in [101] and clarified in [105]. Following this approximation, the combined contribution of all particles to the overall stiffness of the RVE is given by

$$N_{RVE}^{MT} = \varphi N: [\varphi(C_1 - C_0)^{-1}: N + (1 - \varphi)J]^{-1} \quad (5)$$

where  $\varphi$  is the volume fraction of particles,  $J$  is the identity fourth rank tensor, and  $C_1$  is the stiffness tensor of the inhomogeneity material.

In the studied case, the properties of polymer matrix were:  $E_0 = 600MPa$ ,  $\nu_0 = 0.46$  and inhomogeneities:  $E_1 = 500GPa$ ,  $\nu_1 = 0.3$ . Utilizing Mori-Tanaka scheme effective properties of PP polymer filled with CB and MWCNTs were computed (Figure 33). In the case of CB, the volume fraction of particles was 10% and the corresponding effective properties were:  $E_{eff} = 755.83 MPa$ ,  $\nu_{eff} = 0.455$ . In the case of MWCNTs  $\varphi = 4.74\%$  and the corresponding effective properties were:  $E_{eff} = 764.088 MPa$ ,  $\nu_{eff} = 0.4528$ .

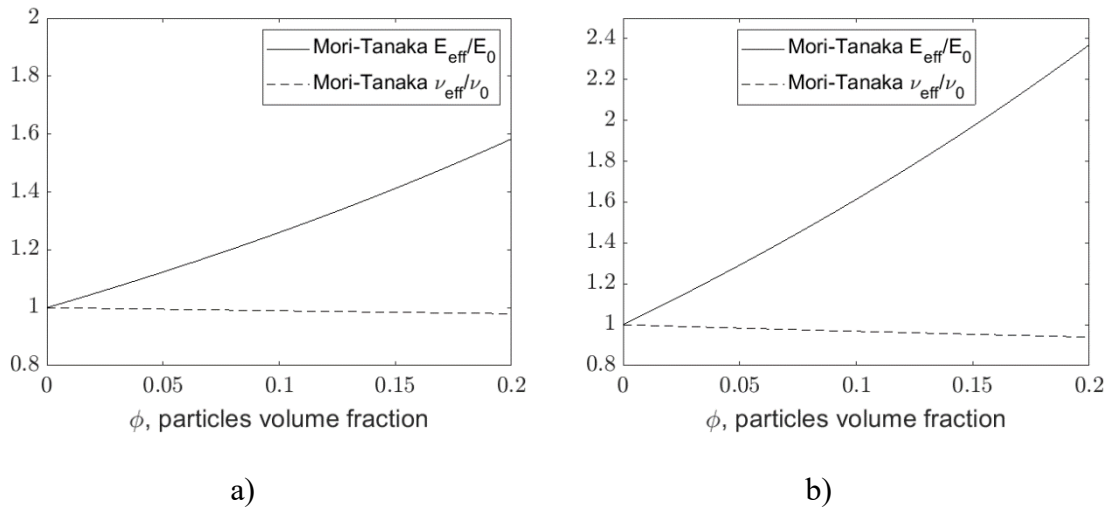


Figure 33. Relative effective mechanical properties of PP matrix filled with: (a) CB and (b) MWCNTs.

As electrical properties data obtained experimentally in Chapter 6 was used.

### 7.1.2. Modeling at the Micro-scale Level

The effective mechanical properties of the tows (warp and weft) were calculated using the numerical homogenization procedure, which begins with the generation of an RVE. The RVEs' packing was assumed to be hexagonal for the warp and weft tows containing 65 % and 70% of E-glass fibers, respectively (Figure 34). Glass fibers were considered isotropic and linearly elastic  $E_{\text{fibers}} = 80\text{GPa}$  and  $\nu_{\text{fibers}} = 0.2$ , the properties of modified PP were calculated at the previous step.

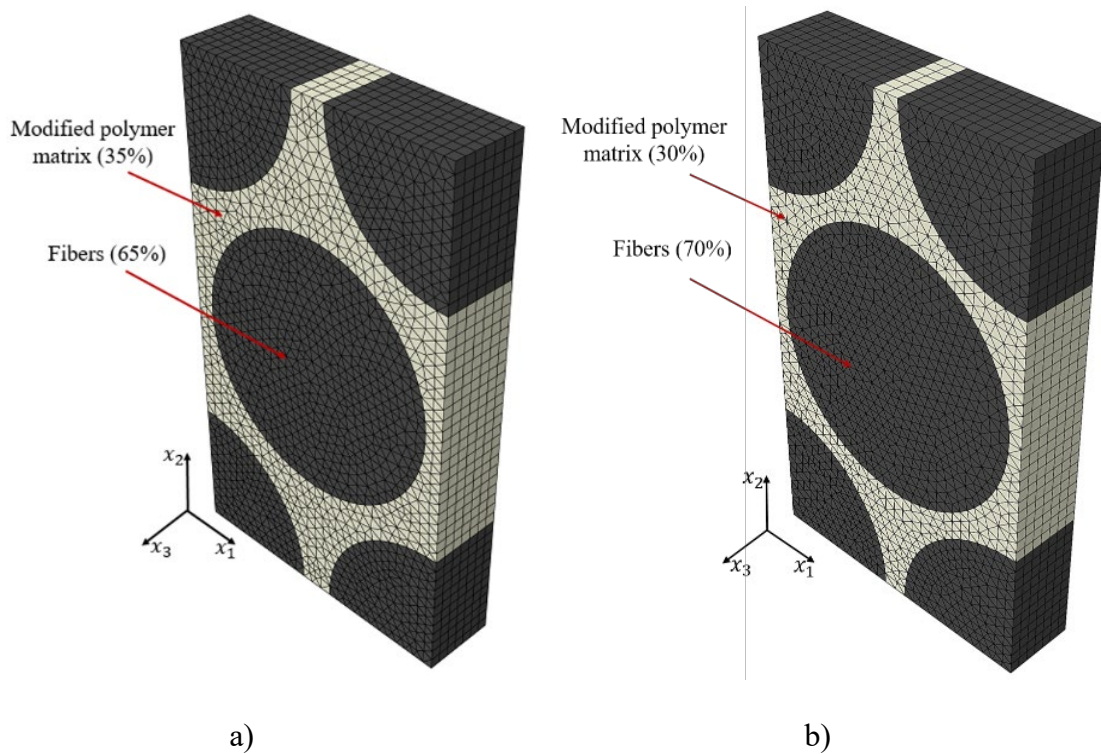


Figure 34. Example of micro-scale RVEs, meshed with  $\sim 20000$  3D wedge elements that have volume fractions of glass fibers equal to: (a) 65% corresponding to the warp tow; (b) 70% corresponding to the weft tow.

Next, to perform homogenization and identify mechanical behavior of composite, a set of six load cases in strains was applied (three uniaxial tension and three shears, see [106]).

Once the numerical simulations were performed, the resultant files were processed using a custom Python script to calculate effective elastic properties of the RVE. First, volume-averaged stress components were calculated for each load case. Given the

averaged stress components and applied strain, the effective stiffness tensor was calculated using Hooke's law:

$$C_{ijkl}^{eff}(\varepsilon_{kl}^0)_m = \langle \sigma_{ij} \rangle_m \quad (6)$$

where  $\langle \sigma_{ij} \rangle_m$  and  $(\varepsilon_{kl}^0)_m$  are the volume-averaged stress and applied strain components, respectively, and  $m$  is the load case number.

For example, from the second load case it is possible to calculate all  $C_{ij22}^{eff}$  components using an expression:

$$C_{ij22}^{eff} = \frac{\langle \sigma_{ij} \rangle_2}{(\varepsilon_{22}^0)_2} \quad (7)$$

Results of the calculations are presented in Table 5.

Table 5. Components of effective stiffness tensor of composite at the micro-scale.

$C_{ijkl}^{eff}$ , GPa	$\varphi_{glass\ fiber} = 65\%$		$\varphi_{glass\ fiber} = 70\%$	
	PP+MWCNT	PP+CB	PP+MWCNT	PP+CB
$C_{1111}^{eff}$	10.228 ±0.001	10.128±0.001	11.929±0.001	11.631±0.001
$C_{1122}^{eff}$	5.608±0.001	5.5531±1e-4	6.238±0.001	6.023±0.001
$C_{1133}^{eff}$	4.514±0.001	4.4691±1e-4	4.923±0.001	4.778±0.001
$C_{3333}^{eff}$	54.060±0.001	53.946±0.001	58.234±0.001	58.144±0.001
$C_{1212}^{eff}$	2.1474±1e-4	2.1264±1e-4	2.994±0.001	2.945±0.001

The electrical properties of the tows (warp and weft) were calculated using the numerical homogenization procedure. The change in the conductivity of the modified matrix under the applied load was computed at the previous stage (Chapter 4), the conductivity of the fibers was assumed to be constant and equals to  $K = 1 \cdot 10^{-10} \text{ S/m}^{-1}$ . At this stage, previously generated RVEs was submitted to the uniaxial tension along with potential of electric field. Since the electrical problem includes second-rank tensors and the composite was transversely isotropic, two loadcases were sufficient to be considered (Table 5, loadcases 1 and 3): uniaxial tension loading along  $x_1$  and  $x_3$  and the potential of electric field in the same directions. Similar to elastic problem, the results of simulations were post processed using custom-made Python script which starts with computation of volume average of electric current:

$$\langle I_q \rangle_m = \frac{1}{V} \sum_{l=1}^N \left( I_q^{(l)} \right)_m \cdot V^{(l)}, \quad (i, j = 1, 2, 3; \quad m = 1, 2, \dots, 6) \quad (8)$$

where  $\langle I_q \rangle_m$  is the volume average component  $q$  calculated as result of application of  $m$ -th loadcase,  $V$  is the overall volume of RVE,  $\left( I_q^{(l)} \right)_m$  is the electric current component  $q$  at the centroid of the FE  $l$  calculated from the  $m$ -th loadcase,  $V^{(l)}$  is the volume of the element  $l$ , and  $N$  is the total number of elements in the model.

Given the averaged electric current components and applied electric potential, the effective stiffness tensor were calculated using Ohm's law:  $\langle I_q \rangle_m = K_{qs}^{eff} (U_{,s}^0)_m$ , where  $K_{qs}^{eff}$  are the components of effective conductivity. For example, from the first loadcase component of conductivity tensor can be calculated as:

$$K_{11}^{eff} = \frac{\langle I_1 \rangle_1}{(U_{,1}^0)_1} \quad (9)$$

As a result, all non-zero components of conductivity tensor were calculated ( $K_{11}^{eff} = K_{22}^{eff}$  и  $K_{33}^{eff}$ ). To calculate the dependency of the change in conductivity ( $K_{ij}^{rel}$ ) on the applied strain, the procedure was repeated for 0.5, 1, 1.5 ... 10% of strain. Figure 35 depicts obtained dependencies of the conductivity on the applied strain.

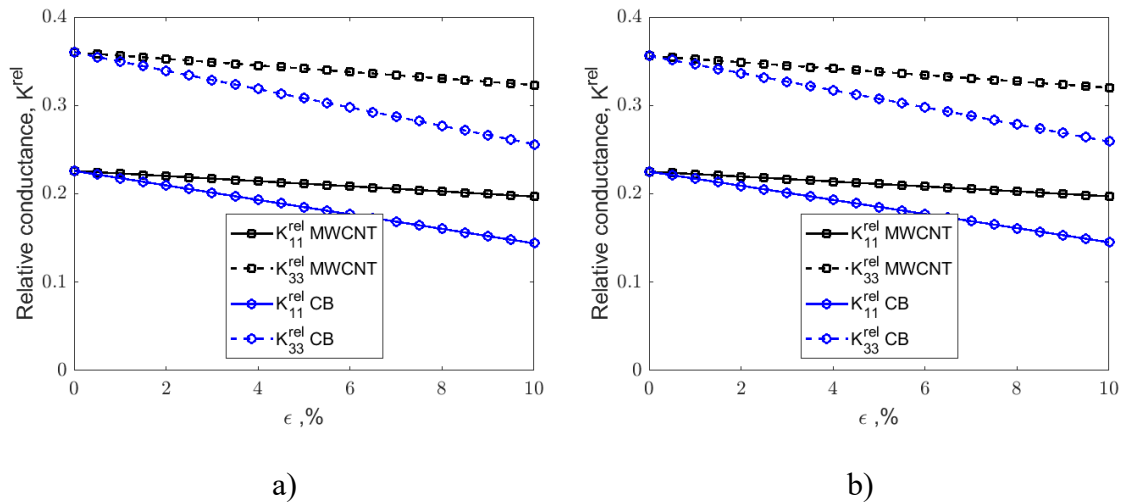


Figure 35. Dependencies of changes in the conductivity of the composite at the micro level on the applied strain: (a) RVE with 65% of fibers; (a) RVE with 70% of fibers.

### 7.1.3. Modeling at the Meso-scale Level

Numerical modeling at the meso-level begins with the generation of RVE. From the analysis of experimental data, it was concluded that the center line of the tow can be modeled by a sinusoidal curve, and that the tows cross sections present ellipses. First, the microscopy data was processed, and the ratio of semi axes of the ellipses were found to be identical for both warp and weft tows and equals to  $\frac{a}{b} = 3.4$ . In the next step, experimental data were used to find the curvature of the tows. To prepare the necessary 3D FEA mesh, a surface mesh of each tow was created first using a MATLAB custom-made script. To create a surface mesh, profiles (ellipses) of tows cross-sections and a central line were created (Figure 36a). Since the profiles were stored as ordered lists of point coordinates, they can be easily combined into triangular elements to get a continuous FEA surface mesh (Figure 36b).

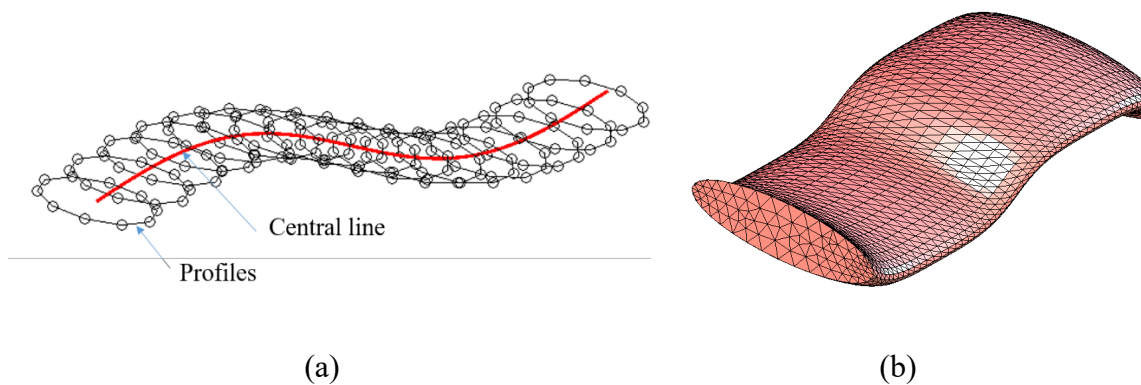


Figure 36. Surface mesh generation procedure for tows: (a) subdivided structure into profiles; (b) final surface mesh with ~8000 elements.

Surface mesh for warp and weft tows was generated and imported into a representative volume, so that the volume fraction of the reinforcement was 50% (see Figure 37). This setup was then auto meshed with linear tetrahedral 3D elements. Next, the properties were assigned to the constituents as follows: (1) mechanical and electrical behavior of tows were transferred from modeling at the micro level, (2) mechanical properties of the modified matrix were taken from the Mori-Tanaka model and electrical properties from the Chapter 6.

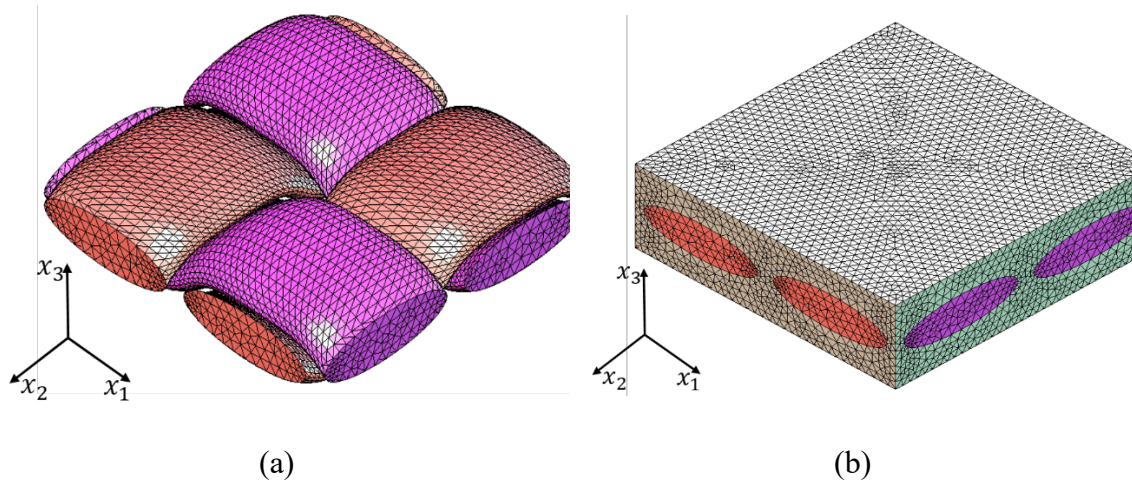


Figure 37. FE model of the RVE at the meso-scale: (a) warp and weft tows; (b) matrix with tows.

To model the changes of the composite conductivity due to the applied load coupled electrical and mechanical problem submitting generated RVE to the uniaxial tension in displacements (along the  $x_1$ ) and electrical potential were solved. The result of FE analysis was used to compute the effective conductivity composite according to the procedure

described in the micro-scale modeling section. Note, only one load case (along  $x_1$ ) was considered since the composite behavior is practically the same in the  $x_2$  while along  $x_3$  it was impossible to conduct experiment due to the small dimension of the composite in that direction.

To compute dependency of the change in conductivity ( $K_{ij}^{rel}$ ) on the applied strain, the procedure was repeated for 0.5, 1, 1.5 ... 10% of strain. Figure 38 depicts obtained dependencies of the conductivity on the applied strain.

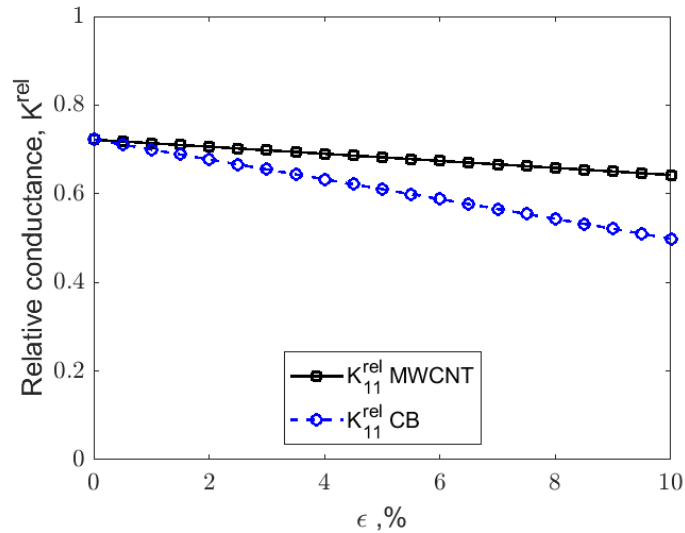
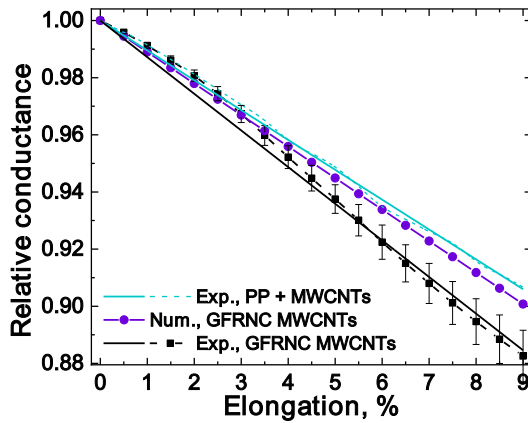


Figure 38. Dependencies of changes in the conductivity of a composite having matrix filled with conductive particles (CB and MWCNTs) on the applied deformation.

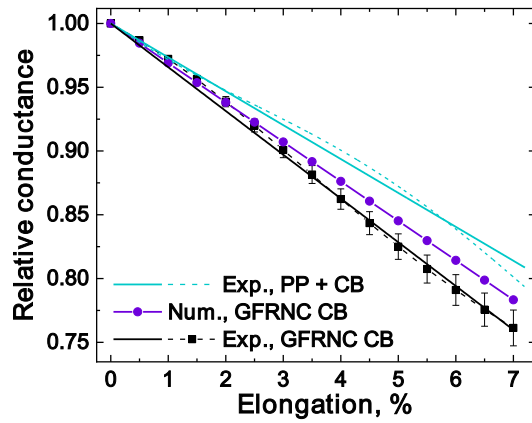
## 7.2. Comparison of the Experimental and Numerical Results

The conductance deformational behavior was characterized by the change in relative conductance (ratio of electrical conductance measured at certain strain divided by the conductance at undeformed state) with respect to the applied strain. All experimental measurements were conducted for a set of 3 identical samples for statistical purposes.

Figure 39a,b shows dependencies of relative conductance from elongation for modified PP and GFRNC samples. Since PP is characterized by good deformability, it was possible to deform GFRNC specimens up to 10% of elongation experimentally. It can be seen that the resulting dependencies are very close to the linear with intercept equals to 1, thus allowing to analyze the results using only values of the slopes (Figure 40a,b). Same is true for the normalized results, obtained numerically (Figure 38).



(a)



(b)

Figure 39. Dependencies of relative electrical conductance on the elongation for the filled with nanoparticles PP and glass fibers reinforced nanocomposite (GFRNC) specimens with (a) CB and (b) MWCNTs used as electroconductive fillers.

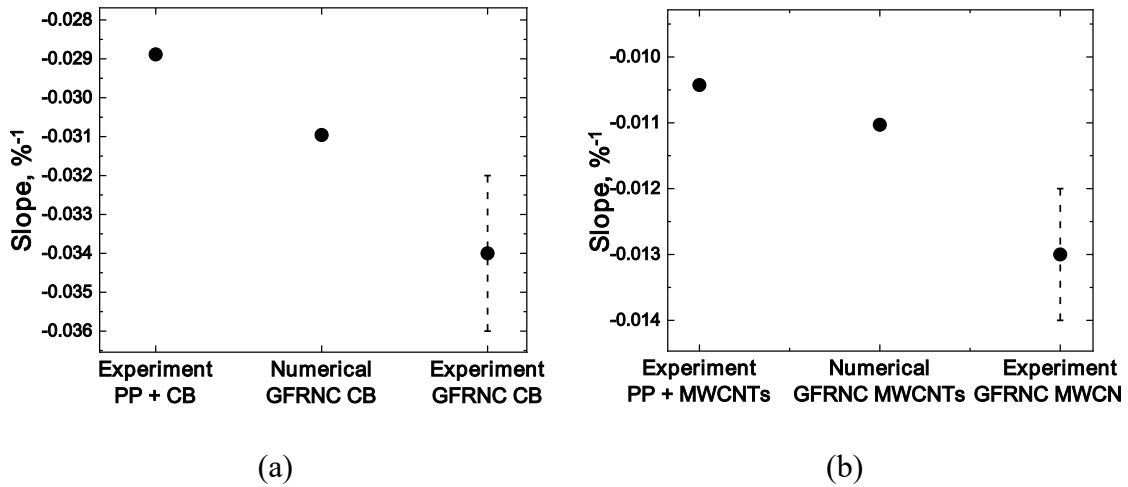


Figure 40. Comparison of the values of slopes of the relative conductance from elongation dependencies for the filled with nanoparticles PP and glass fibers reinforced nanocomposite (GFRNC) specimens with (a) CB and (b) MWCNTs used as electroconductive fillers

An analysis of the slopes of the dependencies between the relative electrical conductivity of the GFRNC and the magnitude of their uniaxial deformation, obtained both numerically and experimentally, shows that the distribution of nanoparticles in the composite, disturbed by the presence of fiberglass, has a different deformation behavior of electrical conductivity, namely, the loss of conductivity becomes sharper, compared to the dependencies obtained for modified PP (Figure 28c,d). It is worth noting, that no strong effect of the number of layers on the rate of change of the electrophysical characteristics

of the composites was observed for GFRNCs obtained with described in Section 5.2 method of manufacturing (Figure 41) for both types of the filler used, allowing conducting comparison only for GFRNC comprising 4 layers of fiberglass textile.

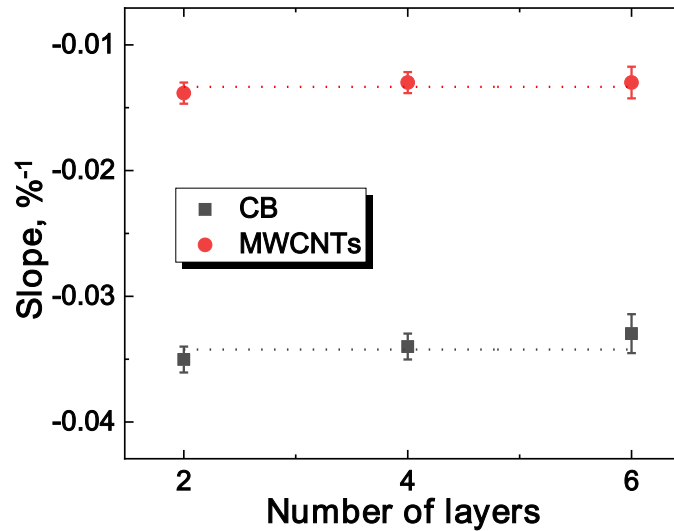


Figure 41. The value of slope of the relative conductance from elongation dependencies versus number of fiberglass textile layers in glass fibers reinforced nanocomposite specimens with CB and MWCNTs used as electroconductive fillers.

One of the factors influencing the value of the slope of these dependencies is that for the glass-fiber-reinforced matrices modified with nanoparticles, the law of change in electrical conductivity with deformation becomes transversely isotropic. Another factor is the inhomogeneous local deformation of the matrix modified by nanoparticles. It strongly depends on the proximity to the fiberglass, which has much higher mechanical characteristics. Finally, since the nanoparticle-modified matrix determines the

electrophysical characteristics of GFRNC, forced segregation of this electrically conductive phase leads to the formation of nontrivial conductive paths that are differently oriented to the direction of the applied deformation. This, in turn, leads to the fact that the law of the change in electrical conductivity from deformation for samples of fiberglass-reinforced composites strongly depends not only on the volume fraction of fiberglass, but also on the fiberglass textile weaving pattern, as well as on the quality of layup of the fiberglass layers themselves. Also, the presence of pores can be one of the contributing factors.

The above considerations may explain the difference between the results of numerical and experimental studies. It was found that the difference between the experimentally determined for the GFRNCs value of the slope of the dependence of electrical conductivity on deformation and that experimentally obtained for modified PP is higher compared to the slope value difference between obtained numerically for GFRNCs and experimentally for modified PP. This leads to the conclusion that the RVE built for numerical investigation may not be sufficiently representative in this case. In order to be able to more accurately reproduce numerically the complexity of the real structure of GFRNC, a more thorough analysis of experimental samples, for example using X-ray computed tomography, may be required.

### **7.3. Conclusions to the Chapter 7**

A multi-scale modeling approach was developed to predict electrical conductance changes with respect to the uniaxial deformation for GFRNC. The results of modeling were

compared against the experimental data. It was noted that the numerical approach can qualitatively reproduce the effect of the glass fibers presence in the GFRNC on the change of conductance with deformation. The quantitative discrepancy can be explained by the idealized representation of the composite at the micro- and meso-scales using the concept of RVE. Indeed, since the strain field that depends on the geometrical parameters of the RVE determines the loss in conductance of the GFRNC, it is important to have a comprehensive set of parameters for accurate numerical representation of the composite at different length scales. The presence of porosity, local changes in tows geometry, tows weaving pattern and fabric layers layout are examples of parameters that can be added to the modeling procedure. For correct verification of the modeling results it is also required to perform more detailed experimental analysis of the specimens in the future, i.e. their X-ray computer tomography.

Thus, it can be said that in the long term, the results of the study can effectively predict the deformation state of materials based on data on their relative electrical conductivity, regardless of the type of nanoscale filler and the complexity of its spatial distribution, provided, for example, by the presence of reinforcing fibers in the composite various weaving. It will be possible to apply the proposed numerical approaches for materials obtained by widely used industrial processing methods (melt mixing), as well as for materials reinforced with fibers or fabric, which can be used simultaneously as functional and structural.

## Chapter 8. General Conclusions

In this work, the multi-scale numerical models were developed for correlation of electrical properties and applied uniaxial deformation for polymer composites with different types of filler distribution. The numerical simulations were performed taking into account real structure of the materials, and verified by experimental methods.

To achieve this goal the analysis and selection of the most suitable types of fillers and methods for their introduction into the polymer matrix were done. It was followed by the manufacturing of representative laboratory batches of samples optimized in structure and properties for studying their physical properties. Study of the structure and properties of composite materials by experimental methods, as well as changes in these properties during the deformation of composites was conducted. Multi-scale numerical modeling of representative composite structures based on experimental data and analytical methods of homogenization to calculate the effective mechanical and electrical properties of composite structures was performed.

Two types of the filler distribution were investigated experimentally and numerically at different scales, deepening the understanding of influence of type of segregated structure on its behavior under external stimuli.

First, a composite with complex 3D extremely segregated structure made of MWCNTs was investigated, based on preliminary studies of deformational behavior of thin layer of densely packed filler. In that case the filler had minimal influence on the mechanical properties of the composite. At the same time, it was shown that a segregated

structure element – thin layer of densely packed filler - had anisotropic deformational response of conductivity.

Second system of interest was electroconductive composite reinforced with woven glass fabric. Electrical conductance of the composite was achieved by modification of polymer thermoplastic matrix with one of two types of nanosized filler, which were present in agglomerated state in the resulting mixtures. Since the conductive phase in that case was modified with nanoparticles polymer, its electrical conductivity deformational response was isotropic.

It was concluded, that deformational response of electrical conductance of composites with segregated structure is highly dependent on how segregation was achieved and what types of components are used. Comparing the results, obtaining for the numerical and experimental studies of response of electrical conductance for composite, where segregation had an extreme character, and the results for composites, where segregation was obtained through introduction in isotropic electroconductive nanocomposite dielectric glass fibers, it was concluded, that contrast of mechanical properties between insulating regions and electroconductive phase in composite materials with segregated structure plays a significant role. Especially it was notable when comparing deformational response of conductance of composite with segregated structure at meso scale and that of volume element of the electroconductive phase in the composite at micro scale. Particularly, in case when contrast of mechanical properties is low, or the deformational behavior of the electroconductive phase at micro-scale is dictated by the surrounding polymer matrix, the

transition to the meso scale leads to decrease of rate of electrical conductance change with deformation. In case of high property contrast situation is opposite.

The conducted study in the future can help predicting electrical conductance deformational response of the constructions or components made of the composite materials manufactured by different processing techniques with segregated structure made of different types of the filler using computationally efficient numerical simulations. The developed models are of great practical importance. Although there is still a room for improvement for the proposed approaches, the obtained results allow to conclude that it is potentially possible to predict with relatively good accuracy ( $\pm\sim 10\%$ ) the material electrical conductance response to the deformation using proposed numerical models. It can be done regardless of what type of the filler used and how complex its distribution is, as long as the numerical model realistically represent experimental data, and assumptions made during the conductance calculations are justifiable. The conducted study in the future can help predicting electrical conductance deformational response of the constructions or components made of the composite materials filled with different types of the filler by different processing techniques using computationally efficient numerical simulations.

As a future development of this work it is planned to investigate several important effects. It is planned to perform calculation of the effective properties of composite materials with a segregated structure, as well as a filler finely distributed in a thin layer, using the fast Fourier transform method. By processing the data obtained by electron microscopy and tomography for the undeformed and deformed state, it is planned to evaluate the absolute values of contact resistances between nanoparticles and the possible

changes in their values during deformation. Also, it is planned to develop a more detailed algorithm for calculating the electrical conductivity of the conducting filler structure, taking into account the shape and mutual orientation of the filler particles, as well as their own electrical conductivity and its change depending on the degree of deformation of nanoparticles. This can be done taking into account the tunneling effect in more detail depending on the distance, type of filler particles and the medium between them. One of the future steps will be obtaining a more contrast picture of the distribution of the filler in the volume of the composite due to the use of particles as a filler that have a significantly different elemental composition from the matrix, such as nanoparticles of gold or titanium oxide.

Since, as it was concluded in Chapter 7, the RVE built for numerical investigation of CFRNC was not sufficiently representative, to be able to more accurately reproduce numerically the complexity of the real structure of GFRNC, a more thorough analysis of experimental samples, for example using X-ray computed tomography, is planned.

## Bibliography

- [1] Schaefer DW, Justice RS. How Nano Are Nanocomposites? *Macromolecules* 2007;40:8501–8517. <https://doi.org/10.1021/ma070356w>.
- [2] Flandin L, Cavaille JY, Brechet Y, Dendievel R. Characterization of the damage in nanocomposite materials by a.c. electrical properties: Experiment and simulation. *J Mater Sci* 1999;34:1753–9. <https://doi.org/10.1023/A:1004546806226>.
- [3] Flandin L, Brechet Y, Canova GRR, Cavaille JY, Bréchet Y, Canova GRR, et al. AC electrical properties as a sensor of the microstructural evolution in nanocomposite materials: experiment and simulation. *Model Simul Mater Sci Eng* 1999;7:865. <https://doi.org/10.1088/0965-0393/7/5/317>.
- [4] Zeng Z, Liu M, Xu H, Liao Y, Duan F, Zhou L, et al. Ultra-broadband frequency responsive sensor based on lightweight and flexible carbon nanostructured polymeric nanocomposites. *Carbon N Y* 2017;121:490–501. <https://doi.org/10.1016/j.carbon.2017.06.011>.
- [5] Mičušík M, Georgousis G, Omastová M, Kontou E, Pissis P, Kyritsis A. Piezoresistivity of conductive polymer nanocomposites: Experiment and modeling. *J Reinf Plast Compos* 2018;37:1085–98. <https://doi.org/10.1177/0731684418783051>.
- [6] Böger L, Wichmann MHG, Meyer LO, Schulte K. Load and health monitoring in glass fibre reinforced composites with an electrically conductive nanocomposite epoxy matrix. *Compos Sci Technol* 2008;68:1886–94. <https://doi.org/https://doi.org/10.1016/j.compscitech.2008.01.001>.

- [7] Bauhofer W, Kovacs JZ. A review and analysis of electrical percolation in carbon nanotube polymer composites. *Compos Sci Technol* 2009;69:1486–98.  
<https://doi.org/10.1016/j.compscitech.2008.06.018>.
- [8] Stauffer D, Aharony A. *Introduction to percolation theory*. 2nd ed. London: Taylor & Francis; 1992.
- [9] Jogi BF. Dispersion and Performance Properties of Carbon Nanotubes (CNTs) Based Polymer Composites: A Review. *J Encapsulation Adsorpt Sci* 2012;02:69–78. <https://doi.org/10.4236/jeas.2012.24010>.
- [10] Pegel S, Pötschke P, Petzold G, Alig I, Dudkin SM, Lellinger D. Dispersion, agglomeration, and network formation of multiwalled carbon nanotubes in polycarbonate melts. *Polymer (Guildf)* 2008;49:974–84.  
<https://doi.org/10.1016/j.polymer.2007.12.024>.
- [11] Kalaitzidou K, Fukushima H, Drzal LT. A route for polymer nanocomposites with engineered electrical conductivity and percolation threshold. *Materials (Basel)* 2010;3:1089–103. <https://doi.org/10.3390/ma3021089>.
- [12] Pang H, Xu L, Yan DX, Li ZM. Conductive polymer composites with segregated structures. *Prog Polym Sci* 2014;39:1908–33.  
<https://doi.org/10.1016/j.progpolymsci.2014.07.007>.
- [13] Li J, Kim JK. Percolation threshold of conducting polymer composites containing 3D randomly distributed graphite nanoplatelets. *Compos Sci Technol* 2007;67:2114–20. <https://doi.org/10.1016/j.compscitech.2006.11.010>.
- [14] Clingerman ML, King JA, Schulz KH, Meyers JD. Evaluation of electrical

- conductivity models for conductive polymer composites. *J Appl Polym Sci* 2002;83:1341–56. <https://doi.org/10.1002/app.10014>.
- [15] Castellino M, Rovere M, Shahzad MI, Tagliaferro A. Conductivity in carbon nanotube polymer composites: A comparison between model and experiment. *Compos Part A Appl Sci Manuf* 2016;87:237–42. <https://doi.org/10.1016/j.compositesa.2016.05.002>.
- [16] Ma PC, Siddiqui NA, Marom G, Kim JK. Dispersion and functionalization of carbon nanotubes for polymer-based nanocomposites: A review. *Compos Part A Appl Sci Manuf* 2010;41:1345–67. <https://doi.org/10.1016/j.compositesa.2010.07.003>.
- [17] Šupová M, Martynková GS, Barabaszová K. Effect of Nanofillers Dispersion in Polymer Matrices: A Review. *Sci Adv Mater* 2011;3:1–25. <https://doi.org/10.1166/sam.2011.1136>.
- [18] Panamoottil SM, Pötschke P, Lin RJT, Bhattacharyya D, Fakirov S. Conductivity of microfibrillar polymer-polymer composites with CNT-loaded microfibrils or compatibilizer: A comparative study. *Express Polym Lett* 2013;7:607–20. <https://doi.org/10.3144/expresspolymlett.2013.58>.
- [19] Lebedev O V., Ozerin AN, Kechek AS, Shevchenko VG, Kurkin TS, Golubev EK, et al. A study of oriented conductive composites with segregated network structure obtained via solid-state processing of UHMWPE reactor powder and carbon nanofillers. *Polym Compos* 2019;40:E146–55. <https://doi.org/10.1002/pc.24532>.
- [20] Lisunova MO, Mamunya YP, Lebovka NI, Melezhyk A V. Percolation behaviour

of ultrahigh molecular weight polyethylene/multi-walled carbon nanotubes composites. *Eur Polym J* 2007;43:949–58.

<https://doi.org/10.1016/j.eurpolymj.2006.12.015>.

- [21] Keчек'yan AS, Mikhailik ES, Monakhova KZ, Kurkin TS, Gritsenko OT, Beshenko MA, et al. Effect of preliminary compression and uniform shear on the deformation behavior of a filled polymer nanocomposite in orientation stretching. *Dokl Chem* 2013;449:94–7. <https://doi.org/10.1134/S0012500813030087>.
- [22] Tallman T, Wang KW. An arbitrary strains carbon nanotube composite piezoresistivity model for finite element integration. *Appl Phys Lett* 2013;102:0–4. <https://doi.org/10.1063/1.4774294>.
- [23] Du F, Fischer JE, Winey KI. Effect of nanotube alignment on percolation conductivity in carbon nanotube/polymer composites. *Phys Rev B - Condens Matter Mater Phys* 2005;72. <https://doi.org/10.1103/PhysRevB.72.121404>.
- [24] Lee BM, Loh KJ, Burton AR, Loyola BR. Modeling the electromechanical and strain response of carbon nanotube-based nanocomposites 2014;9061:906117. <https://doi.org/10.1117/12.2044566>.
- [25] Taherian R. Development of an Equation to Model Electrical Conductivity of Polymer-Based Carbon Nanocomposites. *ECS J Solid State Sci Technol* 2014;3:M26–38. <https://doi.org/10.1149/2.023406jss>.
- [26] Dalmas F, Dendievel R, Chazeau L, Cavailé JY, Gauthier C. Carbon nanotube-filled polymer composites. Numerical simulation of electrical conductivity in three-dimensional entangled fibrous networks. *Acta Mater* 2006;54:2923–31.

<https://doi.org/10.1016/j.actamat.2006.02.028>.

- [27] Song W, Krishnaswamy V, Pucha R V. Computational homogenization in RVE models with material periodic conditions for CNT polymer composites. *Compos Struct* 2016;137:9–17. <https://doi.org/10.1016/j.compstruct.2015.11.013>.
- [28] Xu S, Rezvanian O, Zikry MA. Electrothermomechanical Modeling and Analyses of Carbon Nanotube Polymer Composites. *J Eng Mater Technol* 2013;135:021014. <https://doi.org/10.1115/1.4023912>.
- [29] Zeng QH, Yu AB, Lu GQ. Multiscale modeling and simulation of polymer nanocomposites. *Prog Polym Sci* 2008;33:191–269. <https://doi.org/10.1016/j.progpolymsci.2007.09.002>.
- [30] Shokrieh MM, Rafiee R. On the tensile behavior of an embedded carbon nanotube in polymer matrix with non-bonded interphase region. *Compos Struct* 2010;92:647–52. <https://doi.org/10.1016/j.compstruct.2009.09.033>.
- [31] Romanov VS, Lomov S V., Verpoest I, Gorbatiikh L. Modelling evidence of stress concentration mitigation at the micro-scale in polymer composites by the addition of carbon nanotubes. *Carbon N Y* 2015;82:184–94. <https://doi.org/10.1016/j.carbon.2014.10.061>.
- [32] Romanov VS, Lomov S V., Verpoest I, Gorbatiikh L. Stress magnification due to carbon nanotube agglomeration in composites. *Compos Struct* 2015;133:246–56. <https://doi.org/10.1016/j.compstruct.2015.07.069>.
- [33] Spanos P, Elsbernd P, Ward B, Koenck T, a PTRS. Estimation of the physical properties of nanocomposites by finite-element discretization and Monte Carlo

simulation Estimation of the physical properties of nanocomposites by finite-element discretization and Monte Carlo simulation 2013.

- [34] Srivastava D, Wei C, Cho K. Nanomechanics of carbon nanotubes and composites. *Appl Mech Rev* 2003;56:215. <https://doi.org/10.1115/1.1538625>.
- [35] Lee HS, Yun CH, Kim HM, Lee CJ. Persistence length of multiwalled carbon nanotubes with static bending. *J Phys Chem C* 2007;111:18882–7. <https://doi.org/10.1021/jp075062r>.
- [36] Moniruzzaman M, Winey KI. Polymer nanocomposites containing carbon nanotubes. *Macromolecules* 2006;39:5194–205. <https://doi.org/10.1021/ma060733p>.
- [37] Oliva-Avilés AI, Sosa V, Avilés F. Predicting the piezoresistance contribution of carbon nanotubes in a polymer matrix through finite element modeling. *Rev Mex Fis* 2013;59:511–6.
- [38] Kupke M, Schulte K, Schüler R. Non-destructive testing of FRP by d.c. and a.c. electrical methods. *Compos Sci Technol* 2001;61:837–47. [https://doi.org/10.1016/S0266-3538\(00\)00180-9](https://doi.org/10.1016/S0266-3538(00)00180-9).
- [39] Boisse P. *Advances in composites manufacturing and process design*. 2015.
- [40] Vasiliev V V., Morozov E V. *Advanced mechanics of composite materials*. Elsevier; 2007.
- [41] Smith JG, Connell JW, Delozier DM, Lillehei PT, Watson KA, Lin Y, et al. Space durable polymer/carbon nanotube films for electrostatic charge mitigation. *Polymer (Guildf)* 2004;45:825–36.

- <https://doi.org/https://doi.org/10.1016/j.polymer.2003.11.024>.
- [42] Xu NS, Wu ZS, Deng SZ, Chen J. High-voltage triode flat-panel display using field-emission nanotube-based thin films. *J Vac Sci Technol B Microelectron Nanom Struct Process Meas Phenom* 2001;19:1370–2.  
<https://doi.org/10.1116/1.1387451>.
- [43] Wang QH, Setlur AA, Lauerhaas JM, Dai JY, Seelig EW, Chang RPH. A nanotube-based field-emission flat panel display. *Appl Phys Lett* 1998;72:2912–3.  
<https://doi.org/10.1063/1.121493>.
- [44] Villmow T, Pegel S, John A, Rentenberger R, Pötschke P. Liquid sensing: smart polymer/CNT composites. *Mater Today* 2011;14:340–5.  
[https://doi.org/https://doi.org/10.1016/S1369-7021\(11\)70164-X](https://doi.org/https://doi.org/10.1016/S1369-7021(11)70164-X).
- [45] Li Z-M, Li S-N, Yang M-B, Huang R. A novel approach to preparing carbon nanotube reinforced thermoplastic polymer composites. *Carbon N Y* 2005;43:2413–6. <https://doi.org/https://doi.org/10.1016/j.carbon.2005.04.037>.
- [46] Pötschke P, Bhattacharyya AR, Janke A, Pegel S, Leonhardt A, Täschner C, et al. Melt Mixing as Method to Disperse Carbon Nanotubes into Thermoplastic Polymers. *Fullerenes, Nanotub Carbon Nanostructures* 2005;13:211–24.  
<https://doi.org/10.1081/FST-200039267>.
- [47] Al-Saleh MH, Sundararaj U. A review of vapor grown carbon nanofiber/polymer conductive composites. *Carbon N Y* 2009;47:2–22.  
<https://doi.org/10.1016/j.carbon.2008.09.039>.
- [48] Vilčáková J. *Electrical Percolation Threshold of Composite Materials* 2000.

- [49] Wentzel D, Miller S, Sevostianov I. Dependence of the electrical conductivity of graphene reinforced epoxy resin on the stress level. *Int J Eng Sci* 2017;120:63–70. <https://doi.org/10.1016/j.ijengsci.2017.06.013>.
- [50] Govorov A, Wentzel D, Miller S, Kanaan A, Sevostianov I. Electrical conductivity of epoxy-graphene and epoxy-carbon nanofibers composites subjected to compressive loading. *Int J Eng Sci* 2018;123:174–80. <https://doi.org/10.1016/j.ijengsci.2017.11.014>.
- [51] Pang H, Bao Y, Xu L, Yan DX, Zhang WQ, Wang JH, et al. Double-segregated carbon nanotube-polymer conductive composites as candidates for liquid sensing materials. *J Mater Chem A* 2013;1:4177–81. <https://doi.org/10.1039/c3ta10242d>.
- [52] Du J, Zhao L, Zeng Y, Zhang L, Li F, Liu P, et al. Comparison of electrical properties between multi-walled carbon nanotube and graphene nanosheet/high density polyethylene composites with a segregated network structure. *Carbon N Y* 2011;49:1094–100. <https://doi.org/10.1016/j.carbon.2010.11.013>.
- [53] Gao JF, Li ZM, Meng Q jie, Yang Q. CNTs/ UHMWPE composites with a two-dimensional conductive network. *Mater Lett* 2008;62:3530–2. <https://doi.org/10.1016/j.matlet.2008.03.053>.
- [54] Zhai W, Zhao S, Wang Y, Zheng G, Dai K, Liu C, et al. Segregated conductive polymer composite with synergistically electrical and mechanical properties. *Compos Part A Appl Sci Manuf* 2018;105:68–77. <https://doi.org/10.1016/j.compositesa.2017.11.008>.
- [55] Shields RJ, Bhattacharyya D, Fakirov S. Fibrillar polymer-polymer composites:

morphology, properties and applications. *J Mater Sci* 2008;43:6758–70.

<https://doi.org/10.1007/s10853-008-2693-z>.

- [56] Lin RJT, Bhattacharyya D, Fakirov S. Innovative manufacturing of carbon nanotube-loaded fibrillar polymer composites. *Int J Mod Phys B* 2010;24:2459–65. <https://doi.org/10.1142/S021797921006509X>.
- [57] Gong T, Peng SP, Bao RY, Yang W, Xie BH, Yang MB. Low percolation threshold and balanced electrical and mechanical performances in polypropylene/carbon black composites with a continuous segregated structure. *Compos Part B Eng* 2016;99:348–57. <https://doi.org/10.1016/j.compositesb.2016.06.031>.
- [58] Wu HY, Jia LC, Yan DX, Gao J feng, Zhang XP, Ren PG, et al. Simultaneously improved electromagnetic interference shielding and mechanical performance of segregated carbon nanotube/polypropylene composite via solid phase molding. *Compos Sci Technol* 2018;156:87–94. <https://doi.org/10.1016/j.compscitech.2017.12.027>.
- [59] Di Y, Ren P, Zhang Q. Segregated ultrahigh molecular weight polyethylene composites filled with graphene sheets and hybrid multi-walled carbon nanotubes. *Fuhe Cailiao Xuebao/Acta Mater Compos Sin* 2012;29:36–41.
- [60] Pang H, Chen C, Bao Y, Chen J, Ji X, Lei J, et al. Electrically conductive carbon nanotube/ultrahigh molecular weight polyethylene composites with segregated and double percolated structure. *Mater Lett* 2012;79:96–9. <https://doi.org/10.1016/j.matlet.2012.03.111>.

- [61] Feng CP, Chen L, Wei F, Ni HY, Chen J, Yang W. Highly thermally conductive UHMWPE/graphite composites with segregated structures. *RSC Adv* 2016;6:65709–13. <https://doi.org/10.1039/c6ra13921c>.
- [62] Ren PG, Di YY, Zhang Q, Li L, Pang H, Li ZM. Composites of ultrahigh-molecular-weight polyethylene with graphene sheets and/or MWCNTs with segregated network structure: Preparation and properties. *Macromol Mater Eng* 2012;297:437–43. <https://doi.org/10.1002/mame.201100229>.
- [63] Ozerin AN, Ivanchev SS, Chvalun SN, Aulov VA, Ivancheva NI, Bakeev NF. Properties of oriented film tapes prepared via solid-state processing of a nascent ultrahigh-molecular-weight polyethylene reactor powder synthesized with a postmetallocene catalyst. *Polym Sci Ser A* 2012;54:950–4. <https://doi.org/10.1134/S0965545X12100033>.
- [64] Gu H, Wang J, Yu C. Three-dimensional Modeling of Percolation Behavior of Electrical Conductivity in Segregated Network Polymer Nanocomposites Using Monte Carlo Method. *Adv Mater* 2016;5:1. <https://doi.org/10.11648/j.am.20160501.11>.
- [65] Zhang S, Deng H, Zhang Q, Fu Q. Formation of conductive networks with both segregated and double-percolated characteristic in conductive polymer composites with balanced properties. *ACS Appl Mater Interfaces* 2014;6:6835–44. <https://doi.org/10.1021/am500651v>.
- [66] Hao X, Gai G, Yang Y, Zhang Y, Nan C wen. Development of the conductive polymer matrix composite with low concentration of the conductive filler. *Mater*

- Chem Phys 2008;109:15–9. <https://doi.org/10.1016/j.matchemphys.2007.10.044>.
- [67] Brigandi PJ, Cogen JM, Pearson RA. Electrically conductive multiphase polymer blend carbon-based composites. *Polym Eng Sci* 2014;54:1–16. <https://doi.org/10.1002/pen.23530>.
- [68] Feng Y, Ning N, Zhang L, Tian M, Zou H, Mi J. Evolution of conductive network and properties of nanorod/polymer composite under tensile strain. *J Chem Phys* 2013;139. <https://doi.org/10.1063/1.4812752>.
- [69] Aneli JN, Zaikov GE, Khananashvili LM. Effects of mechanical deformations on the structurization and electric conductivity of electric conducting polymer composites. *J Appl Polym Sci* 1999;74:601–21. [https://doi.org/10.1002/\(SICI\)1097-4628\(19991017\)74:3<601::AID-APP14>3.0.CO;2-K](https://doi.org/10.1002/(SICI)1097-4628(19991017)74:3<601::AID-APP14>3.0.CO;2-K).
- [70] Zhang R, Baxendale M, Peijs T. Universal resistivity-strain dependence of carbon nanotube/polymer composites. *Phys Rev B - Condens Matter Mater Phys* 2007;76:2–6. <https://doi.org/10.1103/PhysRevB.76.195433>.
- [71] Staszewski W, Boller C, Tomlinson GR. *Health Monitoring of Aerospace Structures: Smart Sensor Technologies and Signal Processing*. John Wiley & Sons, Inc.; 2004.
- [72] Iov F, Blaabjerg F. Power electronics and control for wind power systems. 2009 *IEEE Power Electron. Mach. Wind Appl.*, 2009, p. 1–16. <https://doi.org/10.1109/PEMWA.2009.5208339>.
- [73] Brownjohn JMW. Structural health monitoring of civil infrastructure. *Philos Trans*

- R Soc A Math Phys Eng Sci 2007;365:589–622.  
<https://doi.org/10.1098/rsta.2006.1925>.
- [74] Merzbacher CI, Kersey AD, Friebele EJ. Fiber optic sensors in concrete structures: a review. *Smart Mater Struct* 1996;5:196–208. <https://doi.org/10.1088/0964-1726/5/2/008>.
- [75] Gholizadeh S. A review of non-destructive testing methods of composite materials. *Procedia Struct Integr* 2016;1:50–7.  
<https://doi.org/https://doi.org/10.1016/j.prostr.2016.02.008>.
- [76] Wichmann MHG, Buschhorn ST, Gehrman J, Schulte K. Piezoresistive response of epoxy composites with carbon nanoparticles under tensile load. *Phys Rev B - Condens Matter Mater Phys* 2009;80:1–8.  
<https://doi.org/10.1103/PhysRevB.80.245437>.
- [77] Thostenson ET, Chou T-W. Processing-structure-multi-functional property relationship in carbon nanotube/epoxy composites. *Carbon N Y* 2006;44:3022–9.  
<https://doi.org/https://doi.org/10.1016/j.carbon.2006.05.014>.
- [78] Saito R, Dresselhaus G, Dresselhaus MS. *Physical Properties of Carbon Nanotubes*. PUBLISHED BY IMPERIAL COLLEGE PRESS AND DISTRIBUTED BY WORLD SCIENTIFIC PUBLISHING CO.; 1998.  
<https://doi.org/doi:10.1142/p080>.
- [79] Nadiv R, Fernandes RMF, Ochbaum G, Dai J, Buzaglo M, Varenik M, et al. Polymer nanocomposites: Insights on rheology, percolation and molecular mobility. *Polymer (Guildf)* 2018;153:52–60.

<https://doi.org/10.1016/j.polymer.2018.07.079>.

- [80] Li C, Thostenson ET, Chou T-W. Sensors and actuators based on carbon nanotubes and their composites: A review. *Compos Sci Technol* 2008;68:1227–49. <https://doi.org/https://doi.org/10.1016/j.compscitech.2008.01.006>.
- [81] Gao L, Thostenson ET, Zhang Z, Chou T-W. Sensing of Damage Mechanisms in Fiber-Reinforced Composites under Cyclic Loading using Carbon Nanotubes. *Adv Funct Mater* 2009;19:123–30. <https://doi.org/10.1002/adfm.200800865>.
- [82] Moriche R, Sánchez M, Jiménez-Suárez A, Prolongo SG, Ureña A. Electrically conductive functionalized-GNP/epoxy based composites: From nanocomposite to multiscale glass fibre composite material. *Compos Part B Eng* 2016;98:49–55. <https://doi.org/https://doi.org/10.1016/j.compositesb.2016.04.081>.
- [83] Baltopoulos A, Polydorides N, Pambaguan L, Vavouliotis A, Kostopoulos V. Exploiting carbon nanotube networks for damage assessment of fiber reinforced composites. *Compos Part B Eng* 2015;76:149–58. <https://doi.org/https://doi.org/10.1016/j.compositesb.2015.02.022>.
- [84] Lyulin S V, Larin S V, Nazarychev VM, Fal'kovich SG, Kenny JM. Multiscale computer simulation of polymer nanocomposites based on thermoplastics. *Polym Sci Ser C* 2016;58:2–15. <https://doi.org/10.1134/S1811238216010082>.
- [85] Nanocyl n.d. <https://www.nanocyl.com/product/nc7000/>.
- [86] Tuball n.d. <https://tuball.com/en/about-tuball>.
- [87] П267-Э n.d. <https://studylib.ru/doc/2305578/e-lektroprovodnyj-tehnicheskij-uglerod-p-267-e---p-268>.

- [88] III H030 GP/3 n.d. <http://www.sibur-int.com/upload/documents/TDS H030 GP 3 v14.pdf>.
- [89] Lu W, Chou TW, Thostenson ET. A three-dimensional model of electrical percolation thresholds in carbon nanotube-based composites. *Appl Phys Lett* 2010;96:10–3. <https://doi.org/10.1063/1.3443731>.
- [90] Spanos P, Elsbernd P, Ward B, Koenck TA. Estimation of the physical properties of nanocomposites by finite-element discretization and Monte Carlo simulation. *Phil Trans R Soc* 2013;371. <https://doi.org/10.1098/rsta.2012.0494>.
- [91] Liu YJ, Chen XL. Continuum Models of Carbon Nanotube-Based Composites Using the Boundary Element Method. *Electron J Bound Elem* 2003;1:316–35. [https://doi.org/10.1016/S0167-6636\(02\)00200-4](https://doi.org/10.1016/S0167-6636(02)00200-4).
- [92] Liu B, Jiang H, Johnson HT, Huang Y. The influence of mechanical deformation on the electrical properties of single wall carbon nanotubes. *J Mech Phys Solids* 2004;52:1–26. [https://doi.org/10.1016/S0022-5096\(03\)00112-1](https://doi.org/10.1016/S0022-5096(03)00112-1).
- [93] Derosa PA, Michalak T. Polymer-Mediated Tunneling Transport Between Carbon Nanotubes in Nanocomposites. *J Nanosci Nanotechnol* 2014;14:3696–702. <https://doi.org/10.1166/jnn.2014.7973>.
- [94] Gau C, Kuo C-Y, Ko HS. Electron tunneling in carbon nanotube composites. *Nanotechnology* 2009;20:395705. <https://doi.org/10.1088/0957-4484/20/39/395705>.
- [95] Flory PJ. *Statistical mechanics of chain molecules*. 2nd ed. New York: Hanser Publishers; 1989. <https://doi.org/doi:10.1002/bip.1969.360080514>.

- [96] Bao WS, Meguid SA, Zhu ZH, Pan Y, Weng GJ. Effect of carbon nanotube geometry upon tunneling assisted electrical network in nanocomposites. *J Appl Phys* 2013;113. <https://doi.org/10.1063/1.4809767>.
- [97] ASTM. ASTM D3849-14a Method for Carbon Black — Morphological Characterization Using Electron Microscopy. *Astm* 2015:1–8. <https://doi.org/10.1520/D3849-14A.2>.
- [98] Klüppel M, Heinrich G. Fractal Structures in Carbon Black Reinforced Rubbers. *Rubber Chem Technol* 1995;68:623–51. <https://doi.org/https://doi.org/10.5254/1.3538763>.
- [99] Menyhárd A, Suba P, László Z, Fekete HM, Mester O, Horváth Z, et al. Direct correlation between modulus and the crystalline structure in isotactic polypropylene. *Express Polym Lett* 2015;9:308–20. <https://doi.org/10.3144/expresspolymlett.2015.28>.
- [100] Xu S, Rezvanian O, Peters K, Zikry MA. Tunneling effects and electrical conductivity of CNT polymer composites. *Mater Res Soc Symp Proc* 2011;1304:50–6. <https://doi.org/10.1557/opl.2011.606>.
- [101] Mori T, Tanaka K. Average stress in matrix and average elastic energy of materials with misfitting inclusions. *Acta Metall* 1973;21:571–4. [https://doi.org/10.1016/0001-6160\(73\)90064-3](https://doi.org/10.1016/0001-6160(73)90064-3).
- [102] Horii H, Nemat-Nasser S. Overall moduli of solids with microcracks: Load-induced anisotropy. *J Mech Phys Solids* 1983;31:155–71. [https://doi.org/10.1016/0022-5096\(83\)90048-0](https://doi.org/10.1016/0022-5096(83)90048-0).

- [103] Kachanov M, Tsukrov I, Shafiro B. Effective Moduli of Solids With Cavities of Various Shapes. *Appl Mech Rev* 1994;47:S151.  
<https://doi.org/10.1115/1.3122810>.
- [104] Sevostianov I, Kachanov M. Compliance tensors of ellipsoidal inclusions. *Int J Fract* 1999;96:L3–7. <https://doi.org/10.1023/A:1018712913071>.
- [105] Benveniste Y. A new approach to the application of Mori-Tanaka's theory in composite materials. *Mech Mater* 1987;6:147–57. [https://doi.org/10.1016/0167-6636\(87\)90005-6](https://doi.org/10.1016/0167-6636(87)90005-6).
- [106] Trofimov A, Drach B, Sevostianov I. Effective elastic properties of composites with particles of polyhedral shapes. *Int J Solids Struct* 2017;120:157–70.  
<https://doi.org/10.1016/j.ijsolstr.2017.04.037>.